Characterization of adaptation mechanisms in sorghum using a multi-reference back-cross nested association mapping design and envirotyping

Vincent Garin [1,2,3,*], Chiaka Diallo [4,5,*], Mohamed Lamine Tekete [6,9,*], Korotimi Thera [6,*], Baptiste Guitton[2,3], Karim Dagno[6], Abdoulaye G. Diallo[6], Mamoutou Kouressy[6], Willmar Leiser [4], Fred Rattunde[7], Ibrahima Sissoko[4], Aboubacar Toure[4], Baloua Nebie [8], Moussa Samake[9], Jana Kholova[1,10], Julien Frouin [2,3], David Pot [2,3], Michel Vaksmann [2,3], Eva Weltzien [4,7], Niaba Teme[6], and Jean-Francois Rami [2,3]

[1]International Crops Research Institute for the Semi-Arid Tropics, Patancheru, India

[2]CIRAD, UMR AGAP Institut, F-34398 Montpellier, France

[3]UMR AGAP Institut, Univ Montpellier, CIRAD, INRAE, Institut Agro, Montpellier, France

[4]International Crops Research Institute for the Semi-Arid Tropics, Bamako, Mali

[5]Institut polytechnique rural de formation et de recherche appliquée de Katibougou, Bamako, Mali

[6]Institut d'Economie Rurale, Bamako, Mali
[7]Agronomy Department, University of Wisconsin, Madison, Wisconsin, USA

[8]International Maize and Wheat Improvement Center (CIMMYT), Dakar, Senegal

[9]Université des Sciences des Techniques et des Technologies de Bamako - Faculté des Sciences et Techniques, Bamako, Mali

[10]Department of Information Technologies, Faculty of Economics and Management, Czech University of Life Sciences, Prague, Czech Republic

[*]Those authors made equal contributions

The identification of haplotypes influencing traits of agronomic interest, with well-defined effects across environments, is of key importance to develop varieties adapted to their context of use. It requires advanced crossing schemes, multi-environment characterization and relevant statistical tools. Here we present a sorghum multi-reference back-cross nested association mapping (BCNAM) population composed of 3901 lines produced by crossing 24 diverse parents to three elite parents from West and Central Africa (WCA-BCNAM). The population was characterized in environments contrasting for photoperiod, rainfall, temperature, and soil fertility. To analyse this multi-parental and multi-environment design, we developed a new methodology for QTL detection and parental effect estimation. In addition, envirotyping data were mobilized to determine the influence of specific environmental covariables on the genetic effects, which allowed spatial projections of the QTL effects. We mobilized this strategy to analyse the genetic architecture of flowering time and plant height, which represent key adaptation mechanisms in environments like West Africa. Our results allowed a better characterisation of well-known genomic regions influencing flowering time concerning their response to photoperiod with Ma6 and Ma1 being photoperiod sensitive and candidate gene Elf3 being insensitive. We also accessed a better understanding of plant height genetic determinism with the combined effects of phenology dependent (Ma6) and independent (qHT7.1 and Dw3) genomic regions. Therefore, we argue that the WCA-BCNAM constitutes a key genetic resource to feed breeding programs in relevant elite parental lines and develop climate-smart varieties.

Multi-reference BCNAM | genotype by environment interaction | sorghum envirotyping

Correspondence: *jean-francois.rami@cirad.fr*

Introduction

The quantitative nature of complex traits and their context specific expression are major hindrances for marker assisted selection (MAS) (Bernardo 2016; Cobb et al., 2019). The genotype by environment (GxE) effect is particularly problematic for MAS because it can strongly reduce or even reverse the QTL effect (Malosetti et al., 2013). However, the combination of advanced genetic resources, improved statistical methodology, and envirotyping data give us a chance to improve our understanding of the QTL by environment (QTLxE) effects. This understanding should increase our capacity to mobilize those effects for MAS and design varieties able to take advantage of specific environmental conditions.

A. The BCNAM design and its properties

Multiparental populations (MPPs) combining the genomes of several founders have progressively emerged as central genetic resources for research (Scott et al., 2020; Bernardo 2021). The nested association mapping (NAM) design composed of crosses between a recurrent parent and donor parents is a well-spread MPP design (McMullen et al., 2009, Gage et al., 2020), with examples in maize (Bauer et al., 2013), rice (Fragoso et al., 2017), wheat (Kidane et al., 2019, Christopher et al., 2021) and sorghum (Bouchet et al., 2017). Sorghum is also the species that was used to develop the back-cross NAM (BCNAM) design, which consists of introgressing diverse alleles from donors in a recurrent (elite) line using one generation of back-cross followed by several generation of selfing (Jordan et al., 2011, Mace et al., 2021). BCNAM designs allow the introgression of diverse alleles in elite background while limiting the risk of introgressing deleterious alleles by keeping around 75% of the elite genome. It can serve research purposes for genetic analysis and breeding purposes (Scott et al., 2020).

BCNAM design has several interesting properties for genetic analyses. Compared to bi-parental crosses it addresses a larger genetic diversity and captures more recombination events. Compared to association panels, it offers better control over the population structure, which can reduce the detection of false positive signals (Myles et al., 2009). BCNAM designs also allow to trace back the origin of favourable alleles to a specific parent, a highly desirable feature to design future crosses. MPPs like BCNAM increase the rare allele frequencies, which is essential to precisely estimate their additive effects (Myles et al., 2009). Moreover, the possibility to extend the reference NAM design by using several recurrent parents allows the characterization of the genetic effect in multiple genetic backgrounds (Christopher et al., 2021). Finally, BCNAM designs are also interesting for GxE studies because it can be used to measure the expression of an interconnected set of diverse alleles in contrasting environments (Cobb et al., 2019).

B. Improved statistical methods for QTL detection in MPP designs

Several approaches have been developed to detect QTL in MPPs characterized in a single environment. For example, Garin et al. (2017, 2018) proposed a framework assuming different allelic configurations at the QTL position. Li et al. (2011) developed a method based on maximum likelihood parental allelic effect significance. Xavier et al. (2015) used mixed models employed for genome-wide association analysis accounting for crossing structure. More recently Paccapelo et al. (2022), adapted the whole genome interval mapping method for the NAM design. A more general strategy consists of using models with identical by descent probability that can be estimated for any type of MPP designs (Zheng et al., 2015; Li et al., 2021).

Compared to separate within-environment analyses, the QTL detection using MPP data characterized in multiple environments (MPP-ME) in a joint model is more challenging, but it allows a more direct comparison of the simultaneously estimated effects. Until now, phenotypic values were averaged across environments (e.g. Giraud et al., 2014), which does not use the full potential of those data. Therefore, Garin et al. (2020) extended the MPP-ME QTL detection methodology using joint analyses. Diouf et al. (2020) proposed a forward-backward algorithm for MPP-ME analysis. De Walsh et al. (2022) proposed a meta-analysis of single environments analyses. Those MPP-ME models are particularly useful to characterize the trait variability in terms of genetic (parents, genetic background) and non-genetic (environment) effects.

C. Extending genetic modelling with envirotyping

The recent progresses in sensor technologies have considerably increased the availability of large-scale environmental information (Xu 2016, Costa-Neto et al., 2021). Therefore, in this study, we extended MPP-ME QTL detection models by integrating environmental covariables (ECs) to refine our understanding of the GxE interaction by testing the sensitivity of multiple parental alleles with respect to various ECs.

Among the available ECs, photoperiod is a key variable for sorghum development, especially in West Africa. Photoperiodism is the developmental responses of plants to the relative length of daylight or photoperiod (Hopkins 2009). Sorghum is a short-day plant generally sensitive to photoperiod that flowers when days become shorter than a certain length (Wolabu and Tadege 2016). When day length is longer than the critical photoperiod, photoperiod sensitive sorghum delays its panicle initiation. The flowering time can be represented as a broken linear function of the photoperiod with a baseline duration remaining constant until a certain photoperiod then an increasing slope where flowering time increases with the photoperiod (Van Oosterom et al., 2001; Figure 4G). The photoperiod sensitivity is the steepness of the slope. Since adaptation of sorghum to its cultivation site relies largely on its photoperiod sensitivity it is of paramount importance to integrate this environmental dimension in our analysis.

In this article, we present a multi-reference sorghum back-cross nested association mapping populations composed of 24 diverse parents anchored on three West African elite lines that represents one of the most relevant publicly available resources for West and Central Africa sorghum (WCA-BCNAM, Table 2, Figure S1). The sub-populations were phenotyped for flag leaf appearance (FLAG), plant height (PH), number of internodes (NODE_N), average length of the internodes (NODE_L), peduncle length (PED), panicle length (PAN), 1000 grains weight (GWGH), and grain yield (YIELD) in multiple environments contrasting for sowing date (photoperiod), rainfall, temperature, and soil fertility over two seasons.

To analyse those data, we developed a methodology for MPP-ME QTL analysis integrating environmental covariables (Figure 1). We illustrate our approach through a fine characterization of major QTL for flowering and plant height and discuss how the combination of advanced genetic resources and statistical methodology can support the design of climate-smart varieties.

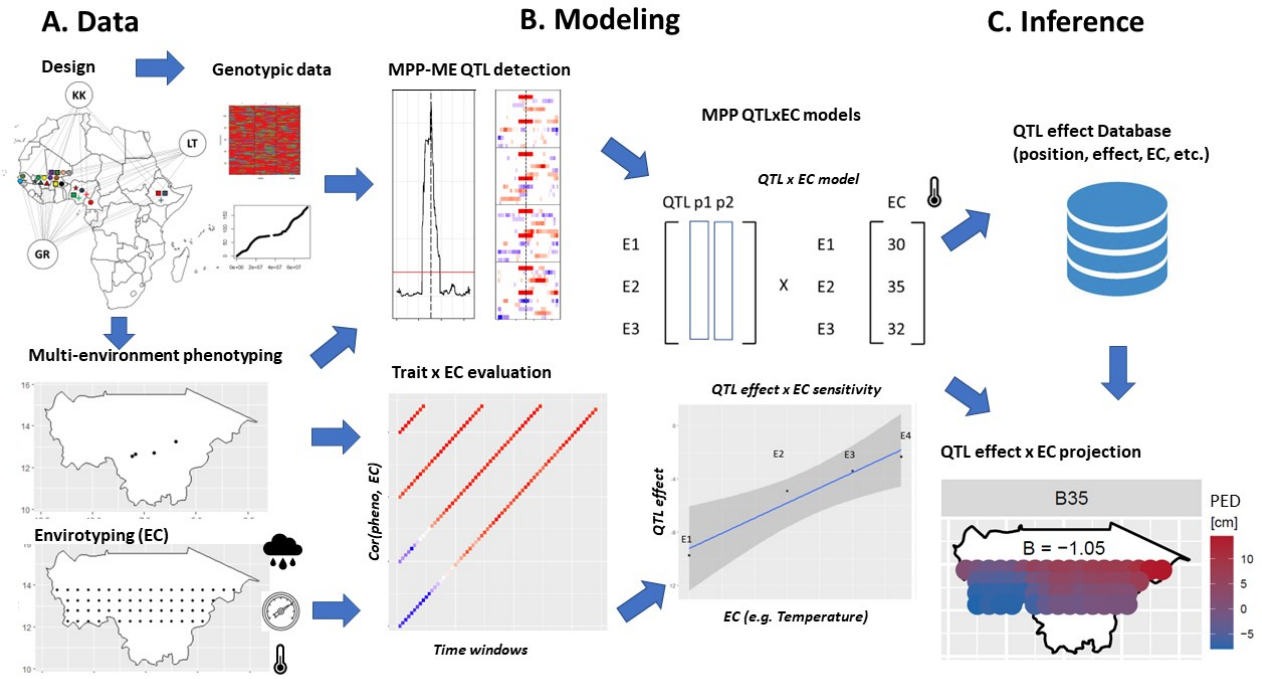

Figure 1. Overview of the analytical strategy. A) Raw genotypic phenotypic and environmental covariable; B) Statistical models for QTL detection in MPP characterized in multiple environment (ME), correlation between trait and environmental covariables (EC) analysis, and synthesis in QTLxEC models; C) Inference using the results gathered in a database and projection of the QTL effect beyond the tested environments.

Results

D. Genetic diversity

Figure 2A illustrates the genetic diversity covered by the parental lines of the WCA-BCNAM population compared to a panel representative of the global sorghum diversity (Methods S1). We compared the number of common polymorphic SNPs of our population, of the US-NAM (Bouchet et al. 2017) and the global diversity panel. Overall, the WCA-BCNAM parents covered 90.2% of the global sorghum genetic diversity considered for the analysis (192K SNP) which offer a slightly better coverage (11 %) than the parents from the sorghum US-NAM which already captured 79.2% of the considered diversity. Principal component analysis of the WCA-BCNAM genetic data (Figures 2 B, C and D) detected three distinct groups corresponding to the three recurrent parents (Figure S2). Clear subdivisions of the populations according to the donor parent race and some specific divergences from this general pattern were observed especially for the populations involving the Hafijeka Guinea Margaritiferum accession.

E. Phenotypic data

The average heritability values over populations were larger for traits like FLAG (0.78-0.95), PH (0.76-0.88) or NODE_L (0.8-0.9) compared to YIELD (0.37-0.64) (Tables S3). Heritability values were larger in the Lata3 sub-population which is due to the within-environment replication as well as the larger similarity between the environmental conditions in which the Lata3 sub-population was phenotyped. In terms of correlation between traits (Figures S3 and S4), we observed an overall negative relationship between FLAG and YIELD. With an average Pearson correlation of -0.28 and a standard deviation of 0.17. This negative relationship was observed in all genetic backgrounds and environments but was stronger at the second sowing (-0.38 ±0.15). FLAG and NODE_N were positively correlated in all backgrounds (Grinkan, Kenin-Keni, and Lata3). This correlation was stronger at the second sowing time (S1: 0.34 ±0.15; S2: 0.45 ±0.15). Concerning the correlation of PH with its components, the strongest one was with NODE_L (0.74 ±0.12), the lowest with NODE_N (0.26 ±0.14). It took intermediary values for PED (0.53 ±0.15) and PAN (0.41 ±0.13). This pattern was observed in all configurations. PH was positively correlated with YIELD (0.23-0.56), except for the Grinkan sub-population measured in 2013 at Sotuba (-0.11 ±0.01). Looking at the correlation between PH, its components (NODE_L, NODE_N, PED, PAN), and YIELD, we noticed that it was undetermined with NODE_N (0.03 ±0.14), and positive with PED (0.17 ±0.18), PAN (0.22 ±0.15), NODE_L (0.24 ±0.14). Finally, GWGH was generally correlated with YIELD (0.27 ±0.18), with a stronger correlation in Kenin-Keni 2012 (0.46 ±0.01). A correlation analysis also helped us to identify the five ECs that were the most correlated with the phenotype and the time window where the association was the strongest (Figures S5 and Tables S4).

F. QTL detection - general results

The total length of the consensus genetic map was 1412 cM with a number of cross-over equal to 47'669, 20'343, and 20'120 in the Grinkan, Kenin-Keni, and Lata3 populations, respectively (Table S1). Overall, we detected 100 significant QTL over the five populations for eight traits, which represented 64 unique QTL (Table S2, Figures S6). Consistently with the heritability estimates, the total variance explained by the QTL effects was rather large for FLAG (32-53), PH (10-48), and NODE_L (11-47), moderate for PED (10-32), NODE_N (10-22), and GWGH (8-30), and low for YIELD (4-14) and PAN (5-9).

G. QTLxEC extend

The 100 significant QTL covered 1056 parental alleles for which we could estimate the significance of the main and GxE additive effects (Tables S5). Around 60% of the parental alleles were significant and around 25% interacted with the environment. Overall, around 15% of the parent alleles interacted with at least one EC. The FLAG, PH and PED QTL were more significantly affected by the EC than the one for PAN and YIELD. For example, photoperiod strongly influenced FLAG, NODE_N and PH QTL. Atmospheric EC like VPD influenced PED and NODE_L QTL sensitivity while YIELD QTL were sensitive to humidity. PAN and NODE_L QTL were sensitive to minimum temperature.

H. QTL with large effects and candidate genes

Eleven QTL showed medium to large effect with strong significance and consistency over several populations and environments (Table 1 and Figures S6). Their parental effect could go up to 300 dd for the FLAG QTL, or up to 1.07 m for PH. On chromosome three, we detected a strong QTL for FLAG (QTL_FL_3_78) significant in all populations and environments. Almost at the same position, we also detected a large effect QTL for NODE_N (QTL_NN_3_78). QTL_FL_3_78 and QTL_NN_3_78 are probably linked to the early flowering (Elf3) candidate gene (Guitton et al., 2018) or SbCN12 (Yang et al., 2014). Another FLAG QTL (QTL_FL_6_3) with a consistent effect in all populations and environments was detected at the beginning of chromosome six. It colocalized with

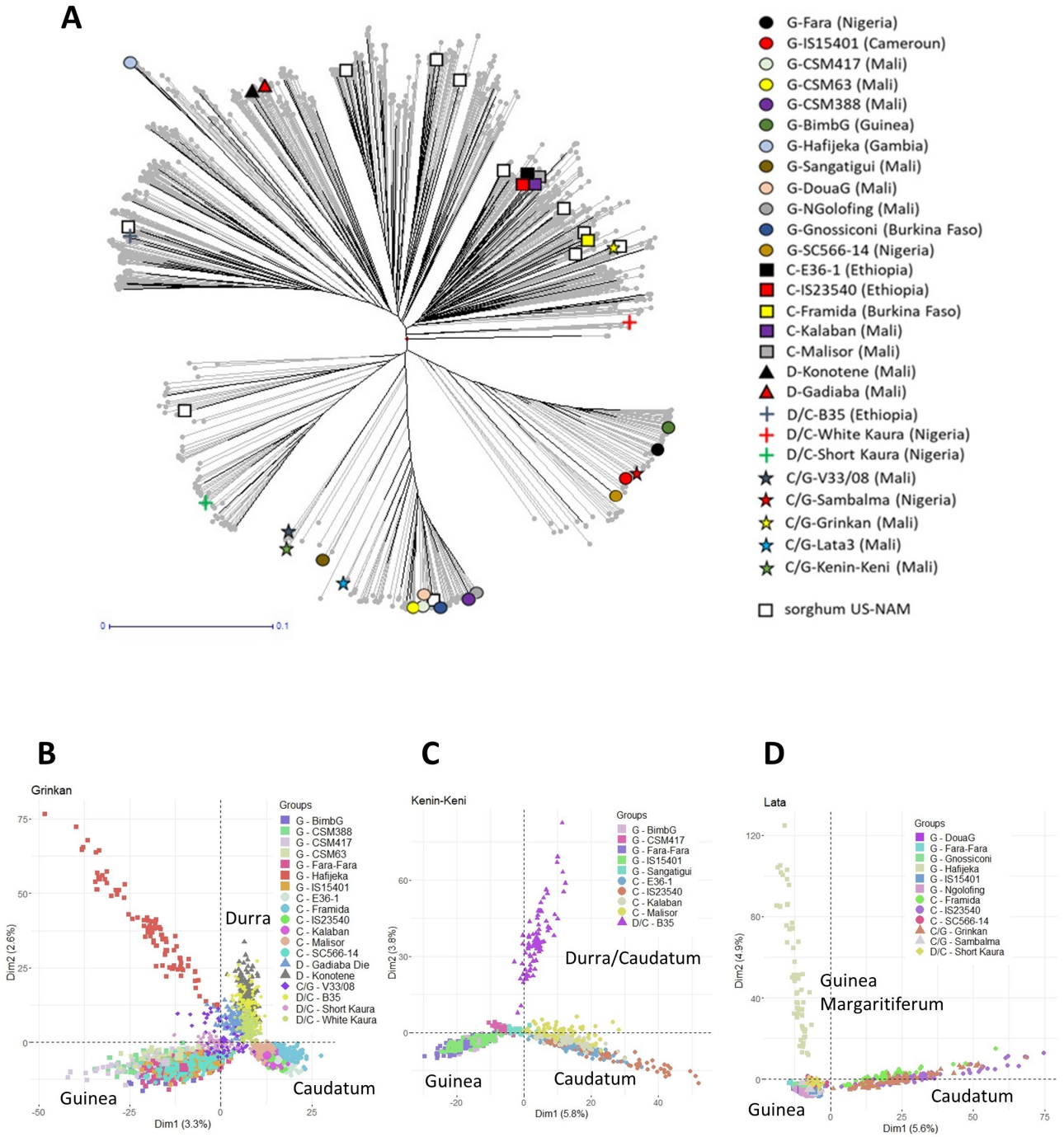

Figure 2. Genetic diversity and structure of the WCA-BCNAM design. A) Coverages of the global sorghum molecular diversity by the WCA-BCNAM and sorghum US-NAM (white square, Bouchet et al. 2017) parents. Principal component bi-plots performed on a subset of 5000 markers randomly selected of the (B) Grinkan (C), Kenin-Keni (D) Lata3 sub- populations.

a QTL for NODE_N (QTL_NN_6_2). Those QTL could be related to the Ma6 gene (Rooney and Aydin 1999; Murphy et al., 2014). We also detected a QTL with medium effects on FLAG on chromosome six around 36 cM (QTL_FL_6_38) falling in the region of the Ma1 gene (Murphy et al., 2011) and another on chromosome nine around 105 cM (QTL_FL_9_105) potentially close to the SbFL9.1 gene (Bouchet et al., 2017).

A strong QTL for PH was detected on chromosome seven around 75 cM (QTL_PH_7_76) with significance in the Grinkan and Kenin-Keni (2013) populations. This QTL colocalized with a highly significant QTL for NODE_L (QTL_NL_7_78) and a strong and highly consistent QTL for PED (QTL_PED_7_78). Nearby this QTL, another QTL

(QTL_PH_7_106) also had a large effect on PH and colocalized with a large effect QTL for NODE_L (QTL_NL_7_98). The QTL region of chromosome seven could be related to one or two genes. The main candidate gene is Dw3 (Multani et al., 2003; Brown et al., 2008). However, according to Li et al. (2015), chromosome seven could harbour two genes: qHT7.1 positioned before Dw3 would influence both the stem and the peduncle length while Dw3 would only influence the stem length.

Table 1. List of large and medium effect QTL with trait, chromosome, position, average R^2, QTLxE effect range, number of parental alleles with significant effects, and candidate genes

QTL ID	trait	chr	range [cM]	range [Mbp]	R^2	QxE range	Npar	Candidate genes
Q_FL_3_78	FLAG	3	77.34-78.36	5.11-5.15	17.1	[-123; 144] [dd]	24	Elf3, SbCN12
Q_NN_3_78	NODE_N	3	78.13-78.75	5.14-5.17	9.3	[-1.8;2.1] [n]	16	Elf3, SbCN12
Q_FL_6_3	FLAG	6	1.49-2.94	0.04-0.08	19.4	[-178; 130] [dd]	24	Ma6
Q_NN_6_2	NODE_N	6	1.49-2.73	0.04-0.08	7.9	[-2.6;1.8] [n]	19	Ma6
Q_FL_6_38	FLAG	6	36.32-39.4	4.04-4.12	6.3	[-192; -27] [dd]	19	Ma1
Q_FL_9_105	FLAG	9	103.7-106.7	5.46-5.54	2.7	[-40;91] [dd]	23	SbFL9.1
Q_PH_7_76	PH	7	74.28-76.69	5.47-5.52	21.9	[-37; 69] [cm]	20	qHT7.1, (Dw3)
Q_NL_7_78	NODE_L	7	76.29-79.59	5.51-5.58	29.9	[-0.1;4.2] [cm]	16	qHT7.1, (Dw3)
Q_PED_7_78	PED	7	74.8-82.1	54.84-56.26	12.6	[-8; 10] [cm]	24	qHT7.1, (Dw3)
Q_NL_7_98	NODE_L	7	96.1-100.7	5.83-5.91	11.8	[-5.8-4.2] [cm]	8	Dw3
Q_PH_7_106	PH	7	102-108.3	5.94-6.07	7.6	[-14;58] [cm]	15	Dw3

I. Complex QTL effect pattern at large effect QTL

The large effect QTL showed a complex pattern with effects distributed over many parents and a wide range of effects modulated by the genetic background and the environment. Those QTL represented 40% of the QTLxEC effects. Almost all donor parents' alleles had at least one significant EC interaction. Such a complex pattern can be illustrated for QTL_FL_3_78 (Figure 3). First, we noticed the contrasting parental effects with parents like CSM417 or CSM388 whose alleles reduced maturity while IS15401 alleles increased it. Then, we observed differences of expression due to the genetic backgrounds. For example, the allele of Fara-Fara had low effect in a Grinkan background while it strongly increased maturity in the Lata3 and Kenin-Keni backgrounds. Finally, we could also observe environmental differences like the stronger cycle reduction of CSM388 allele in 2012 compared to 2013.

J. QTL effect on photoperiodism

The plots of Figures 4 (A-C) represent QTL alleles effect given photoperiod compared to the recurrent (reference) parent score. QTL_FL_6_3 (Ma6) was the most photoperiod sensitive QTL (Figure 4A). At that position compared to Grinkan, the alleles of CSM388 and B35 reduced photoperiodism. For the second sowing date characterized by shorter photoperiod (12.1 h), the difference with Grinkan was small but it increased with longer photoperiod (12.5 h, first sowing). The slope of CSM388 or B35 is therefore less steep than the one of Grinkan. This photoperiod sensitivity reduction was observed in all genetic backgrounds.

QTL_FL_6_38 (Ma1) was also sensitive to photoperiod with five parental alleles interacting significantly with the photoperiod over the different genetic backgrounds. For example, in Grinkan population (2012), the allele of White Kaura increased the photoperiod sensitivity compared to the recurrent parent (Figure 4B). At QTL_FL_3_78 (Elf3), the parental alleles were mostly insensitive to photoperiod. We only detected a reduced photoperiod sensitivity for the Fara-Fara and IS15401 alleles compared to Kenin-Keni (Figure 4C). The alleles of QTL_FL_9_105 (SbFL9.1) were also insensitive to the photoperiod with only two significant interactions out of 15 possible.

K. Dissecting plant height genetic determinism

The phenotypic data for PH and its components (NODE_N, NODE_L, PED, PAN) allowed us to dissect PH genetic architecture. PH can be expressed as PH = (NODE_N * NODE_L) + PED + PAN. Since the phenotypic values of NODE_N are strongly correlated with FLAG, it was not surprising to find overlapping QTL for the two traits on chromosomes three and six (QTL_NN_3_78, QTL_NN_6_2). In terms of photoperiod sensitivity, the QTL for NODE_N followed a similar pattern than the ones from FLAG. QTL_NN_3_78 (Elf3) was rather insensitive to photoperiod with only two parental alleles having a significant interaction while QTL_NN_6_2 (Ma6) was more sensitive with five significant alleles (e.g. Malisor).

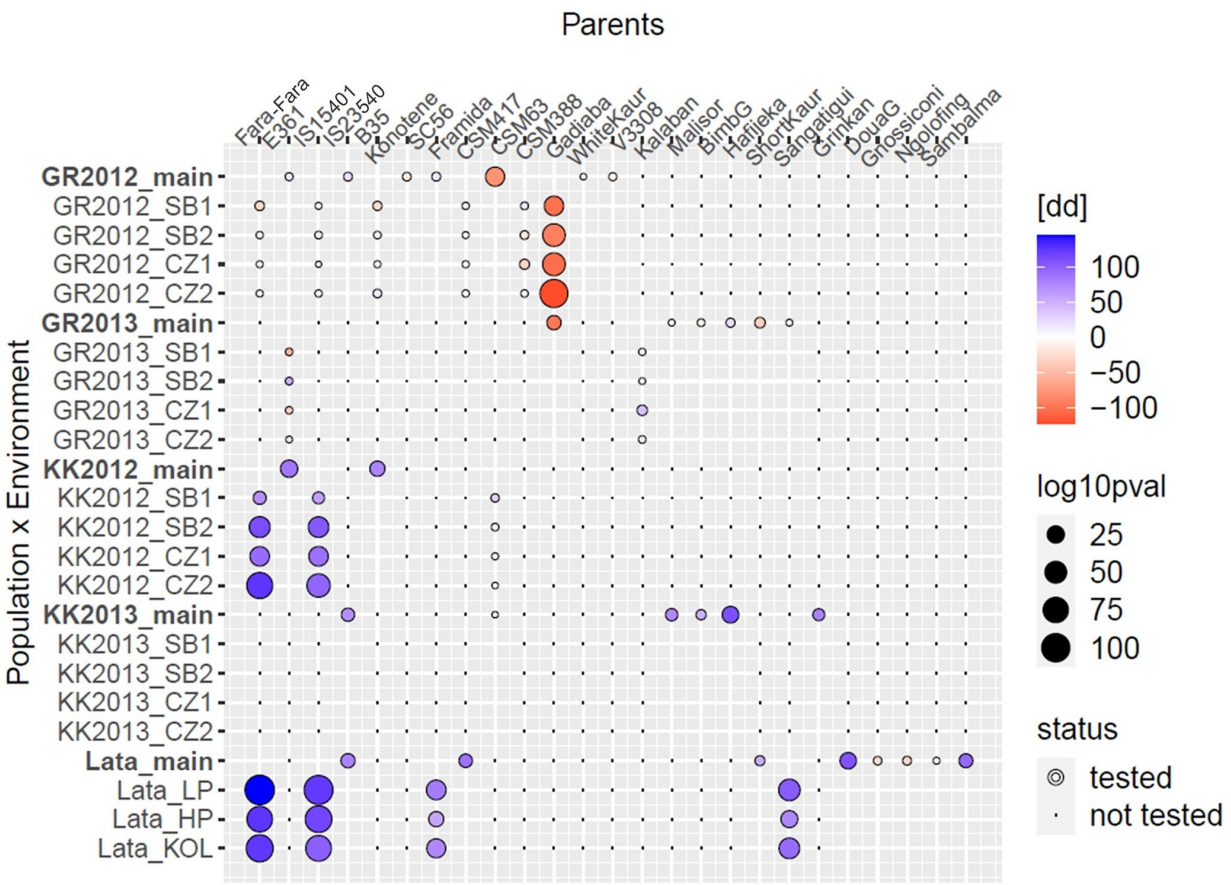

Figure 3. Estimated QTL allelic effect for flag leaf appearance at chromosome three position 77.3 cM for the donor parents (x axis) evaluated in different genetic background (Grinkan, Kenin-Keni, Lata3) and/or environments (SB1-2: Sotuba sowing 1 and 2, CZ1-2: Cinzana sowing 1 and 2, LP/HP: low/high phosphorus, KOL: Kolombada). The colour is proportional to the effect size and direction and the circle size to its significance. An empty space means that the main effect across environments is more significant than the QTLxE effects. Dots means that the parental allele effect was not evaluated in this specific background in this specific trial.

Concerning PH, we also observed a strong agreement between the QTL positions detected for PH and NODE_L on chromosome seven. QTL_PH_7_76 and QTL_NL_7_78 (qHT7.1) colocalized while QTL_PH_7_106 and QTL_NL_7_98 (Dw3) were separated by less than 10 cM. The QTL influencing NODE_L were not sensitive to photoperiod, but other ECs like VPD or potential evapotranspiration modulated the parental allelic effects at those positions. For example, at QTL_PH_7_76, the effects of parents like Hafijeka or Short Kaura were reduced when VPD increased (Figure 4E). Surprisingly, the corresponding QTL (QTL_PH_7_76) detected for PH showed significant interaction with the photoperiod (Figure 4D) in the Grinkan populations. We consider that this apparent effect of photoperiod on QTL_PH_7_76, is due to the fact that PH is proportional to the interaction NODE_N * NODE_L. Therefore, at chromosome seven, the signal is due to the interaction between a photoperiod sensitive component (NODE_N) and a photoperiod insensitive part (NODE_L). The separate analyses of NODE_N and NODE_L helped us to clarify the GxE effects influencing PH.

In terms of PED, QTL_PED_7_78 (qHT7.1) was one of the most environmentally sensitive QTL. This QTL was not photoperiod sensitive but covariables like SVP had a negative effect on the propensity to increase PED compared to the reference parent. This effect was consistent in the Grinkan (2013) population with four parents (BimbG, Hafijeka, Kalaban, V33/08) reducing their propensity to increase PED when SVP increased (Figure 4F). It is interesting to emphasize that drought related ECs (VPD, SVP) influenced both QTL_PH_7_76 and QTL_PED_7_78 with effects going in the same direction.

L. QTL effects on yield

Few QTL were detected for YIELD. However, some of the YIELD QTL colocalized with large or medium effect QTL for FLAG, which gave us the possibility to analyse the influence of FLAG on YIELD. A first example of collocating

FLAG and YIELD QTLs was positioned on chromosome six at 38 cM (QTL_FL_6_38) and 39 cM (QTL_YLD_6_39). Here, we observed that, compared to Grinkan, the allele of parents B35 and SC566-14 reduced the photoperiod sensitivity. Thus, at the first sowing date characterized by a longer photoperiod the plants carrying B35 or SC566-14 alleles had a reduced cycle. Such a reduction could prevent those plants from accumulating biomass that will be reallocated to the grain, which ultimately reduces the yield. Indeed, at QTL_YLD_6_39, we could observe a negative effect on yield for B35 and SC566-14 alleles. Such an indirect QTL effect on yield via the duration of the plant cycle was confirmed by an analysis of the YIELD values residual after regression on FLAG (Table S7) for the B35 allele. For the allele of SC566-14 however we would rather make the hypothesis of an independent effect on both traits due to a unique or two closely located QTL.

In Kenin-Keni 2012, the region of QTL_FL_3_78 contains QTL for FLAG (78 cM) and YIELD (74 cM) with a strong allelic effect of IS15401. Here, the allele of IS15401 increased the cycle length and decreased yield. The analysis of YIELD conditional on FLAG (Table S6) supports the hypothesis of an indirect QTL effect on YIELD through FLAG modulation. At that position, the IS15401 allele increased the cycle length and decreased the yield. The extended maturity given by IS15401 could make the plant falling outside the time when optimal conditions for the Malian agroecology happen. Such a negative effect on yield for varieties flowering outside the optimal time was already observed by Curtis (1968).

M. Expected QTL effect beyond the tested environments

Between 12 and 13.75 degrees of latitude, the Malian environment is characterized by a Southwest to Northeast gradient (Figure S7). The Southwest is cooler with lower temperature range, higher precipitation, and humidity while the Northeast is drier with higher temperature ranges and lower precipitations. A final extension of our results is the projection of QTL allelic effects having a significant interaction with one of the ECs in the Malian environment. For that we substituted the observed EC values from a grid of 60 points in the estimated allele sensitivity equation. This visualisation allowed us to map the expected effect of an allele given environmental conditions.

On Figures 3, we represented the expected behaviour of the BimbG and V33/08 alleles at QTL_PH_7_76 and QTL_PED_7_78, respectively. The BimbG allele was positively influenced by humidity which increases its effect on PH in the more humid southwest part and reduces it in the drier northeast regions (Figure 5B). Figure 5C illustrates the effect of VPD on the effect of V33/08 allele at QTL_PED_7_78 on PED extension. PED extension was reduced in the Northeast drier regions, while it was increased in the more humid southwest part of Mali. We can emphasize that those two alleles react similarly to the environmental gradient by increasing more the plant height in the southwest part.

M Expected QTL effect beyond the tested environments

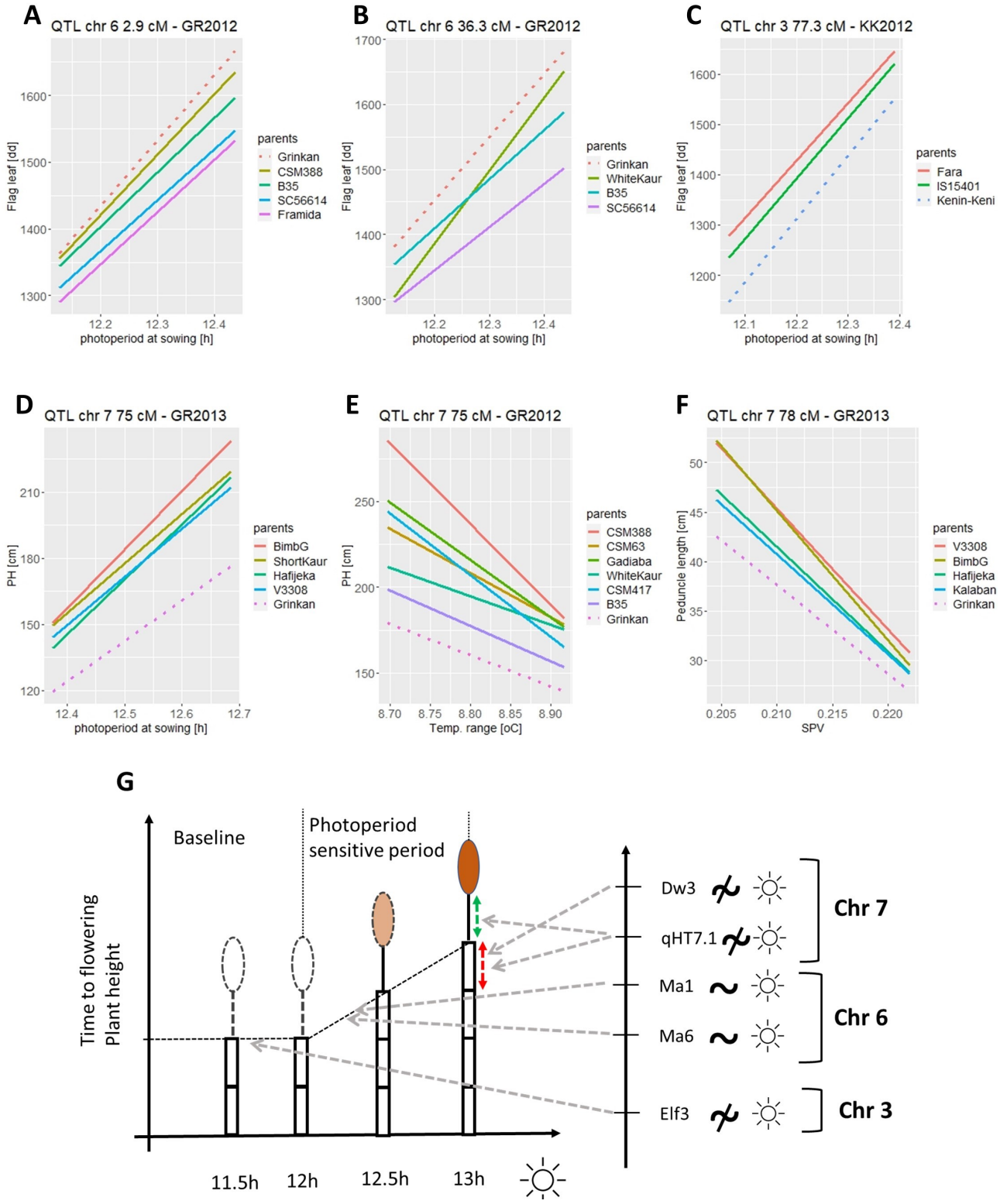

Figure 4. Sensitivity of QTL parental alleles effects to environmental covariables. The plain lines represent the regression between the value of parental allele effect in 4 environments and the value of an environment covariate in the same environments. A) QTL chr 6 (3 cM) in Grinkan 2012; B) QTL chr 6 (36.3 cM) in Grinkan 2012; and C) QTL chr 3 (77.3 cM) in Kenin-Keni 2012. D) Significant parental allelic effects on plant height given photoperiod at QTL chr 7 (76 cM) in Grinkan 2013. E) Significant parental allelic effects on plant height given VPD at QTL chr 7 (76 cM) in Grinkan 2013. F) Significant parental allelic effect on peduncle length given SVP at QTL chr 7 (78 cM) in Grinkan 2013. G) Photoperiodism illustration and summary of the candidate gene effects on plant cycle (time to flowering) and plant height represented as a function of photoperiod (day length [h]). Flowering time is a broken linear function with a constant baseline period and a slope describing the sensitivity to photoperiod. PH is decomposed into number of internodes, internode length, peduncle and panicle lengths.

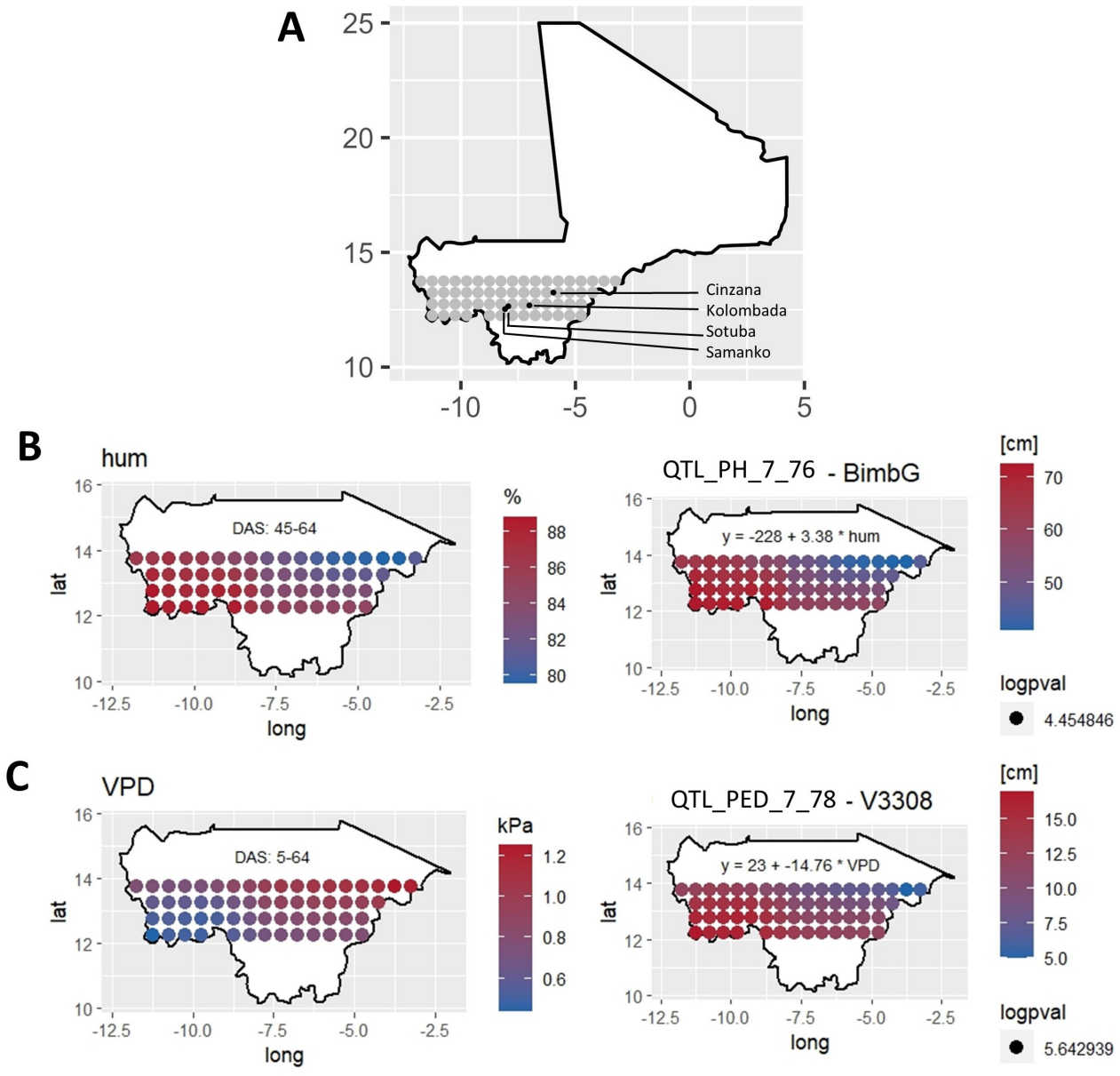

Figure 5. A) Map of Mali with testing locations and neighbouring areas of projection. B-C) Projections of QTL parental allelic effects for plant height and peduncle length in the environment of interest given sensitivity to humidity and VPD, respectively. The two QTL positions and parental allele were B) QTL_PH_7_76 BimbG x humidity; and C) QTL_PED_7_78 V33/08 x VPD. The projections were obtained by substituting observed environmental covariable in a grid of 60 points of the Malian environment in the QTL allele by environmental covariable sensitivity equation.

Discussion

N. Multi-reference BCNAM design properties

A major contribution of this work is the development of a new sorghum genetic resource taking the form of a multi-reference BCNAM design. Its usefulness can be evaluated given criteria like genetic diversity, mapping power and resolution, and potential for genetic gain, which will have different relative importance given usage of the population (research or breeding, Gage et al., 2020, Scott et al., 2020). In terms of breeding, the use of three recurrent parents instead of one like in almost all the (BC)NAM populations (e.g. Jordan et al., 2011, Bouchet et al., 2017, Mace et al., 2021) substantially increases the exploitable genetic diversity generated.

In terms of QTL detection, the usefulness of a design can be evaluated in terms of detection power, capacity to estimate and trace the QTL effect, and resolution. The power gain offered by NAM design compared to bi-parental populations (Li et al., 2011) or association panels (Bouchet et al., 2017) was already demonstrated. This should also be valid for our population. The most relevant advantage of a multi-reference BCNAM design is the possibility to test allelic contribution in several genetic backgrounds. Similarly to Christopher et al. (2021), we could show that parent allelic effect can be strongly modulated by the genetic background (Figure 3). More generally, in terms of QTL effect characterisation, MPPs like the (BC)NAM designs increase the allele frequencies and allow the user to trace back the allelic effect to a specific parent (Myles et al., 2009), which is fundamental to characterize the genetic effects and, if relevant, to mobilize it for breeding purposes. A second important contribution of this work is the capacity to link source of adaptation to specific parental allele. The main disadvantage of (BC)NAM design is the low resolution compared to designs involving further intercrossing like the multiparent advanced generation intercross (MAGIC, Klasen et al., 2012; Garin et al., 2021). Even if (BC)NAM design involves more recombination than bi-parental populations, recombination is still restricted within the cross which considerably extends the linkage disequilibrium decay. Even if the combination of our design to strategies like RapMap (Zhang et al. 2021) could improve the mapping resolution, populations like association panels could already be helpful to better distinguish between one or two QTL scenarios for PH at chromosome seven, for example.

In terms of genetic gain, Bernardo (2021) showed that populations like MAGIC do not have a significant advantage compared to multiple cross populations like the BCNAM. Moreover, populations involving further intercrossing like MAGIC request more resources. The (BC)NAM populations whose design is closer to the standard breeding crossing practice can also have an interest for genomic selection because of the genetic similarity it contains (Scott et al., 2020).

An important question specific to the multi-reference BCNAM design is the need to cross all donor parents to the recurrent parents (full factorial) or only a subset. Such a problem represents a trade-off between a) the advantage of estimating the QTL allelic effect in multiple genetic backgrounds, and b) an increase of the covered genetic diversity (more donor parents) or of the cross size by reducing their number, which increases the QTL detection power (Garin et al., 2021). Even if the quality of the QTL effect estimation is important we consider that it is conditioned on the covered genetic diversity and the QTL detection power. Therefore, performing only a selected number of crosses in a multi-reference (BC)NAM design could be an interesting strategy. More definitive answers to this question could be obtained by simulations.

O. Statistical methodology properties

At the moment of writing this article, no statistical package for MPP-ME QTL detection was publicly available, which made a direct comparison impossible. Nevertheless, we can compare our methodology to general properties from similar methods. The most important criterion is the precision of the QTL effect estimation, which influences the detection power and the interpretation of the effect. This criterion is often balanced with computational power requirements.

We used a mixed model with unstructured variance covariance (VCOV) structure to control for the genetic (co)variance. We could reduce the scanning time using approximation, but we estimated the final QTL effect with a full model. Considering QTL as fixed allowed us to use well established mixed model estimates and Wald test for significance. A small disadvantage of fixed QTL effect is the need to interpret the effect with respect to a reference. The use of a random QTL effect like in Li et al. (2022) with parental effect expressed as deviation from zero could facilitate the QTL effect comparison but it creates other challenges for significance estimation and computational speed. The procedure from De Walsche et al. (2022) proposes to perform MPP-ME QTL detection as a meta-analysis of single environment analysis. Such an approach is very fast, but we expect the joint multi-environment analysis to be more precise concerning the QTL effect estimation because it jointly accounts for multiple sources of variations (Malosetti

et al. 2013).

The main innovation of our methodology was the extension with envirotyping data like the ones generated by Nasapower. The benefit of extending the genetic models with environmental covariates to increase their prediction ability was already demonstrated (e.g. Westhues et al. 2022). This opens the door to dynamic predictions beyond the tested environments that should be used with caution because the estimated sensitivity equations are potentially strongly influenced by the tested environments. The possibility to increase the number and the representativity of the testing sites should improve the model prediction ability.

P. Developing climate-smart varieties

An important contribution of this study is to demonstrate the connection between maturity and plant height at the molecular level via large effects QTLs and underlying genes showing various degrees of photoperiodism (Figure 4G). This understanding could support the development of climate-smart varieties in terms of maturity and biomass accumulation.

The expected rise in the variability and intensity of the African climate in terms of temperature, drought and flood events should affect flowering time (WMO 2022). To develop varieties with a wide geographical adaptation, sorghum breeding programs have mainly selected early flowering and photoperiod insensitive genotypes. This approach failed to produce efficient varieties because, in the sub-Saharan African context, photoperiod sensitivity is the main adaptation trait to climate variability (Sultan et al., 2013). Photoperiod sensitivity ensures the synchronization of flowering with the probable end of the rainy season independently of the sowing date (Kouressy et al., 2008). As we could see, at least two QTL regions influencing the cycle length might have an indirect effect on yield by synchronizing or desynchronizing the plant with the optimal flowering time.

Contrary to Mace et al. (2013) who strongly constrained the maturity of their population genotypes, we could identify QTL with large effects on flag leaf appearance. Those QTL could be used in breeding programs. The QTLxEC analysis revealed that the parental alleles of QTL_3_FL_78 (Elf3) and QTL_FL_9_105 (SbFL9.1) were mostly insensitive to photoperiod. Those QTL mostly affect the flowering baseline duration (Guitton et al., 2018) while the QTL on chromosome six (QTL_FL_6_3 and QTL_FL_6_38) linked to the Ma6 and Ma1 regions influenced both the baseline flowering duration and the photoperiod sensitivity. The photoperiod sensitive nature of the Ma6 was also identified by Takai et al. (2012). The availability of different effects allows the development of alternative breeding strategies: a) varying the duration of the cycle without affecting the photoperiod sensitivity (e.g. QTL_FL_3_78 CSM417: -80 dd); b) influencing only the photoperiod sensitivity (e.g. QTL_FL_6_3 CSM388 : -62 dd/h), or c) influencing both the baseline duration and the photoperiod sensitivity (e.g. QTL_FL_6_38 White Kaura: -49 dd and +47 dd/h).

We could also gain knowledge about important genetic regions affecting plant height. Plant height is connected to plant cycle via the Ma6, Ma1, and Elf3 genes that affect both flag leaf appearance and the number of internodes (Figure 4G). The genetic association between FLAG and NODE_N makes sense because the internode organogenesis is a function of the plant cycle (Takai et al., 2012). Given sufficient nutrients, longer maturity allows the plant to accumulate more internodes.

The other important genetic determinants of plant height were located on chromosome seven with very strong effects on the length of the internode and on the peduncle length. Our data support the results from Li et al. (2015) concerning the existence of two distinct genes (qHT7.1 and Dw3) because the QTL effects of chromosome seven were detected at different positions (around 75 cM and 100 cM) in the different populations. The phenotypic effects of those positions was also consistent with Li et al. (2015) observations because the 75 cM position influenced both the internode and the peduncle lengths while the 100 cM position only influenced internode length.

The different genes controlling plant height could also be mobilized for different breeding strategies: a) vary plant height via the internode length independently of the environment (e.g. QTL_NL_7_76 IS23540: +3.1 cm); b) vary plant height via the number of internodes conditionally on photoperiod (e.g. QTL_NN_6_2 SC566-14 -1.1 n +22.7 n/h) or unconditionally (e.g. QTL_NN_3_78 Sangatigui + 1.5 n). Those QTL could help to develop dual-purpose varieties given a parallel improvement of the fodder quality.

The environmental sensitivity of the peduncle length could also help to design climate-smart varieties with resistance to grain mold and pest attack on the panicle given local conditions. Indeed, on Figure 5C we showed that the allele of V33/08 was sensitive to VPD (-15 cm/KPa). V33/08 allele increased more the peduncle length in the more humid

southwest region than in the drier northeast zones. Since peduncle length is one of the traits that can reduce grain mold and pest attack by avoiding a too close contact between the panicle and the flag leaf, we could use the climate dependent PED sensitivity of V33/08 to improve cultivar resistance. Those examples illustrate the strong application potential resulting from our design and methodology.

Material and Methods

Q. Plant material

The WCA-BCNAM is composed of three BCNAM populations produced after the crossing of the Grinkan, Kenin-Keni, and Lata3 recurrent parents with 24 donor parents representative of the Western African sorghum diversity with lines from Central and East Africa (Table 2, Methods S5: list of parents name synonyms). The whole population contains 3901 BC1F4 genotypes from 41 crosses (GR: 2109 genotypes, 19 crosses; KK: 896 genotypes 10 crosses; Lata: 896 genotypes, 12 crosses, Figure S1). The Lata3 population crosses involved male sterile sister lines of Lata3 to produce BC1 generation, while the BC1 generations of Grinkan and Kenin-Keni crosses were produced using manual emasculation. The recurrent parents are elite lines selected in Mali through farmer variety testing. Grinkan was developed through pedigree breeding methods. Kenin-Keni was derived from a directed recurrent selection population involving local parents of different botanical types (Leroy et al., 2014). Lata3 was selected from a random mating population of Guinea parents (Diallo et al., 2019). The recurrent parents were chosen for their productivity, their adaptation to soil and climate, as well as their resistance to major biotic and abiotic stresses. The recurrent lines also have weaknesses like poor grain quality and mold susceptibility (Grinkan), suboptimal glume opening and/or susceptibility to Striga (Lata3), and low productivity and yield stability (Kenin-Keni).

The 24 donor parents cover diverse racial (Guinea, Caudatum, Durra) and geographical origins (Table 2). They are characterized by key adaptive traits like height, maturity, or photoperiod sensitivity (Kp3). Those parents were also selected for presenting more positive specific traits like tolerance to Striga, to soil phosphorus deficiency and/or to drought, good grain quality, or panicle desirability that could increase farmer acceptance. Several donor parents were tested in multiple genetic backgrounds. Fara-Fara, IS15401, and IS23540 were crossed with the three recurrent parents. Ten donor parents were tested in two genetic backgrounds. During the development of the populations, a moderate selection pressure was applied at BC1F2 generation against too early flowering and too high genotypes.

Table 2. WCA-BCNAM parents with racial classification, origin, relative height (PH), relative maturity, reaction to photoperiod sensitivity (Kp3), and specific advantages. The last three columns specify the crossing scheme with the year when the cross was phenotyped (2012 and/or 2013)

Parent	Race	Origin	PH	Mat	Kp3	Specific advantage	Reference	GR	KK	Lata
Grinkan	G/C	Mali	av	av	av	Elite line	Guitton et al. (2018)			13
Kenin-Keni	G/C	Mali	av	av	av	Elite Line	Leroy et al. (2014)			
Lata3	G/C	Mali	+	av	av	Elite Line	Diallo et al. (2019)			
Fara-Fara	G	Nigeria	+	+	+	Diversity	Andrews (1973)	12	12	13
E36-1	C	Ethiopia	-	av	-	Drought tolerance	Mahalakshmi et al. (2002)	12/13	12	
IS15401	G	Cameroon	+	+	+	Striga resistance	FAO (2008)	12	12	13
IS23540	C	Ethiopia	-	av	-	Sweet stem	FAO (2023)	12	13	13
B35	D/C	Ethiopia	-	-	-	Drought tolerance	Rama Reddy et al. (2014)	12	12	
Konotene	D	Mali	+	+	-	Grain weight	Clément et al. (1980)	12		
SC566-14	C	Nigeria	-	-	-	Al tolerance	Magalhaes et al. (2004)	12		13
Framida	C	S. Africa	-	+	-	Striga resistance	Haussmann et al. (2001)	12		13
CSM417	G	Mali	+	+	+	Grain quality	Clément et al. (1980)	12	12/13	
CSM63	G	Mali	av	-	-	Precocity	Chantereau et al. (1998)	12		
CSM388	G	Mali	+	+	+	Grain quality	Folliard et al. (2004)	12/13		
Gadiaba Dié	D	Mali	+	+	+	Grain weight	Clément et al. (1980)	12		
W. Kaura	D/C	Nigeria	-	+	+	Diversity	Goma et al. (2012)	12		
V33/08	G/C	Mali	av	+	av	Grain quality	Soumaré et al. (2008)	13		
Kalaban	C	Mali	-	av	-	Productivity	FAO (2008)	13	13	
Malisor 84-7	C	Mali	-	-	+	Head bug resistance	Ratnadass et al. (2002)	13	13	
BimbG	G	Guinea	+	+	+	Grain quality	Sagnard et al. (2013)	13	13	
Hafijeka	G	Gambia	+	+	+	Grain quality	Folkertsma et al. (2005)	13		13
S. Kaura	D/C	Nigeria	+	+	+	Diversity	Kassam et al. (1975)	13		13
Sangatigui	G	Mali	av	av	av	Diversity	CEDEAO-UEMOA-CILSS (2016)		13	
DouaG	G	Mali	+	+	+	Low-P adaptation	Kante et al. (2017)			13
Gnossiconi	G	Burkina F.	av	av	av	Yield stability	vom Brocke et al. (2014)			13
Ngolofing	G	Mali	+	av	+	Grain quality	Clément et al. (1980)			13
Sambalma	G/C	Nigeria	+	+	+	Al tolerance	Kante et al. (2019)			13

Q.1. Genotypic data. The 3901 offspring and their parents were genotyped using genotype by sequencing (GBS, Elshire et al., 2011) with 384-plex libraries on an Illumina HiSeq 2000 sequencer. The offspring were genotyped at generation BC1F3. The sequence data were analysed running the reference genome-based TASSEL GBS pipeline (Glaubitz et al., 2014). Unique tags (3'844'911) were aligned on the sorghum reference genome v2.1 (Paterson et al., 2009). After the filtering of raw genotype data for minor allele frequencies (MAF < 0.05) and

single marker missing data (<0.9), 51'545 segregating SNPs were identified between the parents with between 11'856 to 26'128 SNPs segregating in the individual crosses. Missing values in the parents were imputed using Beagle (Browning et al., 2018). Missing values in the offspring genotypes were imputed using FSFHap (Bradbury et al., 2007). We determined a unique genetic consensus map (Table S1) by projecting the 51'545 markers physical distance on a high-quality genetic consensus map (Guindo et al., 2019) using the R package ziplinR (https://github.com/jframi/ziplinR).

R. Phenotypic data

The Grinkan and Kenin-Keni populations were partly phenotyped in 2012 and partly in 2013 (Table 2, Figure S1). We considered each population within a year as a separate population (GR2012, GR2013, KK2012, KK2013). Each population was phenotyped at a combination of two locations (Sotuba and Cinzana, Figure 5A) and two sowing dates (Sowing 1: end of June, Sowing 2: three to four weeks later, Table S8), which gave a total of four environments (SB1, SB2, CZ1, CZ2; Figure S8). The Sotuba environment is characterized by around 900 mm/year of precipitation and lower temperatures while the Cinzana environment is characterized by lower precipitation (600-700 mm/year) and warmer temperature. In both environments, the second sowing date had a lower level of precipitation and humidity and higher temperatures (Figure S7, Table S9). In each environment, the progenies of Grinkan and Kenin-Keni populations were laid out as augmented design (Kempton, 1984) with the three recurrent parents used as checks. The Lata3 population was entirely phenotyped in 2013 in three environments defined by two levels of phosphorus fertilization (Low-P and high-P) at the Samanko station and standard conditions at Kolombada station (Figure 5A). In each environment, the genotypes were laid out as an alpha-lattice design (Kempton, 1984) with two replications (Diallo et al., 2019).

We measured eight traits listed with crop ontology (CO) code. Flag leaf appearance (FLAG, CO_324:0000631) was the number of days after sowing when half of the plot had their ligulated flag leaves visible. For the QTL analysis FLAG data were converted into degree day. Plant height (PH, CO_324:0000623) was the distance in cm between the soil and the panicle top. The number of internodes (NODE_N, CO_324:0000605) was the number of nodes on the main stem minus one and the average length of the internodes (NODE_L) the main stem length divided by NODE_N. The peduncle length (PED, CO_324:0000622) was the distance in cm between the final node and the panicle bottom. The panicle length (PAN, CO_324:0000620) was the distance in cm from the end of the peduncle to the panicle top. GWGH (CO_324:0000424) was the weight in grams of 1000 grains. Finally, YIELD (CO_324:0000403) was measured in kg/ha at the plot level. All traits except FLAG were measured at harvest. Some traits like GWGH and PAN were not measured in all environments (Table S10).

S. environmental covariables - EC

We complemented the data by 15 daily observed ECs (Table S11) to evaluate the environmental influence on plant adaptation of the Grinkan and Kenin-Keni populations. With four environments (SB1, SB2, CZ1, CZ2) we could observe environmental gradients, which was not possible for Lata3 data because the low-P and high-P trials were performed at the same time and location which reduce the number of environments to two. The ECs were divided in three categories. The atmospheric ECs contained: cumulated rain [mm], humidity [%], vapour pressure deficit (VPD - kPa), slope of saturation VP curve (SVP – kPa/d), potential evapotranspiration (ETP – mm/day), atmospheric water deficit (PETP – mm/day). The temperature ECs covered: maximum and minimum temperatures [d], temperature range [d], the effect of temperature on radiation use efficiency (FRUE; 0-1), and cumulated degree day (DD). The radiation ECs were the cumulated hours of sun (hSun), the photoperiod (day length) [h], and the solar radiation [MJ/m^2/day]. We also included the photothermal time as the product between photoperiod and DD. A principal component analysis of environments based on the EC value showed a good coverage of the EC space by the four Sotuba and Cinzana environments (Figures S8).

The ECs values came from weather stations at the locations complemented by Nasapower satellite observations (Spark 2018) and transformation using the R package EnvRtype (Costa-Neto et al., 2021). We projected the genetic effects beyond the tested environments, using compiled environmental data from various sources extended with EnvRtype for a grid of 60 points between 12.25 and 13.75 degrees of latitude and -12.5 and -2 of longitude.

Phenotypic data analysis

We estimated the genotypic variance component and broad-sense heritability (h^2) using the following mixed model

$$y_{icjkl} = env_j + rep(env)_{jk} + block(rep, env)_{jkl} + cr_c + geno(cr)_{ic} + geno * env(cr)_{ijc} + e_{icjklm} \quad \textbf{(1)}$$

Where, y_{icjkl} = plot phenotypic observation of the ith genotype from cross c in environment j, replication k, and block l; env_j = environment effect; $rep(env)_{jk}$ = replication effect within-environment (only for Lata sub-population); $block(rep, env)_{jkl}$ = block effect within replication and environment; cr_c = cross effect; $geno(cr)_{ic}$ = genotype effect conditional on cross; $geno * env(cr)_{ijc}$ = GxE effect conditional on cross. The underlined terms were considered as random, the other ones as fixed.

The genotype, GxE and error terms were normally distributed with cross-specific variance ($\sigma^2_{G(cr)}$, $\sigma^2_{GE(cr)}$, $\sigma^2_{e(cr)}$). We estimated the model components using Genstat 18 (VSN International 2022). Given those, we calculated the broad sense h^2 using the formula of Hung et al. (2012):

$$\frac{\sigma^2_{G(cr)}}{\sigma^2_{G(cr)} + \frac{\sigma^2_{GE(cr)}}{N_{env}} + \frac{\sigma^2_{e(cr)}}{N_{env} * N_{rep}}} \quad \textbf{(2)}$$

Where, N_{env} is the number of environments and N_{rep} the number of replications. For the multi-environment QTL analysis, we calculated within-environment best linear unbiased estimates by removing the environment and cross term from model 1 and by considering the genotype term as fixed. We used the plot field coordinates to model the spatial variation using a 2D P-spline (SpATS model, Rodriguez-Alvarez et al., 2018).
For each configuration of population (GR2012, GR2013, KK2012, KK2013) by trait, we selected the five most influential ECs and time window for which the EC effect were maximal to be introduced in the QTLxEC analysis later using the method developed by Li et al. (2018) (Methods S2).

T. MPP QTLxEC modeling

To detect QTL, we extended the linear mixed model 3 proposed by Garin et al. (2020):

$$y_{icj} = env_j + cross_{cj} + x_{ip} * \beta_{pj} + GE_{ijc} + e_{icj} \quad \textbf{(3)}$$

Where, y_{icj} = BLUE of genotype i from cross c in environment j. env_j = environment effect and $cross_{cj}$ = cross within-environment effect. x_{ip} is the number of alleles from parent p carried by genotype i at the QTL position and β_{pj} represents the QTL allelic effect of parent p in environment j. We assumed that each parent carried a different allele at the QTL position (Garin et al., 2017). The GE_{icj} term is the residual genetic variation and e_{icj} the plot error term that cannot be estimated separately due to the unreplicated nature of the BLUEs. To model the ($GE_{icj} + e_{icj}$) term we extended the model from Garin et al. (2020) using an unstructured variance covariance structure (Boer et al., 2007). The unstructured model estimates one (co)variance ($\sigma^2_{(j,j')}$) for each pair of environments.

We detected QTL by performing a simple interval mapping followed by a composite interval mapping. The final list of QTL contained the positions significant at a -log10(p-val) detection threshold accounting for multiple testing (Li and Ji 2005). For further details see Methods S3. We grouped QTL detected for the same trait but in different populations into unique QTL positions if those positions were distant by less than 10 cMs. We searched for candidate genes using the sorghum QTL atlas (Mace et al., 2019).

We extended the QTL analysis by fitting a QTL by EC (QTLxEC) model for the QTL that showed a larger significance when modelled with a QTLxE term compared to a QTL main effect term. For those QTL, we extended the $x_{ip} * \beta_{pj}$ term from model 2 to $x_{ip} * (\beta_p + EC_e * S_p + l_{pe})$ where β_p is the main parental allelic effect across environments, EC_e is the EC value (e.g. humidity) in each environment, S_p is the parental allele sensitivity to EC_e change and l_{pe} the residual effect. We estimated the sensitivity to the five most influential ECs previously determined ($Q_{eff} = \hat{\beta}_p + EC_e * \hat{S}_p$). We could estimate the expected allelic effect beyond tested environments by substituting in the QTL sensitivity equation the average EC_e values over the next seasons (2014-2020) for the grid of 60 points. For the QTL detection, the effect and significance were estimated using and approximate Wald test similar to the generalized least square strategy implemented in Kruijer et al. (2015; Methods S4) while for the final QTL effects model we used an exact restricted maximum likelihood solution. The methodology was added to the mppR package (Garin et al., 2023).

U. Authors contributions

Data collection: CD, MLT, KT, MV, BG, JFR, KD, AD, MK, WL, IS, MS, NT
Statistical methodology, software, and application: VG
Data analysis: VG, CD, MLT, KT, NT, JFR, MV, DP, JF
Manuscript writing, edition: VG, MLT, CD, KT, DP, MV, JK, NT, JFR

Project coordination: JFR, NT, EW, MV, FR, BN, AT, JK, VG

V. Acknowledgements

The authors thank Madina Diancoumba and Jan Jarolímek for providing the part of the environmental data that were used to realize the projection in the Malian environment.

W. Funding

This work was supported by a grant from the Generation Challenge Programme (Project Numbers G7010.05.01 and G7010.05.02). The work of Vincent Garin was supported by a grant from the Swiss National Science Foundation (Postoc.Mobility grant no: P500PB_203030). Dr Kholova contribution was financed by an internal grant agency of the Faculty of Economics and Management from the Czech University of Life Sciences Prague (Grant Life Sciences 4.0 Plus no. 2022B0006)

X. Conflicts of interest

The authors declare no conflicts of interest.

Y. Data availability statement

The genotypic and phenotypic data are available here (...) [the link to the data repository will be added on acceptance of the manuscript]. The scripts to reproduce the results are available here: https://github.com/vincentgarin/sorghum_BCNAM_analysis. The results were gathered into an interactive database available here https://github.com/vincentgarin/SQE.

Bibliography

Andrews, D. J. (1973). Effects of date of sowing on photosensitive Nigerian Sorghums. Exp. Agric 9: 337-46. https://doi.org/10.1017/S0014479700010139.

Bauer, E., Falque, M., Walter, H., Bauland, C., Camisan, C., Campo, L., ... and Schön, C. C. (2013). Intraspecific variation of recombination rate in maize. Genome biology, 14(9), 1-17.

Bernardo, R. (2016). Bandwagons I, too, have known. Theoretical and applied genetics, 129(12), 2323-2332.

Bernardo, R. (2021). Multiparental populations in line development: Genetic gain, diversity, and practical limitations. Crop Science, 61(6), 4139-4150.

Blum, A., Golan, G., Mayer, J.,Sinmena, B. (1997). The effect of dwarfing genes on sorghum grain filling from remobilized stem reserves, under stress. Field Crops Research, 52(1-2), 43-54.

Bouchet, S., Olatoye, M. O., Marla, S. R., Perumal, R., Tesso, T., Yu, J., ... and Morris, G. P. (2017). Increased power to dissect adaptive traits in global sorghum diversity using a nested association mapping population. Genetics, 206(2), 573-585.

Bradbury, P. J., Zhang, Z., Kroon, D. E., Casstevens, T. M., Ramdoss, Y., and Buckler, E. S. (2007). TASSEL: software for association mapping of complex traits in diverse samples. Bioinformatics, 23(19), 2633-2635. Broman, K. W., Wu, H., Sen, Ś., and Churchill, G. A. (2003). R/qtl: QTL mapping in experimental crosses. bioinformatics, 19(7), 889-890.

Browning, B. L., Zhou, Y., and Browning, S. R. (2018). A one-penny imputed genome from next-generation reference panels. The American Journal of Human Genetics, 103(3), 338-348.

Brown, P. J., Rooney, W. L., Franks, C., and Kresovich, S. (2008). Efficient mapping of plant height quantitative trait loci in a sorghum association population with introgressed dwarfing genes. Genetics, 180(1), 629-637.

Cavanagh, C., Morell, M., Mackay, I., and Powell, W. (2008). From mutations to MAGIC: resources for gene discovery, validation and delivery in crop plants. Current opinion in plant biology, 11(2), 215-221.

CEDEAO-UEMOA-CILSS (2016). Catalogue Régional des Espèces et Variétés Végétales CEDEAO-UEMOA-CILSS.

Chantereau J., Hamada M. AG., Bretaudeau A., and Tembely S.O. (1998). Etude de nouvelles variétés de sorgho en milieu paysan dans la zone cotonnière Cmdt au Mali (1995 - 1996). Actes de l'atelier ICRISAT - CIRAD

Chantereau, J., Trouche, G., Rami, J. F., Deu, M., Barro, C., and Grivet, L. (2001). RFLP mapping of QTLs for photoperiod response in tropical sorghum. Euphytica, 120(2), 183-194.

Christopher, M., Paccapelo, V., Kelly, A., Macdonald, B., Hickey, L., Richard, C., Verbyla, A., Chenu, K., Borrell, A., Amin, A., Christopher, J. (2021). QTL identified for stay-green in a multi-reference nested association mapping population of wheat exhibit context dependent expression and parent-specific alleles. Field Crops Res. 270, 108181. https://doi.org/10.1016/j.fcr.2021.108181

Clément, J. C., and J. M. Leblanc (1980). Prospection des Mils pénicillaires, Sorghos et Graminées mineures en Afrique de l'Ouest. Campagne 1978. République du Mali. IBPGR-ORSTOM.

Cobb, J. N., Biswas, P. S., and Platten, J. D. (2019). Back to the future: revisiting MAS as a tool for modern plant breeding. Theoretical and Applied Genetics, 132(3), 647-667.

Costa-Neto, G., Galli, G., Carvalho, H. F., Crossa, J., and Fritsche-Neto, R. (2021). EnvRtype: a software to interplay enviromics and quantitative genomics in agriculture. G3, 11(4), jkab040.

Curtis, D. L. (1968). The relation between the date of heading of Nigerian sorghums and the duration of the growing season. Journal of Applied Ecology, 215-226.

De Walsche, A., Mezmouk, S., Charcosset, A., Mary-Huard, T. (2022). Meta-analysis of GWAS for studying GxE interactions. 18th Eucarpia Biometrics in Plant Breeding Conference.

Diakite, O. S. (2018). Breeding Sorghum [Sorghum Bicolor (L.) Moench] for High Quality Stover for Niger. Doctoral dissertation, University of Ghana.

Diallo, C., Rattunde, H. F. W., Gracen, V., Touré, A., Nebié, B., Leiser, W., ... and Weltzien, E. (2019). Genetic diversification and selection strategies for improving Sorghum grain yield under phosphorous-deficient conditions in West Africa. Agronomy, 9(11), 742.

Diouf, I., Derivot, L., Koussevitzky, S., Carretero, Y., Bitton, F., Moreau, L., and Causse, M. (2020). Genetic basis of phenotypic plasticity and genotype×environment interactions in a multi-parental tomato population. Journal of experimental botany, 71(18), 5365-5376.

Elshire, R. J., Glaubitz, J. C., Sun, Q., Poland, J. A., Kawamoto, K., Buckler, E. S., and Mitchell, S. E. (2011). A robust, simple genotyping-by-sequencing (GBS) approach for high diversity species. PloS one, 6(5), e19379.

FAO (2008). Catalogue ouest africain des espèces et variétés végétales. Rome. http://www.insah.org/doc/pdf/catalogue_french.pdf.

FAO (2023). Global information system. Rome. https://doi.org/10.18730/NMYBY

Folkertsma, R. T., H. F. W. Rattunde, S. Chandra, G. S. Raju, et C. T. Hash. (2005). The pattern of genetic diversity of Guinea-race Sorghum bicolor (L.) Moench landraces as revealed with SSR markers. Theoretical and Applied Genetics 111 (3): 399-409.

Folliard, A, Traoré P.C.S, Vaksmann, M, and Kouressy, M (2004). Modeling of Sorghum Response to Photoperiod: A Threshold–Hyperbolic Approach. Field Crops Research 89 (1): 59-70. https://doi.org/10.1016/j.fcr.2004.01.006.

Fragoso, C. A., Moreno, M., Wang, Z., Heffelfinger, C., Arbelaez, L. J., Aguirre, J. A., ... and Lorieux, M. (2017). Genetic architecture of a rice nested association mapping population. G3: Genes, Genomes, Genetics, 7(6), 1913-1926.

Gage, J. L., Monier, B., Giri, A., and Buckler, E. S. (2020). Ten years of the maize nested association mapping population: impact, limitations, and future directions. The Plant Cell, 32(7), 2083-2093.

Garin, V., Wimmer, V., Mezmouk, S., Malosetti, M., and Van Eeuwijk, F. A. (2017). How do the type of QTL effect and the form of the residual term influence QTL detection in multi-parent populations? A case study in the maize EU-NAM population. Theoretical and Applied Genetics, 130(8), 1753-1764.

Garin V., Wimmer V., Borchardt D., Van Eeuwijk F. A., Malosetti M. (2018) mppR: multi-parent population QTL analysis. https://CRAN.R-project.org/package=mppR. R package version 1.3.0

Garin, V., Malosetti, M., and Van Eeuwijk, F. A. (2020). Multi-parent multi-environment QTL analysis: an illustration with the EU-NAM Flint population. Theoretical and Applied Genetics, 133(9), 2627-2638.

Garin, V., Wimmer, V., Borchardt, D., Malosetti, M., and Van Eeuwijk, F. A. (2021). The influence of QTL allelic diversity on QTL detection in multi-parent populations: a simulation study in sugar beet. BMC genomic data, 22(1), 1-12.

Giraud, H., Lehermeier, C., Bauer, E., Falque, M., Segura, V., Bauland, C., ... and Moreau, L. (2014). Linkage disequilibrium with linkage analysis of multiline crosses reveals different multiallelic QTL for hybrid performance in the flint and dent heterotic groups of maize. Genetics, 198(4), 1717-1734.

Glaubitz, J. C., Casstevens, T. M., Lu, F., Harriman, J., Elshire, R. J., Sun, Q., and Buckler, E. S. (2014). TASSEL-GBS: a high capacity genotyping by sequencing analysis pipeline. PloS one, 9(2), e90346.

Goma, L, H Man, B Tanimu, L Aliyu, L . Garba, et H. J Jantar (2012). Growth parameters of sorghum (Sorghum

bicolor (L.) Moench) varieties as influenced by planting pattern and nitrogen rates. Agricultural society of Nigeria. 609-18.

Guindo, D., Teme, N., Vaksmann, M., Doumbia, M., Vilmus, I., Guitton, B., ... and Rami, J. F. (2019). Quantitative trait loci for sorghum grain morphology and quality traits: Toward breeding for a traditional food preparation of West-Africa. Journal of Cereal Science, 85, 256-272.

Guitton, B., Théra, K., Tékété, M. L., Pot, D., Kouressy, M., Témé, N., Rami, J.-F., and Vaksmann, M. (2018). Integrating genetic analysis and crop modeling: A major QTL can finely adjust photoperiod-sensitive sorghum flowering. Field Crops Research, 221, 7-18.

Haussmann, B. I. G., D. E. Hess, B. V. S. Reddy, S. Z. Mukuru, M. Kayentao, H. G. Welz, et H. H. Geiger. (2001). Pattern analysis of genotype x environment interaction for striga resistance and grain yield in African sorghum trials. Euphytica 122 (2): 297-308.

Hopkins, W. G. (2009). Introduction to Plant Physiology. Wiley

Hung, H. Y., Browne, C., Guill, K., Coles, N., Eller, M., Garcia, A., ... and Holland, J. B. (2012). The relationship between parental genetic or phenotypic divergence and progeny variation in the maize nested association mapping population. Heredity, 108(5), 490-499.

Kante, M., Rattunde, H. F. W., Leiser, W. L., Nebié, B., Diallo, B., Diallo, A., et al. (2017). Can Tall Guinea-Race Sorghum Hybrids Deliver Yield Advantage to Smallholder Farmers in West and Central Africa? Crop Science, 57(2), 833-842. doi:10.2135/cropsci2016.09.0765

Kante, Moctar, Fred Rattunde, Baloua Nébié, Ibrahima Sissoko, Bocar Diallo, Abdoulaye Diallo, Abocar Touré, Eva Weltzien, Bettina I. G. Haussmann, et Willmar L. Leiser. (2019). Sorghum Hybrids for Low-Input Farming Systems in West Africa: Quantitative Genetic Parameters to Guide Hybrid Breeding. Crop Science 59 (6): 2544-61. https://doi.org/10.2135/cropsci2019.03.0172.

Kassam, A. H., et D. J. Andrews. 1975. « Effects of sowing date on growth, development and yield of photosensitive sorghum at Samaru, Northern Nigeria ». Experimental Agriculture 11 (3): 227-40. Kempton, R. A. (1984). The design and analysis of unreplicated field trials. Vorträge für Pflanzenzüchtung (Germany).

Kidane, Y. G., Gesesse, C. A., Hailemariam, B. N., Desta, E. A., Mengistu, D. K., Fadda, C., ... and Dell'Acqua, M. (2019). A large nested association mapping population for breeding and quantitative trait locus mapping in Ethiopian durum wheat. Plant biotechnology journal, 17(7), 1380-1393.

Klasen, J. R., Piepho, H. P., and Stich, B. (2012). QTL detection power of multi-parental RIL populations in Arabidopsis thaliana. Heredity, 108(6), 626-632.

Kouressy, M., Dingkuhn, M., Vaksmann, M., and Heinemann, A. B. (2008). Adaptation to diverse semi-arid environments of sorghum genotypes having different plant type and sensitivity to photoperiod. Agricultural and Forest Meteorology, 148(3), 357-371.

Kruijer, W., Boer, M. P., Malosetti, M., Flood, P. J., Engel, B., Kooke, R., ... and van Eeuwijk, F. A. (2015). Marker-based estimation of heritability in immortal populations. Genetics, 199(2), 379-398.

Leroy, T., Coumaré, O., Kouressy, M., Trouche, G., Sidibé, A., Sissoko, S., et al. (2014). Inscription d'une variété de sorgho obtenue par sélection participative au Mali dans des projets multiacteurs. Agronomie, Environnement et Sociétés, 4(2), 143-152.

Li, J., and Ji, L. (2005). Adjusting multiple testing in multilocus analyses using the eigenvalues of a correlation matrix. Heredity, 95(3), 221-227.

Li, H., Bradbury, P., Ersoz, E., Buckler, E. S., and Wang, J. (2011). Joint QTL linkage mapping for multiple-cross mating design sharing one common parent. PloS one, 6(3), e17573.

Li, X., Li, X., Fridman, E., Tesso, T. T., and Yu, J. (2015). Dissecting repulsion linkage in the dwarfing gene Dw3 region for sorghum plant height provides insights into heterosis. Proceedings of the National Academy of Sciences, 112(38), 11823-11828.

Li, X., Guo, T., Mu, Q., Li, X., and Yu, J. (2018). Genomic and environmental determinants and their interplay underlying phenotypic plasticity. Proceedings of the National Academy of Sciences, 115(26), 6679-6684.

Li, W., Boer, M. P., Zheng, C., Joosen, R. V., and Van Eeuwijk, F. A. (2021). An IBD-based mixed model approach for QTL mapping in multiparental populations. Theoretical and Applied Genetics, 134(11), 3643-3660.

Li, W., Boer, M. P., van Rossum, B. J., Zheng, C., Joosen, R. V., and Van Eeuwijk, F. A. (2022). statgenMPP: an R package implementing an IBD-based mixed model approach for QTL mapping in a wide range of multi-parent populations. Bioinformatics, 38(22), 5134-5136.

Mace, E. S., Hunt, C. H., and Jordan, D. R. (2013). Supermodels: sorghum and maize provide mutual insight into the genetics of flowering time. Theoretical and applied genetics, 126(5), 1377-1395.

Mace, E. S., Cruickshank, A. W., Tao, Y., Hunt, C. H., and Jordan, D. R. (2021). A global resource for exploring and exploiting genetic variation in sorghum crop wild relatives. Crop Science, 61(1), 150-162.

Magalhaes, Jurandir V., David F. Garvin, Yihong Wang, Mark E. Sorrells, Patricia E. Klein, Robert E. Schaffert, Li Li, et Leon V. Kochian. (2004). Comparative Mapping of a Major Aluminum Tolerance Gene in Sorghum and Other Species in the Poaceae. Genetics 167 (4): 1905-14. https://doi.org/10.1534/genetics.103.023580.

Mahalakshmi, Viswanathan, et Francis R. Bidinger (2002). Evaluation of Stay-Green Sorghum Germplasm Lines at ICRISAT. Crop Science 42 (3): 965-74.

Malosetti, M., Ribaut, J. M., and Van Eeuwijk, F. A. (2013). The statistical analysis of multi-environment data: modeling genotype-by-environment interaction and its genetic basis. Frontiers in physiology, 4, 44.

McMullen, M. D., Kresovich, S., Villeda, H. S., Bradbury, P., Li, H., Sun, Q., ... and Buckler, E. S. (2009). Genetic properties of the maize nested association mapping population. Science, 325(5941), 737-740.

Multani, D. S., Briggs, S. P., Chamberlin, M. A., Blakeslee, J. J., Murphy, A. S., and Johal, G. S. (2003). Loss of an MDR transporter in compact stalks of maize br2 and sorghum dw3 mutants. Science, 302(5642), 81-84.

Murphy, R. L., Klein, R. R., Morishige, D. T., Brady, J. A., Rooney, W. L., Miller, F. R., ... and Mullet, J. E. (2011). Coincident light and clock regulation of pseudoresponse regulator protein 37 (PRR37) controls photoperiodic flowering in sorghum. Proceedings of the National Academy of Sciences, 108(39), 16469-16474.

Myles, S., Peiffer, J., Brown, P. J., Ersoz, E. S., Zhang, Z., Costich, D. E., and Buckler, E. S. (2009). Association mapping: critical considerations shift from genotyping to experimental design. The Plant Cell, 21(8), 2194-2202.

Paterson, A. H., Bowers, J. E., Bruggmann, R., Dubchak, I., Grimwood, J., Gundlach, H., ... and Rokhsar, D. S. (2009). The Sorghum bicolor genome and the diversification of grasses. Nature, 457(7229), 551-556.

Paccapelo, M.V., Kelly, A.M., Christopher, J.T. and Verbyla A.P. (2022) WGNAM: whole-genome nested association mapping. Theor Appl Genet . https://doi.org/10.1007/s00122-022-04107-x

Perrier, X., Jacquemoud-Collet, J.P. (2006). DARwin software (https://darwin.cirad.fr/)

Rama Reddy, Nagaraja, Madhusudhana Ragimasalawada, Murali Sabbavarapu, Seetharama Nadoor, et Jagannatha Patil (2014). Detection and validation of stay-green QTL in post-rainy sorghum involving widely adapted cultivar, M35-1 and a popular stay-green genotype B35. BMC Genomics 15 (1): 909.

Ratnadass, A., J. Chantereau, M. F. Coulibaly, et C. Cilas. (2002). Inheritance of Resistance to the Panicle-Feeding Bug Eurystylus Oldi and the Sorghum Midge Stenodiplosis Sorghicola in Sorghum. Euphytica 123 (1): 131-38. https://doi.org/10.1023/A:1014451103520.

Rodriguez-Alvarez, M.X, Boer, M.P., Van Eeuwijk, F.A., and Eilers, P.H.C. (2018). Correcting for spatial heterogeneity in plant breeding experiments with P-splines. Spatial Statistics, 23, 52 – 71. https://doi.org/10.1016/j.spasta.2017.10.003

Rooney, W. L., and Aydin, S. (1999). Genetic control of a photoperiod-sensitive response in Sorghum bicolor (L.) Moench. Crop science, 39(2), 397-400.

Sagnard F, Deu M, Leblois R, Toure L, Diakite M, Calatayud C, Vaksmann M, Bouchet S, Malle Y, Togola S, Traore PCS. 2011. Genetic diversity, structure, geneflow and evolutionary relationships within the sorghum wild-weedy-crop complex in a western African region. Theoretical and Applied Genetics 123: 1231-1246

Scott, M. F., Ladejobi, O., Amer, S., Bentley, A. R., Biernaskie, J., Boden, S. A., ... and Mott, R. (2020). Multi-parent populations in crops: a toolbox integrating genomics and genetic mapping with breeding. Heredity, 125(6), 396-416.

Soumaré, Mamy, Mamoutou Kouressy, Michel Vaksmann, Ibrahim Maikano, Didier Bazile, Pierre Sibiry Traoré, Seydou Traoré, et al. (2008) Prévision de l'aire de diffusion des sorghos photopériodiques en Afrique de l'ouest. Cahiers Agricultures 17 (2): 160-64.

Sparks, A. H. (2018). nasapower: a NASA POWER global meteorology, surface solar energy and climatology data client for R. Journal of Open Source Software, 3(30), 1035.

Sultan, B., Roudier, P., Quirion, P., Alhassane, A., Muller, B., Dingkuhn, M., ... and Baron, C. (2013). Assessing climate change impacts on sorghum and millet yields in the Sudanian and Sahelian savannas of West Africa. Environmental Research Letters, 8(1), 014040.

Takai, T., Yonemaru, J. I., Kaidai, H., and Kasuga, S. (2012). Quantitative trait locus analysis for days-to-heading and morphological traits in an RIL population derived from an extremely late flowering F1 hybrid of sorghum. Euphytica, 187(3), 411-420.

Thera, K. (2017). Analyse des déterminants génétiques contrôlant la production et la composition de la tige chez le sorgho (Sorghum bicolor L. Moench). Intégration des approches bi-et multi-parentales. Ph.D. dissertation, Montpellier SupAgro.

Van Oosterom, E. J., Carberry, P. S., Hargreaves, J. N. G., and O'leary, G. J. (2001). Simulating growth, development, and yield of tillering pearl millet: II. Simulation of canopy development. Field Crops Research, 72(1), 67-91.

Vom Brocke, K., Trouche, G., Weltzien, E., Kondombo-Barro, C. P., Sidibé, A., Zougmoré, R., and Gozé, E. (2014). Helping farmers adapt to climate and cropping system change through increased access to sorghum genetic resources adapted to prevalent sorghum cropping systems in Burkina Faso. Experimental Agriculture, 50(2), 284-305.

VSN International (2022). Genstat for Windows 22nd Edition. VSN International, Hemel Hempstead, UK. https://genstat.kb.vsni.co.uk/

Westhues, C. C., Simianer, H., and Beissinger, T. M. (2022). learnMET: an R package to apply machine learning methods for genomic prediction using multi-environment trial data. G3, 12(11), jkac226

White, J. W., Alagarswamy, G., Ottman, M. J., Porter, C. H., Singh, U., and Hoogenboom, G. (2015). An Overview of CERES–Sorghum as Implemented in the Cropping System Model Version 4.5. Agronomy Journal, 107(6), 1987-2002 World Meteorological Organization - WMO. (2022) State of the climate in Africa in 2021

Wolabu, T. W., and Tadege, M. (2016). Photoperiod response and floral transition in sorghum. Plant signaling and behavior, 11(12), e1261232.

Xavier, A., Xu, S., Muir, W. M., and Rainey, K. M. (2015). NAM: association studies in multiple populations. Bioinformatics, 31(23), 3862-3864.

Xu, Y. (2016). Envirotyping for deciphering environmental impacts on crop plants. Theoretical and Applied Genetics,

129(4), 653-673.

Yang, S., Murphy, R. L., Morishige, D. T., Klein, P. E., Rooney, W. L., and Mullet, J. E. (2014). Sorghum phytochrome B inhibits flowering in long days by activating expression of SbPRR37 and SbGHD7, repressors of SbEHD1, SbCN8 and SbCN12. PloS one, 9(8), e105352.

Zhang, J., Zhang, D., Fan, Y., Li, C., Xu, P., Li, W., ... and Li, Y. (2021). The identification of grain size genes by RapMap reveals directional selection during rice domestication. Nature communications, 12(1), 1-18.

Zheng, C., Boer, M. P., and Van Eeuwijk, F. A. (2015). Reconstruction of genome ancestry blocks in multiparental populations. Genetics, 200(4), 1073-1087.

Characterization of adaptation mechanisms in sorghum using a multi-reference back-cross nested association mapping design and envirotyping - Supplementary material

Vincent Garin, Chiaka Diallo, Mohamed Tekete, Korotimi Thera, Baptiste Guitton, Karim Dagno, Abdoulaye Diallo, Mamoutou Kouressy, Willmar Leiser, Fred Rattunde, Ibrahima Sissoko, Aboubacar Toure, Baloua Nebie, Moussa Samake, Jana Kholova, Julien Frouin, David Pot, Michel Vaksmann, Eva Weltzien, Niaba Teme, Jean-Francois Rami

Supporting figures

Figure S1: Illustration of the crossing scheme with each parent represented as a circle and cross as a line. The larger ellipses represent the phenotyping experiments

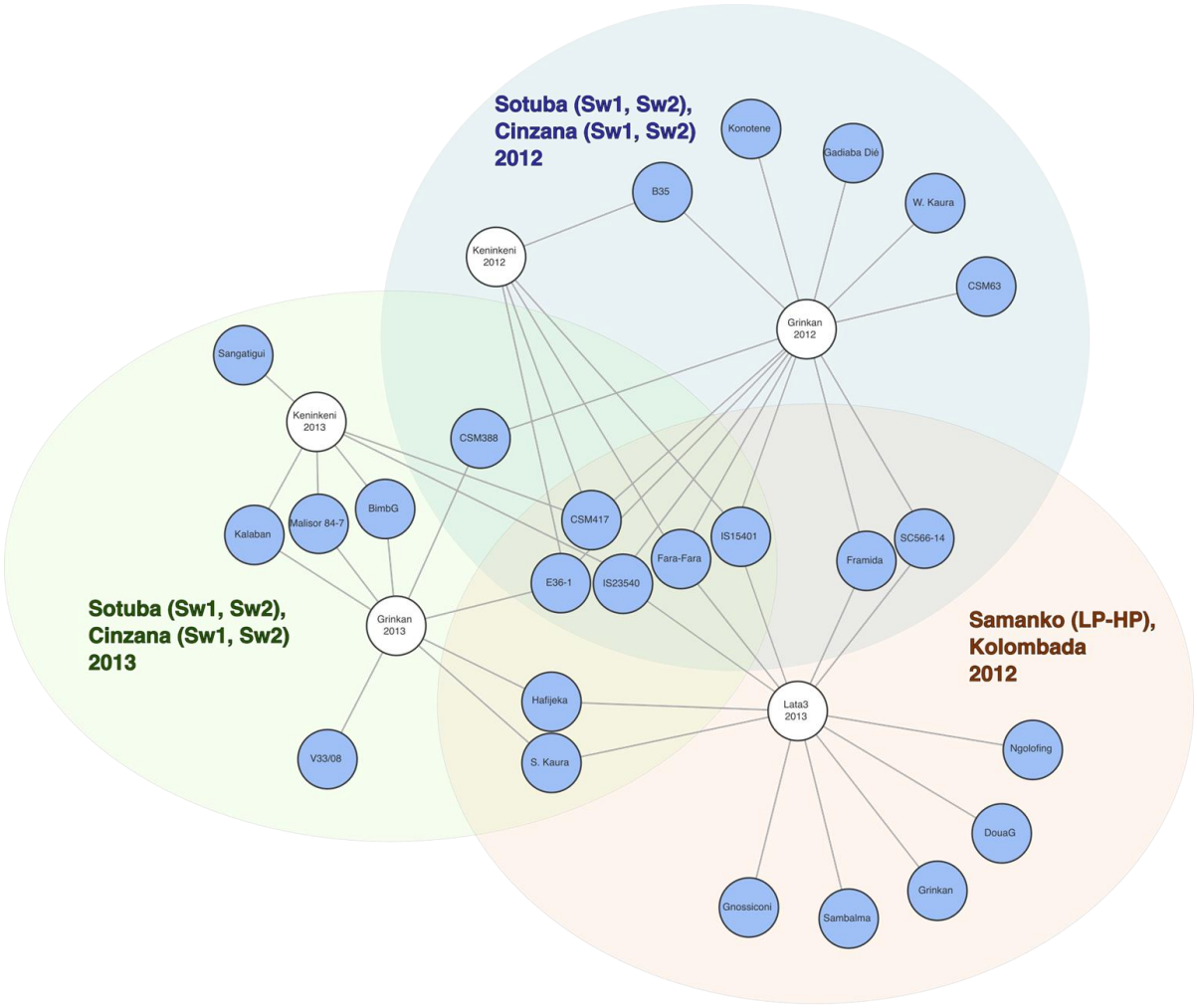

Figures S2: Principal component analysis of genetic information

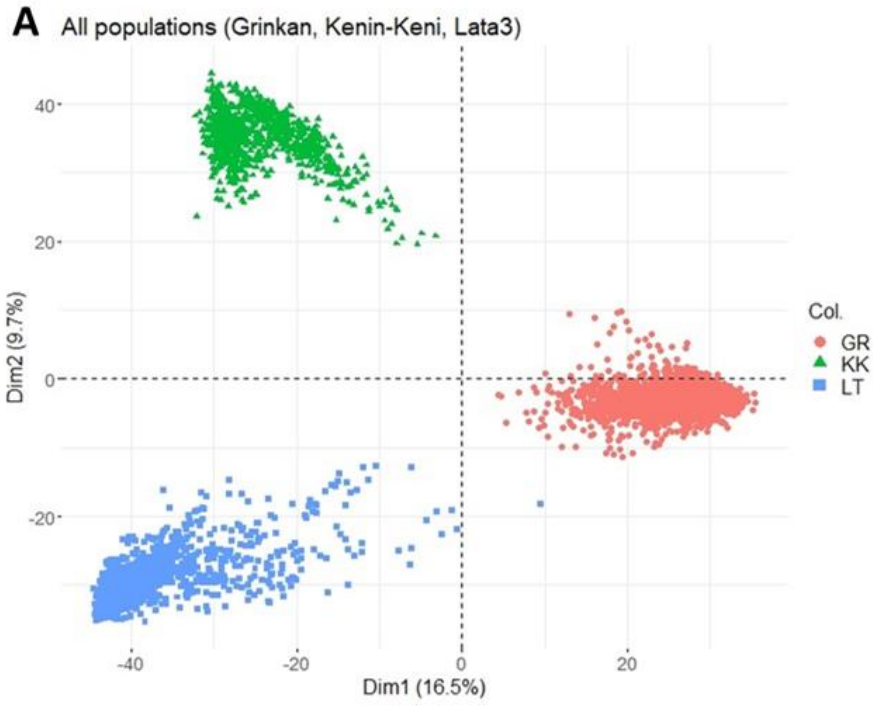

Principal component bi-plots performed on a subset of 5000 markers randomly selected of the three sub-populations Grinkan (GR), Kenin-Keni (KK) and Lata3 (LT) populations.

Figures S3: Principal component plots of the phenotypic traits for each population and year of phenotyping combination

Grinkan 2012

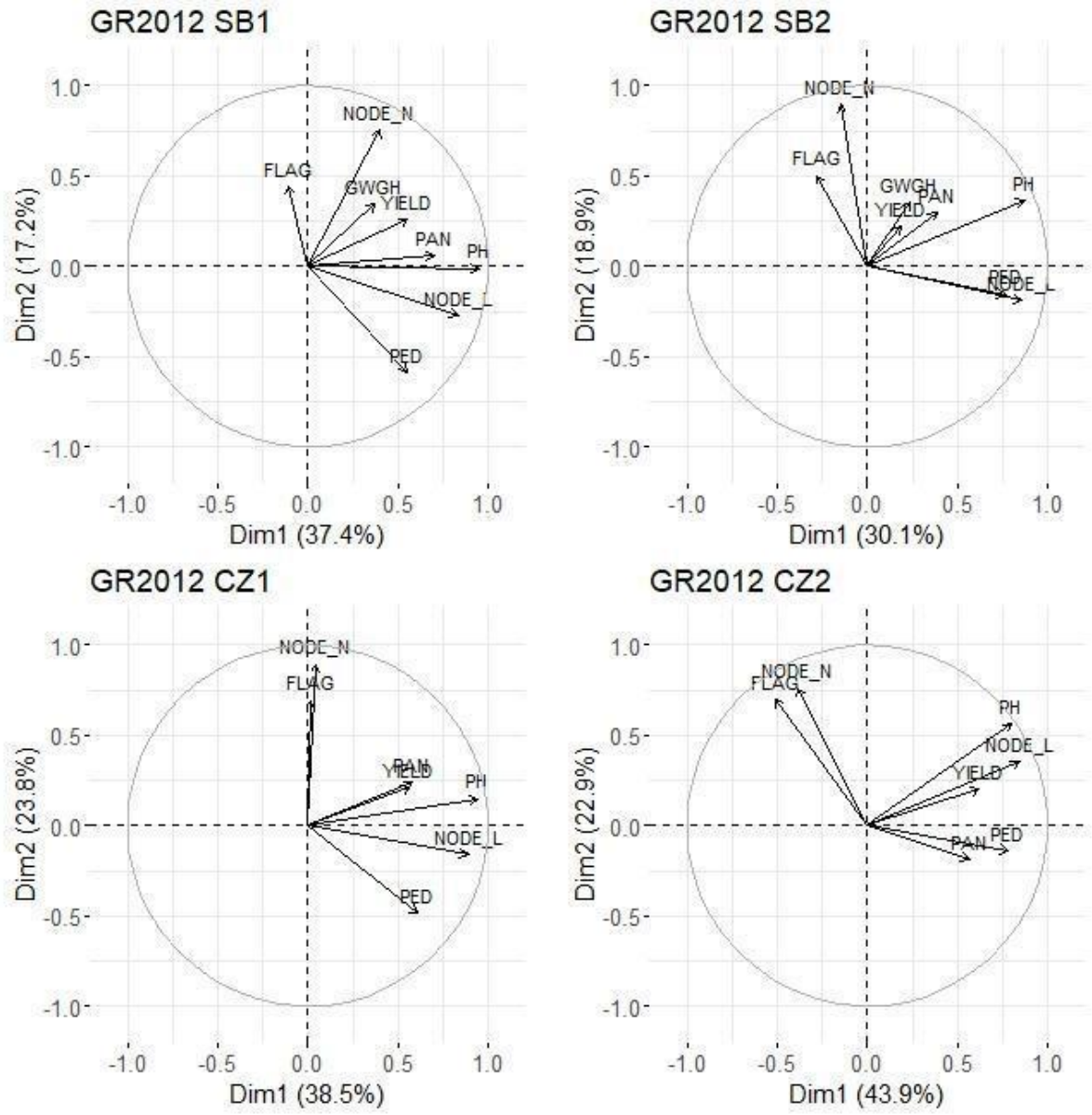

Principal component plots of the adjusted mean phenotypic traits (BLUEs) in the four environments where Grinkan population part was phenotyped in 2012 (SB1, 2: Sotuba sowing 1 and 2; CZ1, 2: Cinzana sowing 1 and 2) FLAG: flag leaf appearance, PH: plant height, NODE_N: number of nodes, NODE_L: average length of the internode, PED: peduncle length, PAN: panicle length, GWGH: 1000 grain weight, YIELD: grain yield

Grinkan 2013

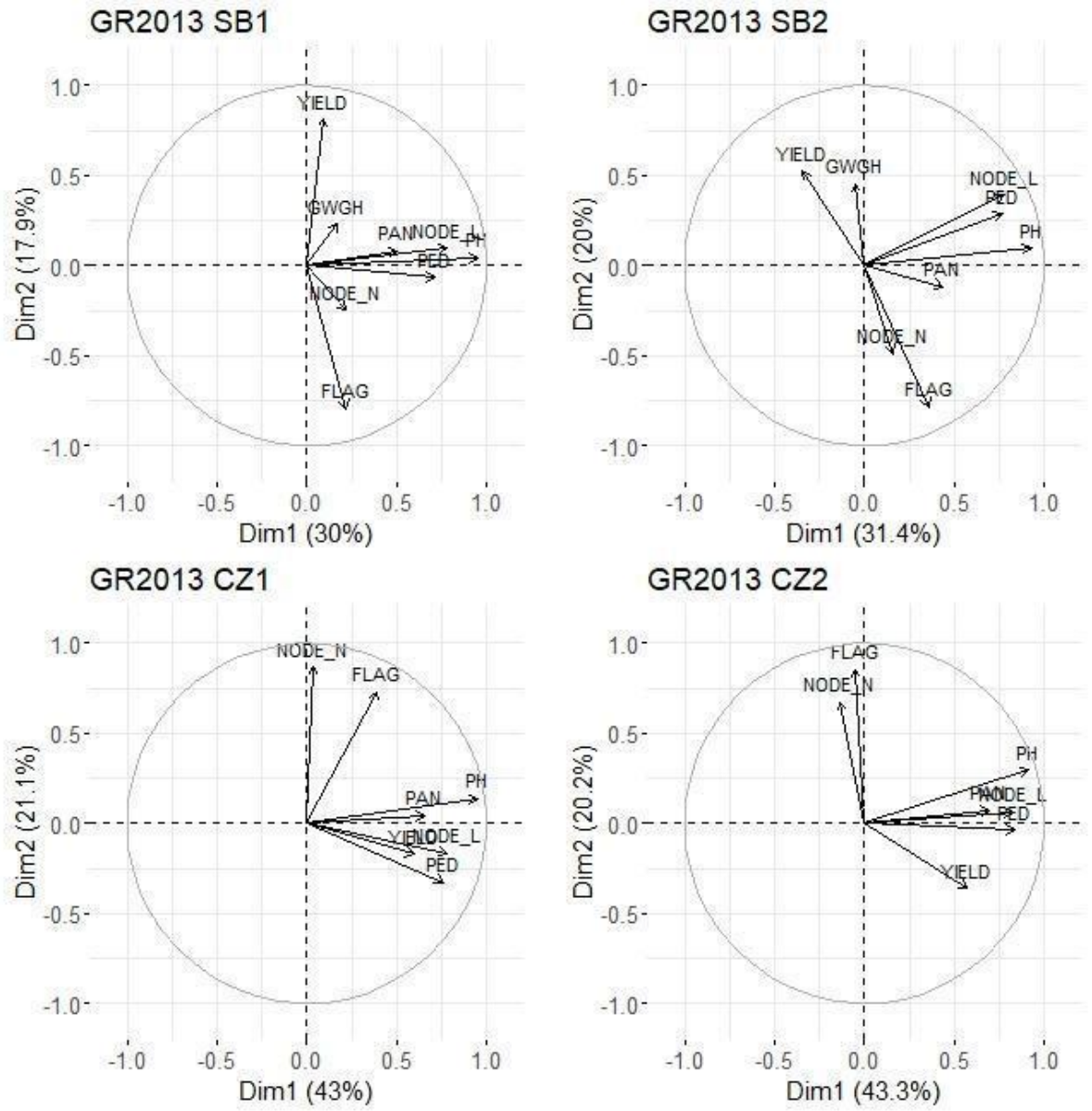

Principal component plots of the adjusted mean phenotypic traits (BLUEs) in the four environments where Grinkan population part was phenotyped in 2013 (SB1, 2: Sotuba sowing 1 and 2; CZ1, 2: Cinzana sowing 1 and 2) FLAG: flag leaf appearance, PH: plant height, NODE_N: number of nodes, NODE_L: average length of the internode, PED: peduncle length, PAN: panicle length, GWGH: 1000 grain weight, YIELD: grain yield

Kenin-Keni 2012

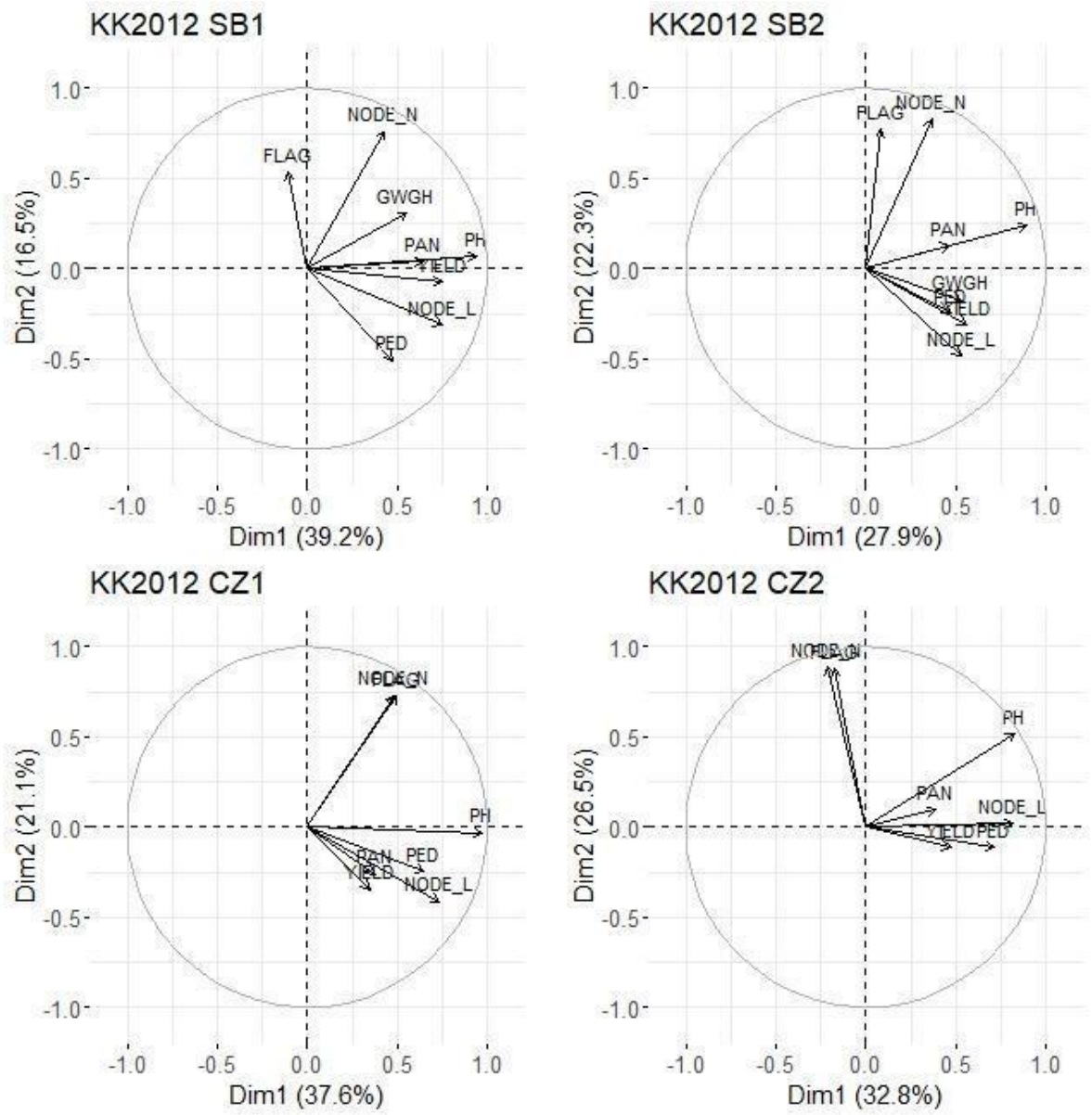

Principal component plots of the adjusted mean phenotypic traits (BLUEs) in the four environments where Kenin-Keni population part was phenotyped in 2012 (SB1, 2: Sotuba sowing 1 and 2; CZ1, 2: Cinzana sowing 1 and 2) FLAG: flag leaf appearance, PH: plant height, NODE_N: number of nodes, NODE_L: average length of the internode, PED: peduncle length, PAN: panicle length, GWGH: 1000 grain weight, YIELD: grain yield

Kenin-Keni 2013

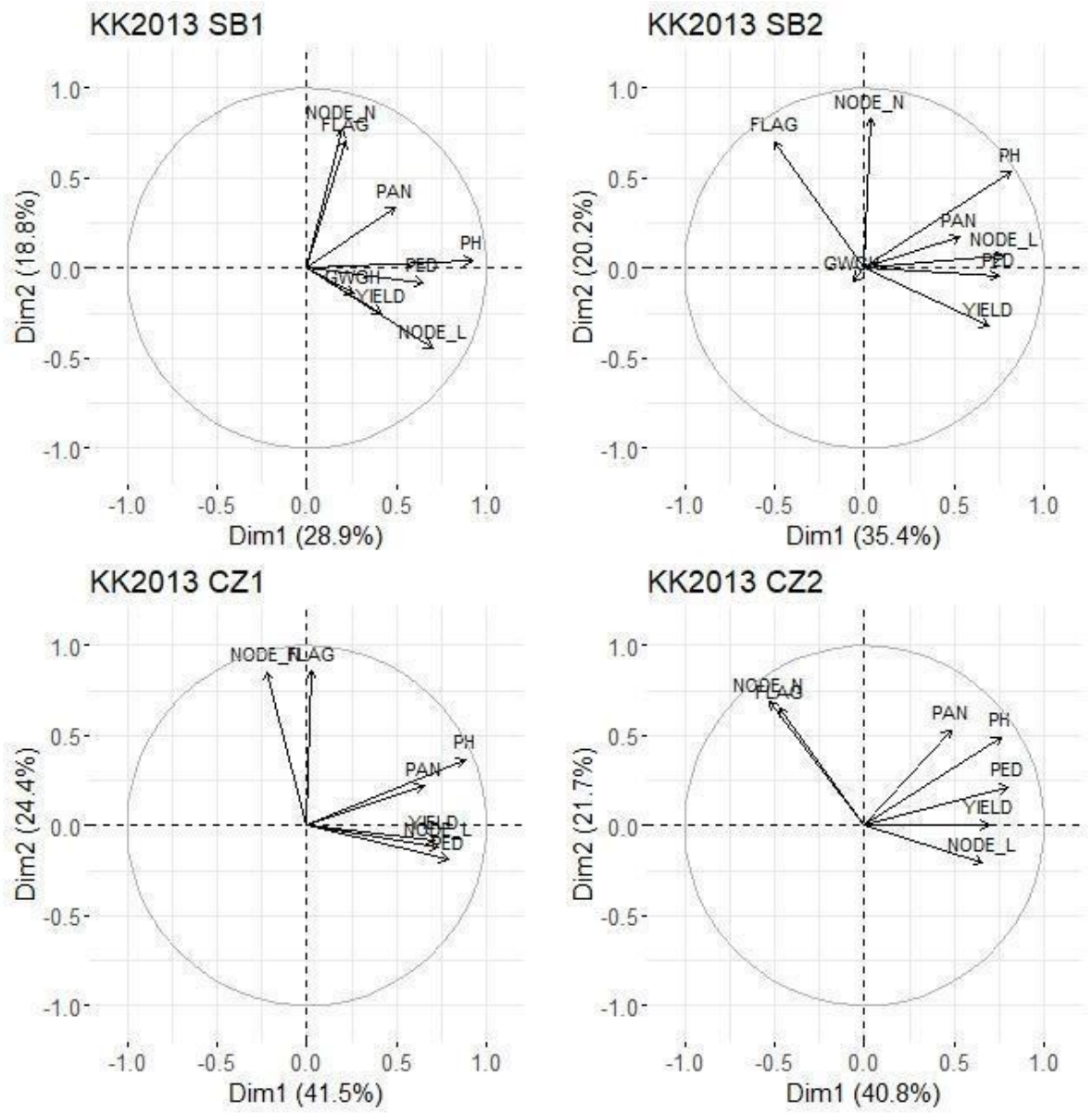

Principal component plots of the adjusted mean phenotypic traits (BLUEs) in the four environments where Kenin-Keni population part was phenotyped in 2013 (SB1, 2: Sotuba sowing 1 and 2; CZ1, 2: Cinzana sowing 1 and 2) FLAG: flag leaf appearance, PH: plant height, NODE_N: number of nodes, NODE_L: average length of the internode, PED: peduncle length, PAN: panicle length, GWGH: 1000 grain weight, YIELD: grain yield

Lata (2013)

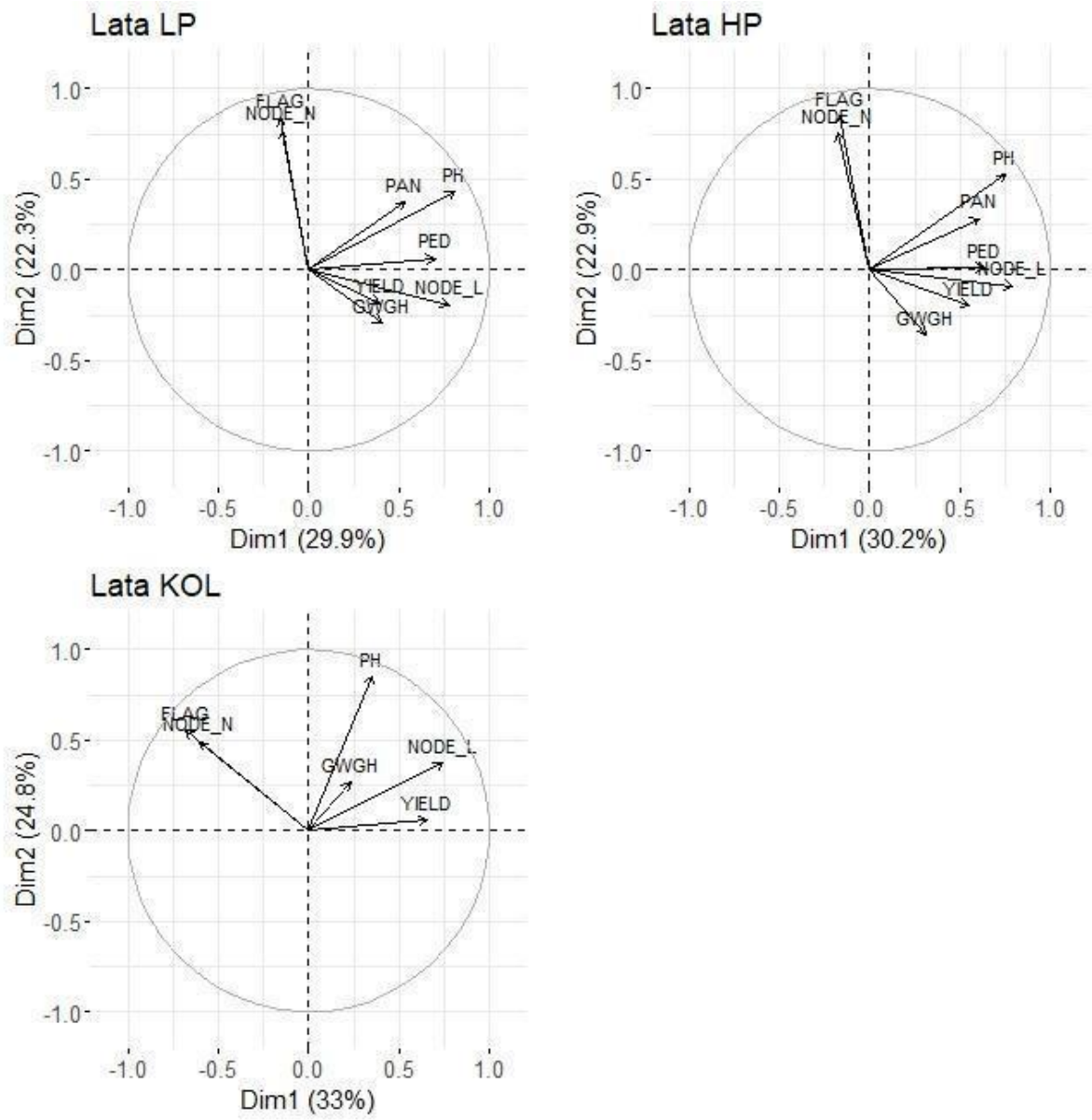

Principal component plots of the adjusted mean phenotypic traits (BLUEs) in the three environments where Lata3 population was phenotyped (LP: low P, HP: high P, KOL: Kolombada station). FLAG: flag leaf appearance, PH: plant height, NODE_N: number of nodes, NODE_L: average length of the internode, PED: peduncle length, PAN: panicle length, GWGH: 1000 grain weight, YIELD: grain yield

Figures S4: Pearson correlation matrix plots of the phenotypic traits for each population and year of phenotyping combination

Grinkan 2012

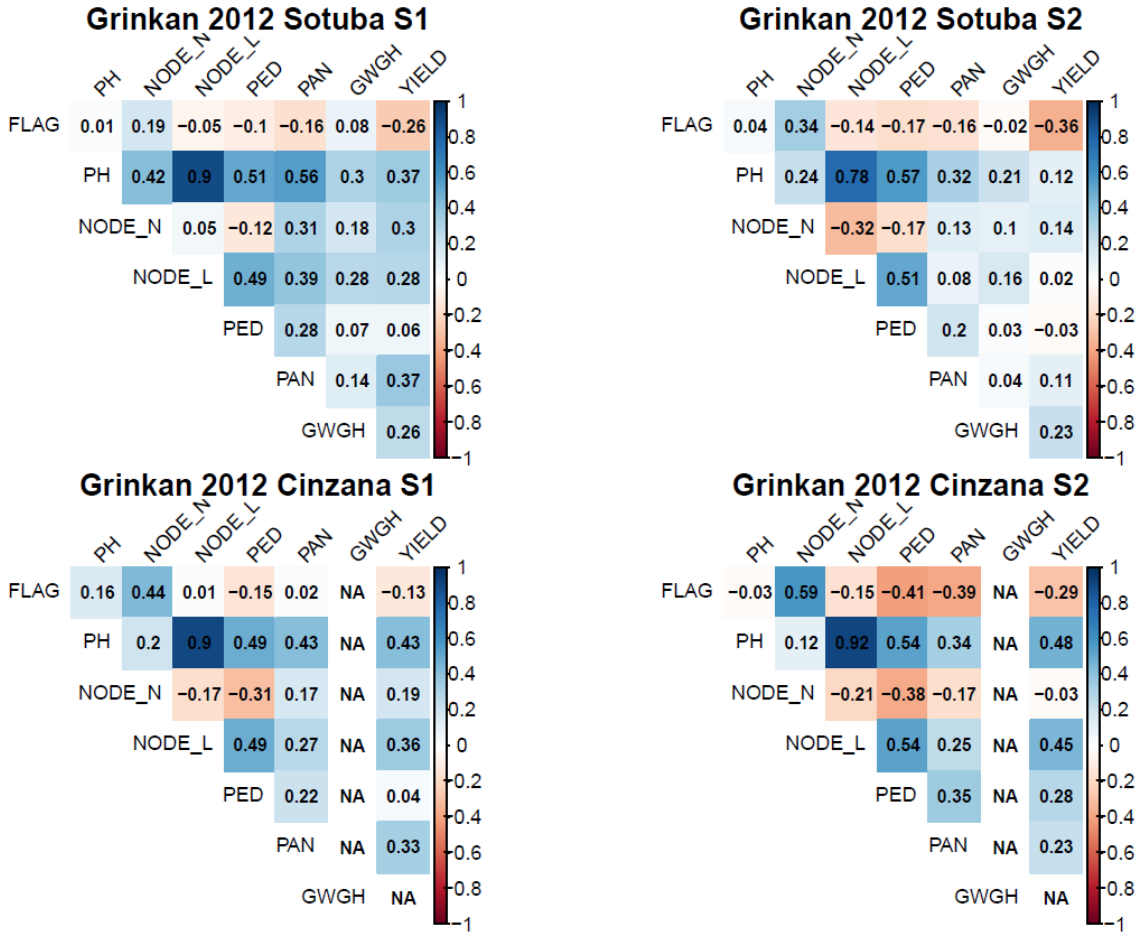

Grinkan 2013

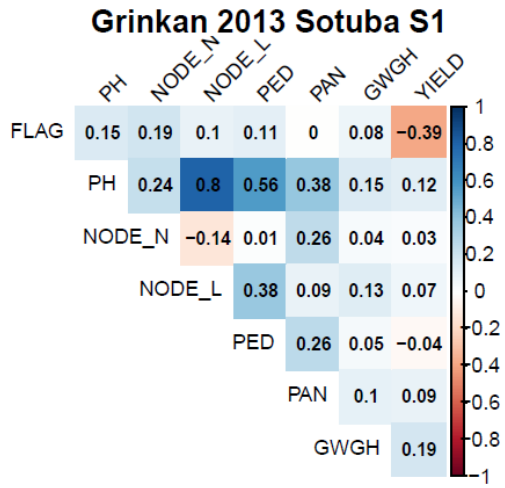

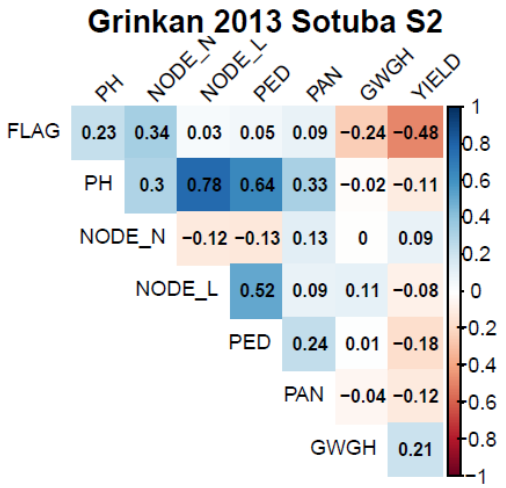

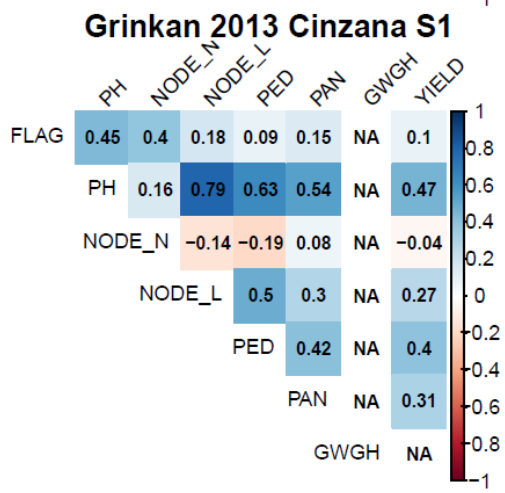

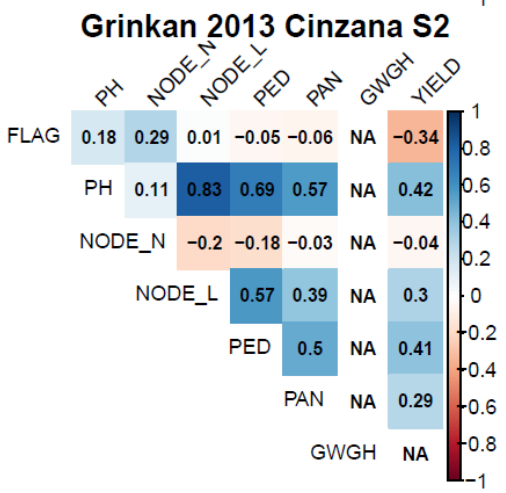

Kenin-Keni 2012

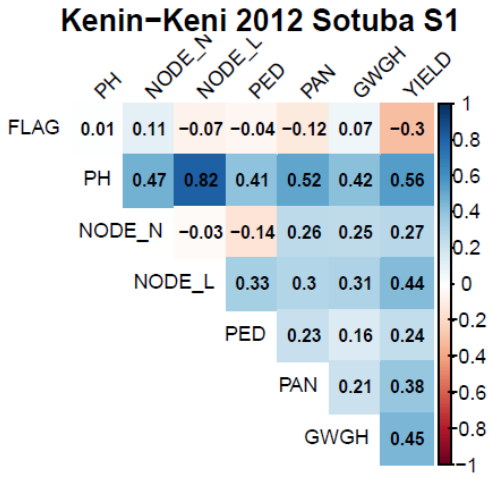

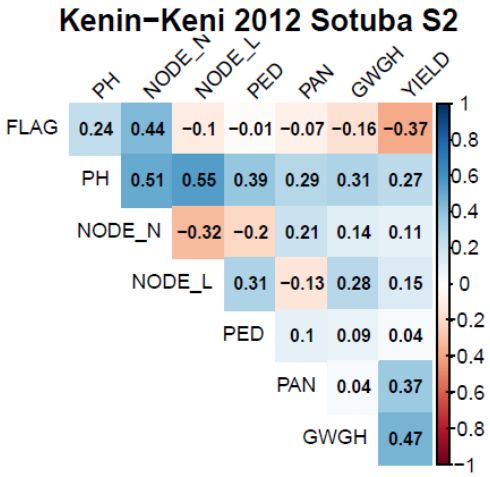

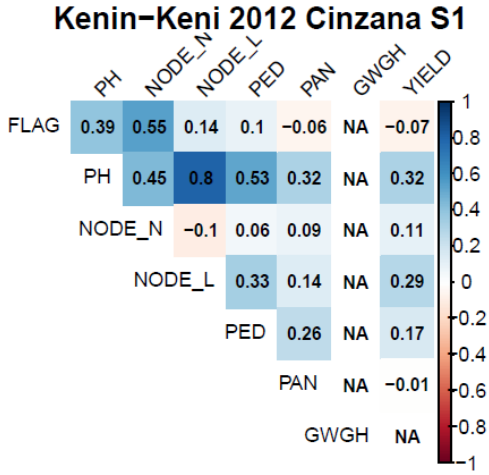

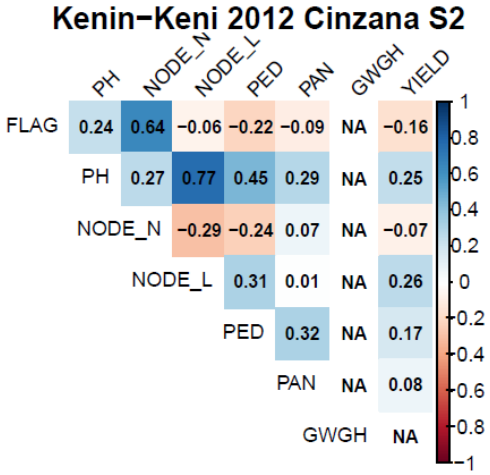

Kenin-Keni 2013

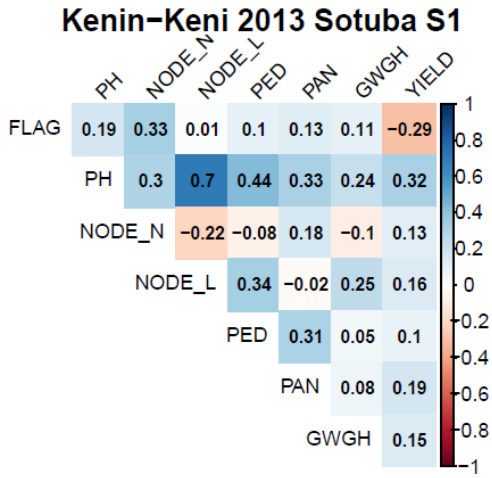

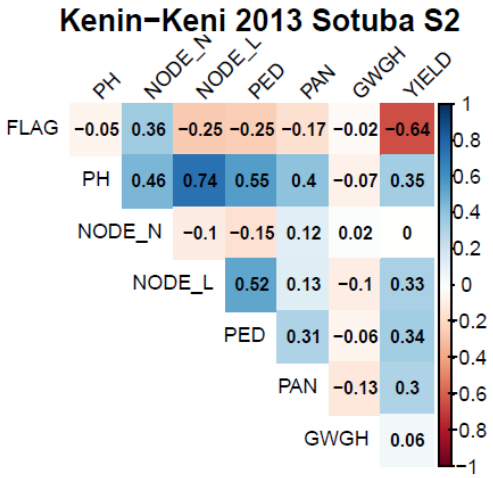

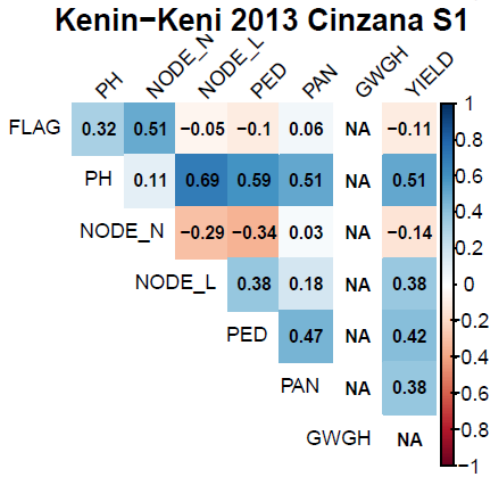

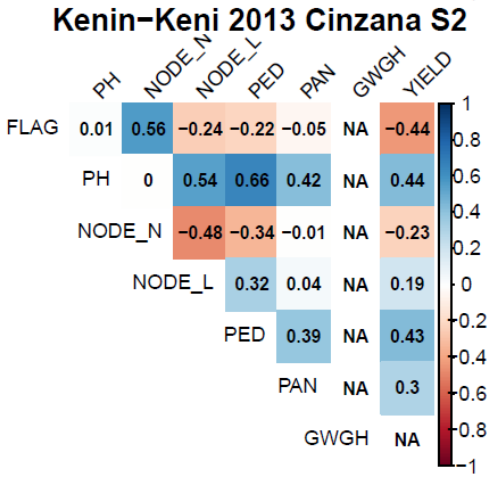

Lata3 2013

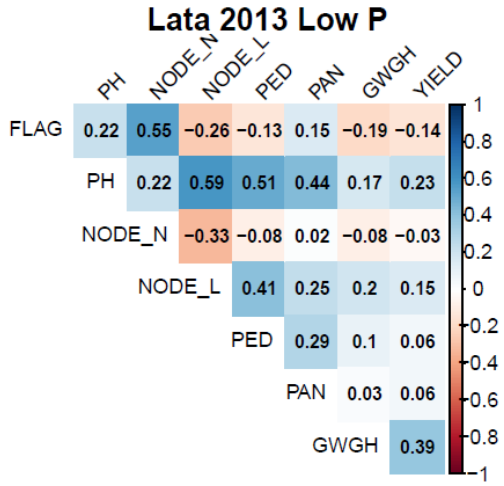

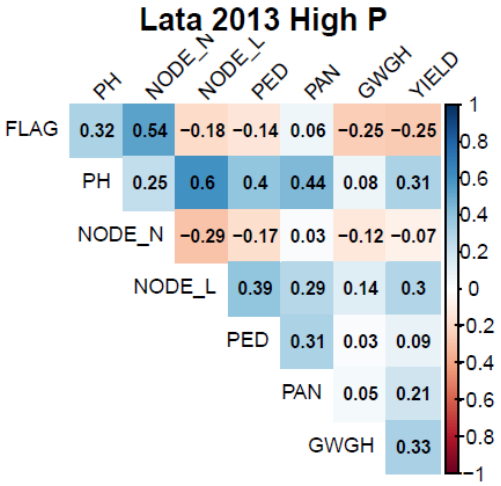

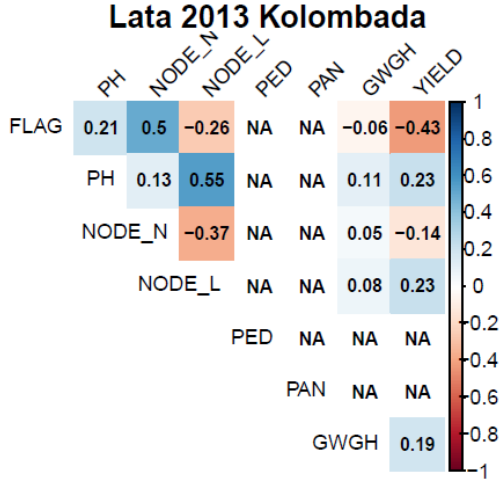

Figures S5: Phenotype by environmental covariables analysis visualisation

Flag leaf appearance (FLAG)

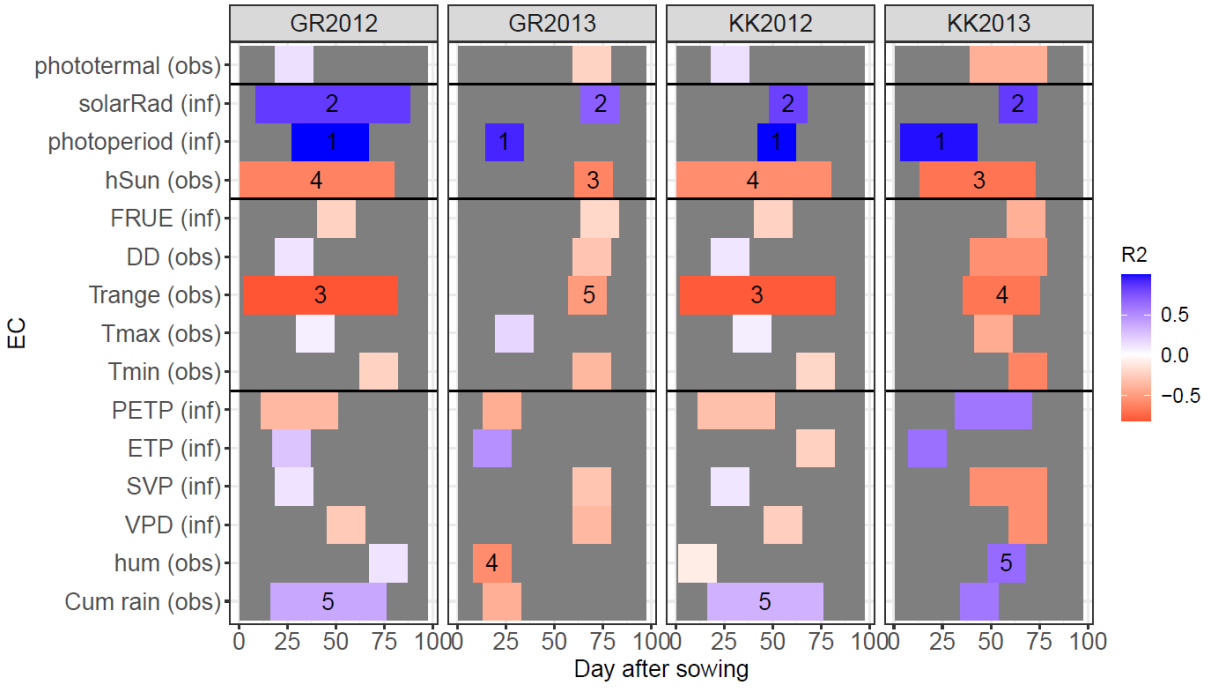

Effect of the environmental covariables (EC) on flag leaf appearance for the Grinkan and Kenin-Keni populations measured in environments Sotuba sowing 1-2 and Cinzana sowing 1-2 over seasons 2012 and 2013. The ECs and time window were selected using method S1. The intensity of the colour is proportional to the r squared (R^2) between the within environment adjusted means and the environmental covariable (EC) value with direction of the effect (blue positive, red negative) and time window during which the effect is the strongest. The five most influential ECs are indicated with numbers (1 corresponding to the most influential one)

Plant height

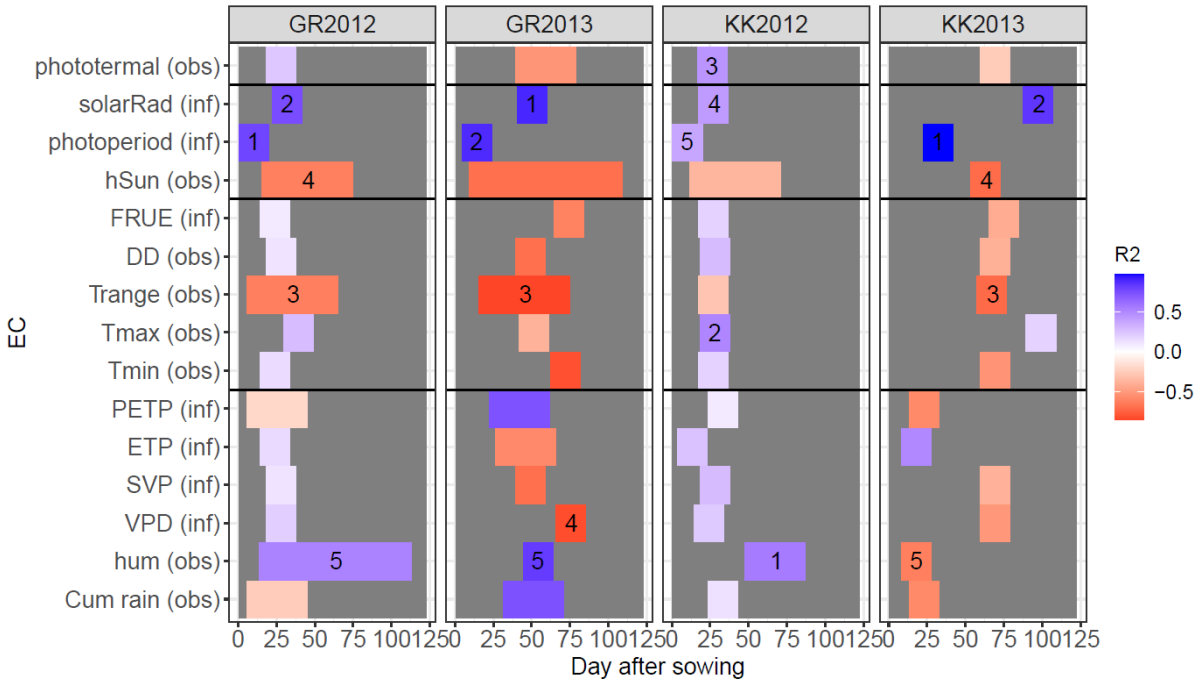

Effect of the environmental covariables (EC) on plant height for the Grinkan and Kenin-Keni populations measured in environments Sotuba sowing 1-2 and Cinzana sowing 1-2 over seasons 2012 and 2013. The ECs and time window were selected using method S1. The intensity of the colour is proportional to the r squared (R^2) between the within environment adjusted means and the environmental covariable (EC) value with direction of the effect (blue positive, red negative) and time window during which the effect is the strongest. The five most influential ECs are indicated with numbers (1 corresponding to the most influential one)

Number of internodes

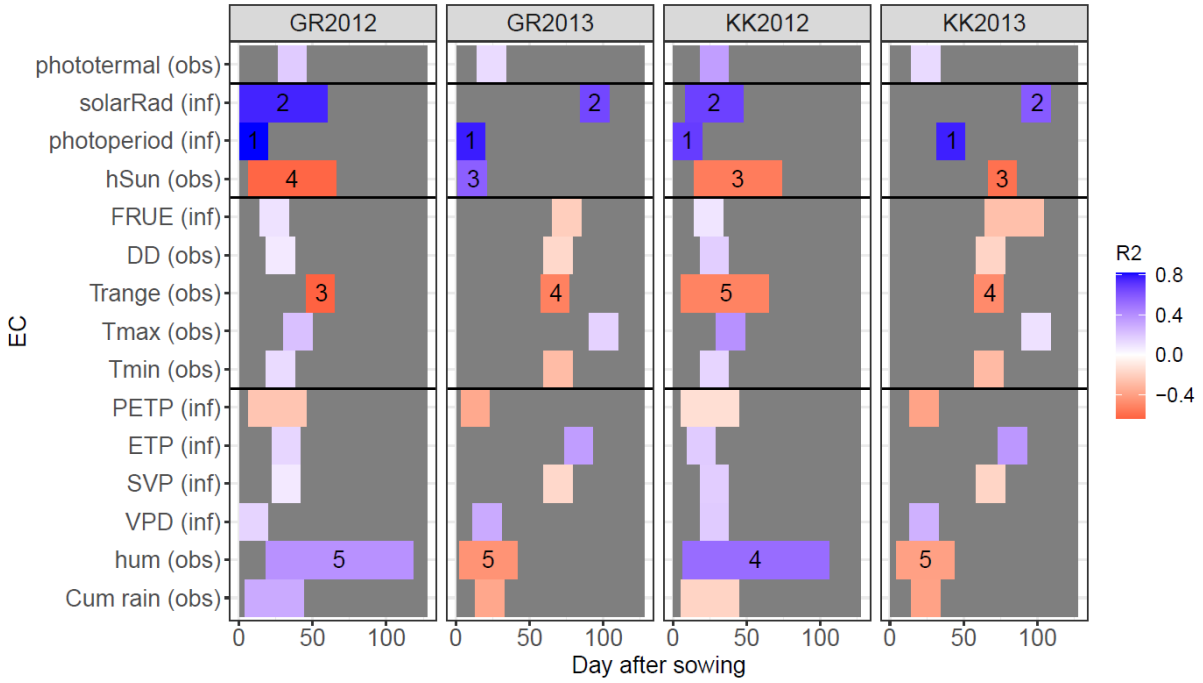

Effect of the environmental covariables (EC) on the number of internodes for the Grinkan and Kenin-Keni populations measured in environments Sotuba sowing 1-2 and Cinzana sowing 1-2 over seasons 2012 and 2013. The ECs and time window were selected using method S1. The intensity of the colour is proportional to the r squared (R^2) between the within environment adjusted means and the environmental covariable (EC) value with direction of the effect (blue positive, red negative) and time window during which the effect is the strongest. The five most influential ECs are indicated with numbers (1 corresponding to the most influential one)

Average internode length

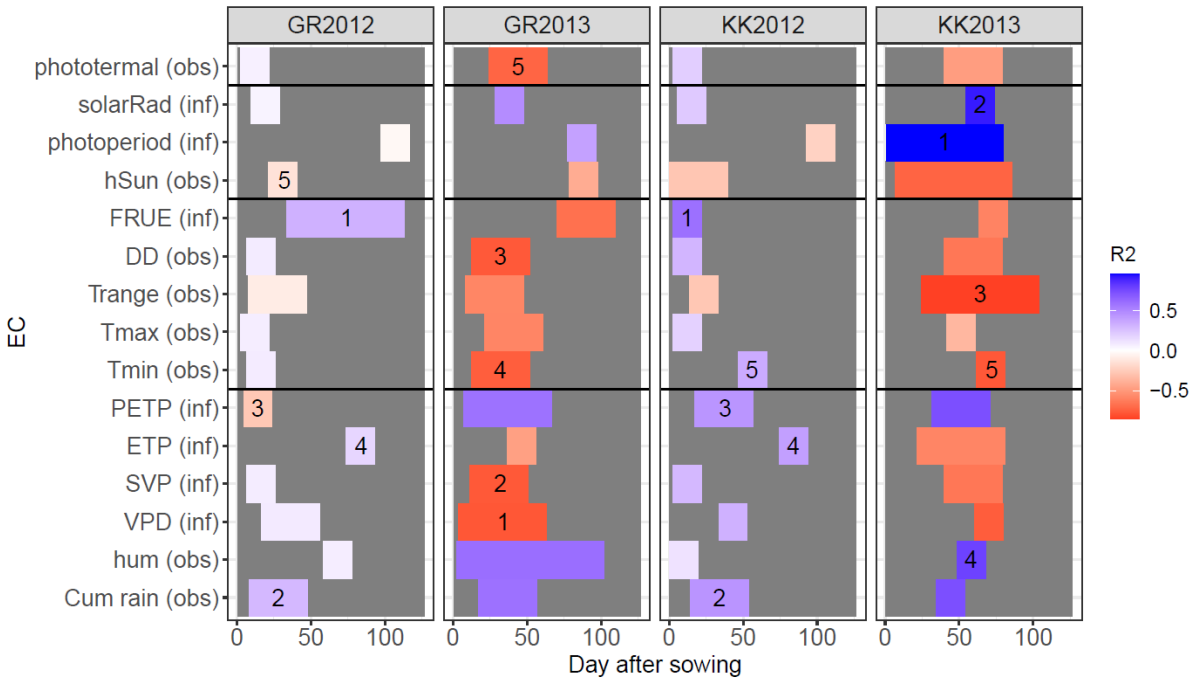

Effect of the environmental covariables (EC) on the average internode length for the Grinkan and Kenin-Keni populations measured in environments Sotuba sowing 1-2 and Cinzana sowing 1-2 over seasons 2012 and 2013. The ECs and time window were selected using method S1 The intensity of the colour is proportional to the r squared (R^2) between the within environment adjusted means and the environmental covariable (EC) value with direction of the effect (blue positive, red negative) and time window during which the effect is the strongest. The five most influential ECs are indicated with numbers (1 corresponding to the most influential one)

Peduncle length

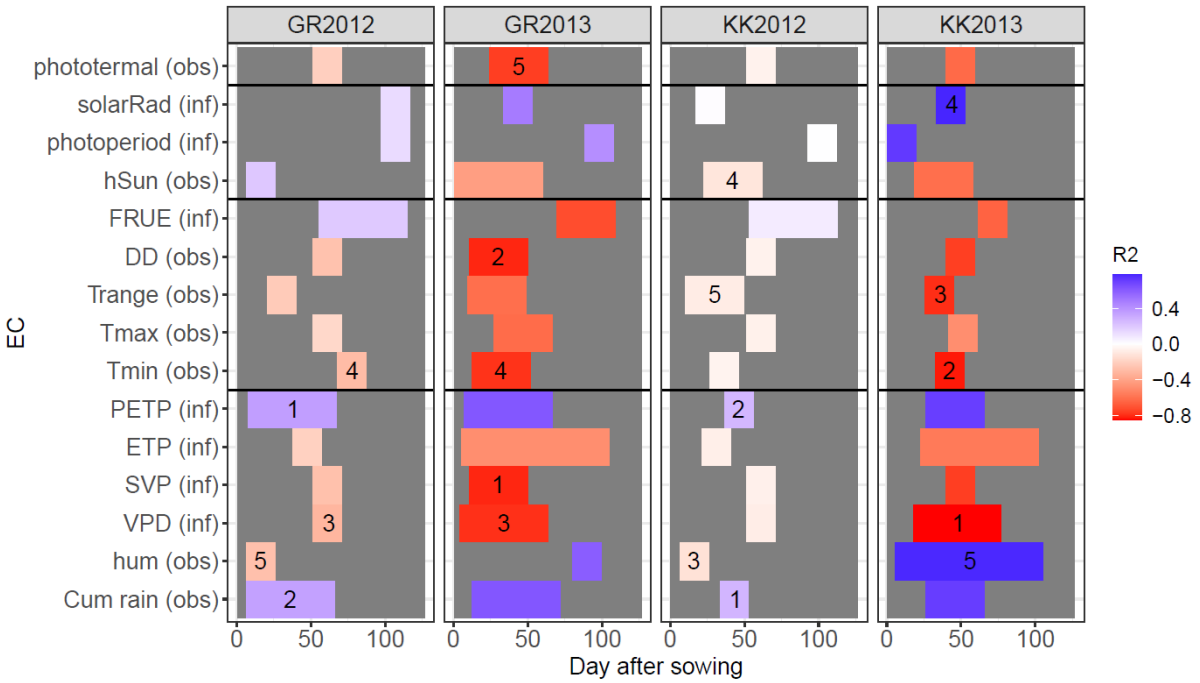

Effect of the environmental covariables (EC) on the peduncle length for the Grinkan and Kenin-Keni populations measured in environments Sotuba sowing 1-2 and Cinzana sowing 1-2 over seasons 2012 and 2013. The ECs and time window were selected using method S1. The intensity of the colour is proportional to the r squared (R^2) between the within environment adjusted means and the environmental covariable (EC) value with direction of the effect (blue positive, red negative) and time window during which the effect is the strongest. The five most influential ECs are indicated with numbers (1 corresponding to the most influential one)

Panicle length

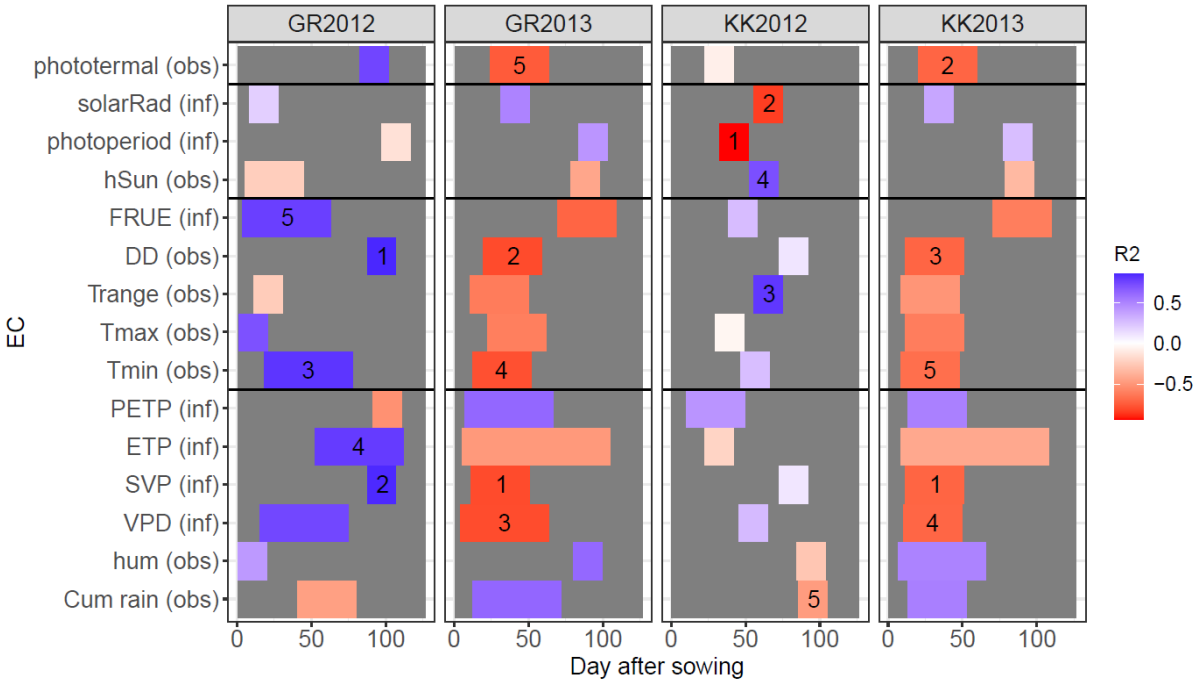

Effect of the environmental covariables (EC) on the panicle length for the Grinkan and Kenin-Keni populations measured in environments Sotuba sowing 1-2 and Cinzana sowing 1-2 over seasons 2012 and 2013. The ECs and time window were selected using method S1. The intensity of the colour is proportional to the r squared (R^2) between the within environment adjusted means and the environmental covariable (EC) value with direction of the effect (blue positive, red negative) and time window during which the effect is the strongest. The five most influential ECs are indicated with numbers (1 corresponding to the most influential one)

Grain yield (YIELD)

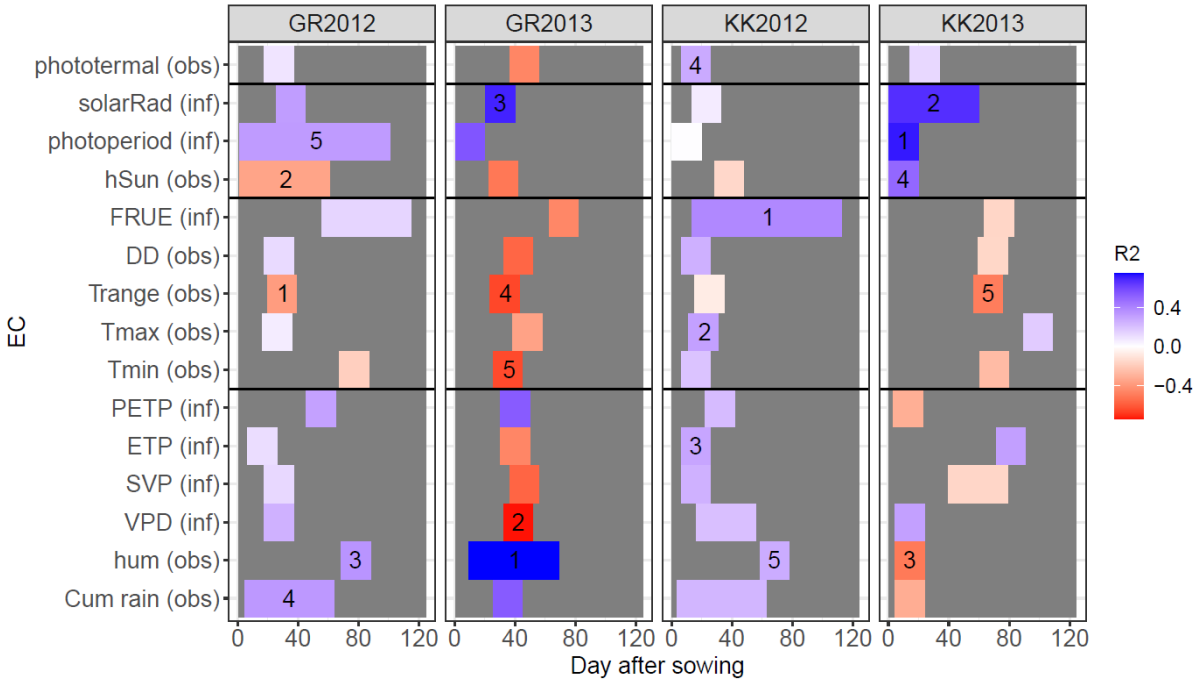

Effect of the environmental covariables (EC) on grain yield for the Grinkan and Kenin-Keni populations measured in environments Sotuba sowing 1-2 and Cinzana sowing 1-2 over seasons 2012 and 2013. The ECs and time window were selected using method S1. The intensity of the colour is proportional to the r squared (R^2) between the within environment adjusted means and the environmental covariable (EC) value with direction of the effect (blue positive, red negative) and time window during which the effect is the strongest. The five most influential ECs are indicated with numbers (1 corresponding to the most influential one)

Figures S6: Effect plot of the detected QTLs over trait, populations and environments

Flag leaf appearance (FLAG)

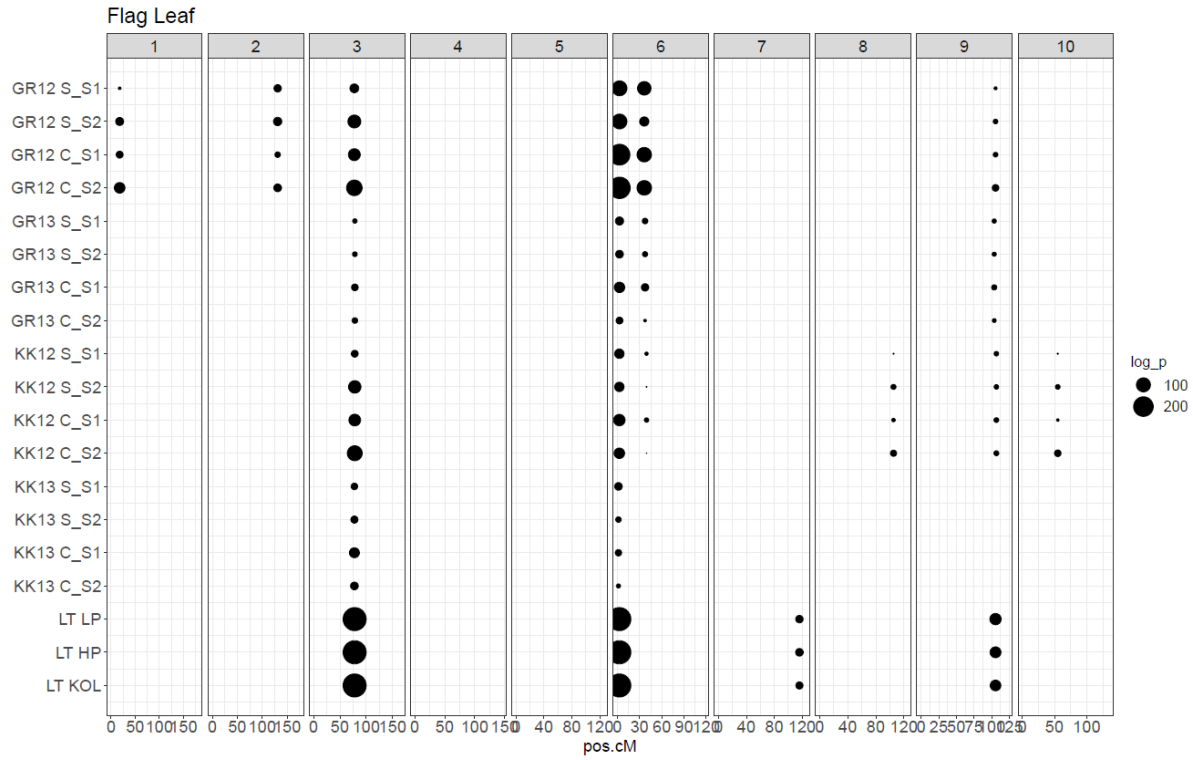

Significance of the QTL effect on flag leaf appearance given the different populations: Grinkan 2012 (GR12), Grinkan 2013 (GR13), Kenin-Keni 2012 (KK12), Kenin-Keni 2013 (KK13), and Lata within the tested environments: Sotuba sowing 1 and 2 (S_S1-2), Cinzana sowing 1 and 2 (C_S1, 2), low/high phosphorus (LP, HP), and Kolombada. The size of the dot is proportional to the within environment significance

Plant height

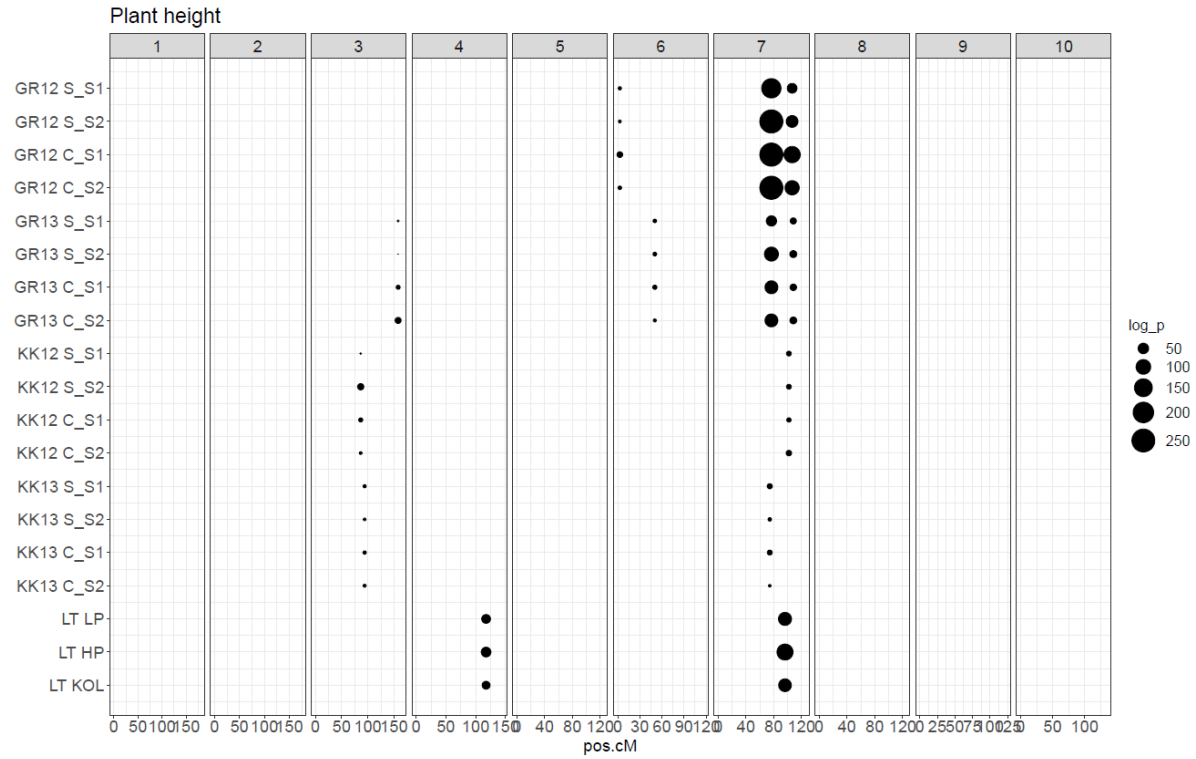

Significance of the QTL effect on flag leaf appearance given the different populations: Grinkan 2012 (GR12), Grinkan 2013 (GR13), Kenin-Keni 2012 (KK12), Kenin-Keni 2013 (KK13), and Lata within the tested environments: Sotuba sowing 1 and 2 (S_S1-2), Cinzana sowing 1 and 2 (C_S1, 2), low/high phosphorus (LP, HP), and Kolombada. The size of the dot is proportional to the within environment significance

Number of internodes (NODE_N)

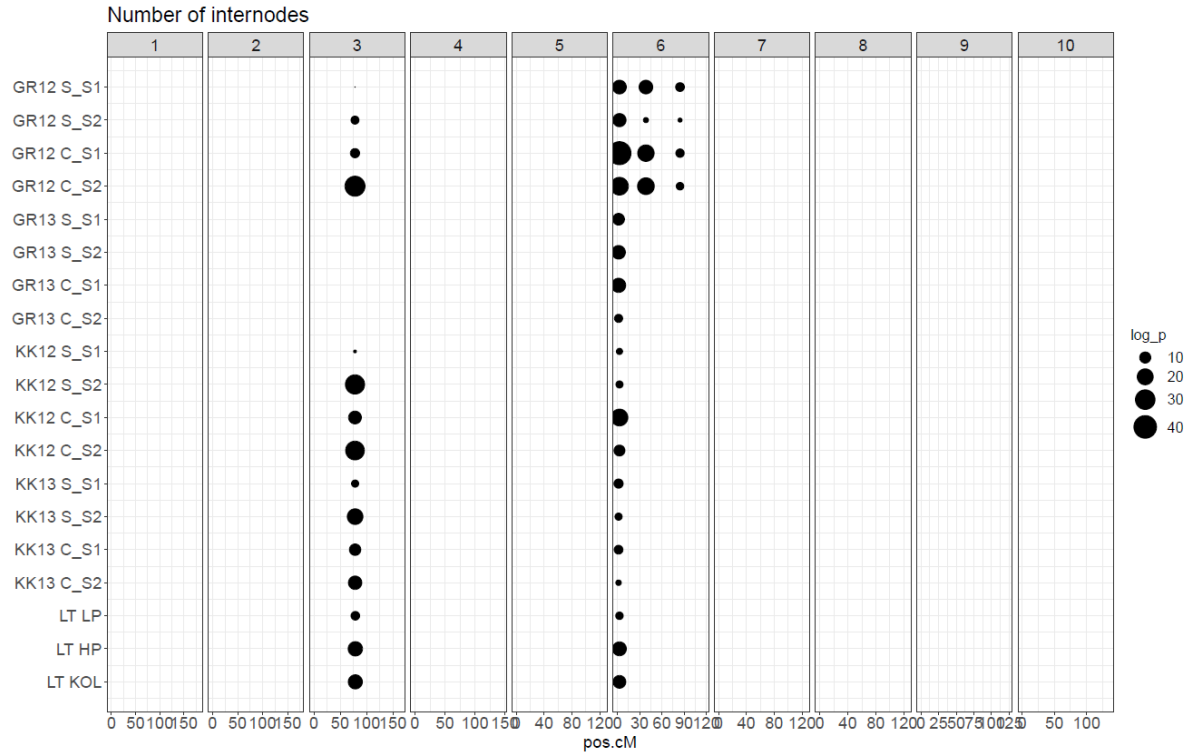

Significance of the QTL effect on the number of internodes given the different populations: Grinkan 2012 (GR12), Grinkan 2013 (GR13), Kenin-Keni 2012 (KK12), Kenin-Keni 2013 (KK13), and Lata within the tested environments: Sotuba sowing 1 and 2 (S_S1-2), Cinzana sowing 1 and 2 (C_S1, 2), low/high phosphorus (LP, HP), and Kolombada. The size of the dot is proportional to the within environment significance

Average internode length (NODE_L)

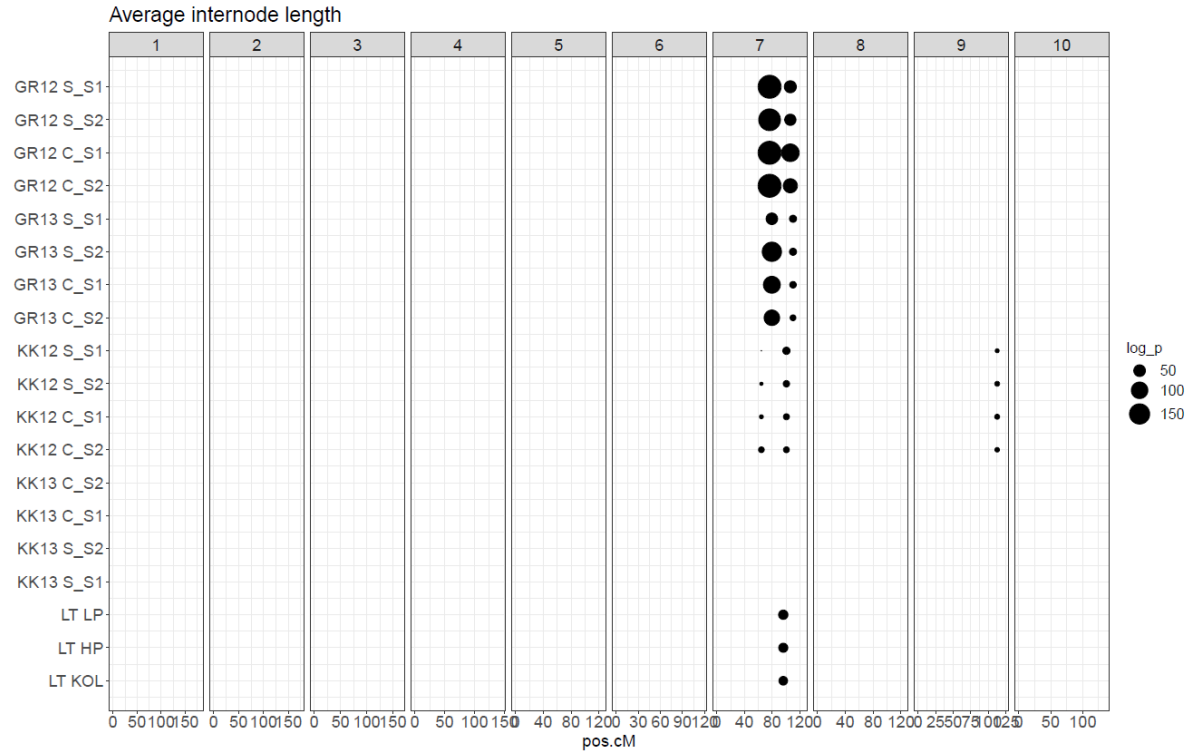

Significance of the QTL effect on the average internode length given the different populations: Grinkan 2012 (GR12), Grinkan 2013 (GR13), Kenin-Keni 2012 (KK12), Kenin-Keni 2013 (KK13), and Lata within the tested environments: Sotuba sowing 1 and 2 (S_S1-2), Cinzana sowing 1 and 2 (C_S1, 2), low/high phosphorus (LP, HP), and Kolombada. The size of the dot is proportional to the within environment significance

Peduncle length (PED)

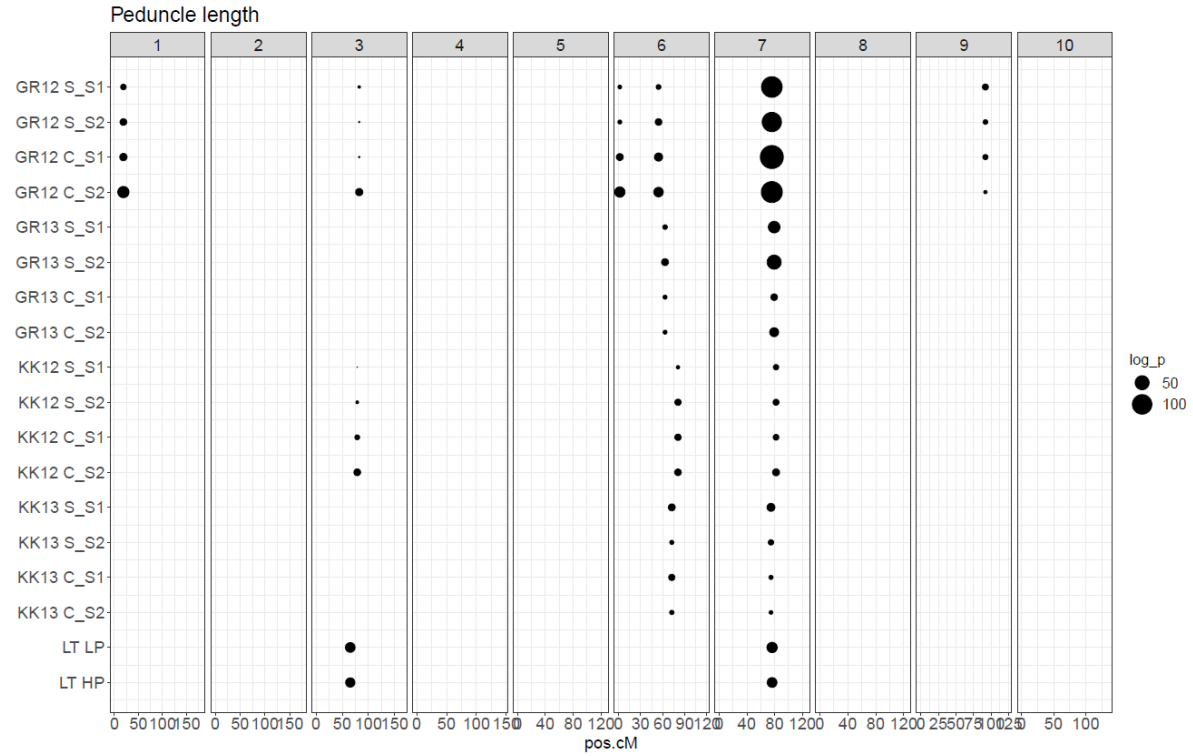

Significance of the QTL effect on the peduncle length given the different populations: Grinkan 2012 (GR12), Grinkan 2013 (GR13), Kenin-Keni 2012 (KK12), Kenin-Keni 2013 (KK13), and Lata within the tested environments: Sotuba sowing 1 and 2 (S_S1-2), Cinzana sowing 1 and 2 (C_S1, 2), low/high phosphorus (LP, HP), and Kolombada. The size of the dot is proportional to the within environment significance

Panicle length (PAN)

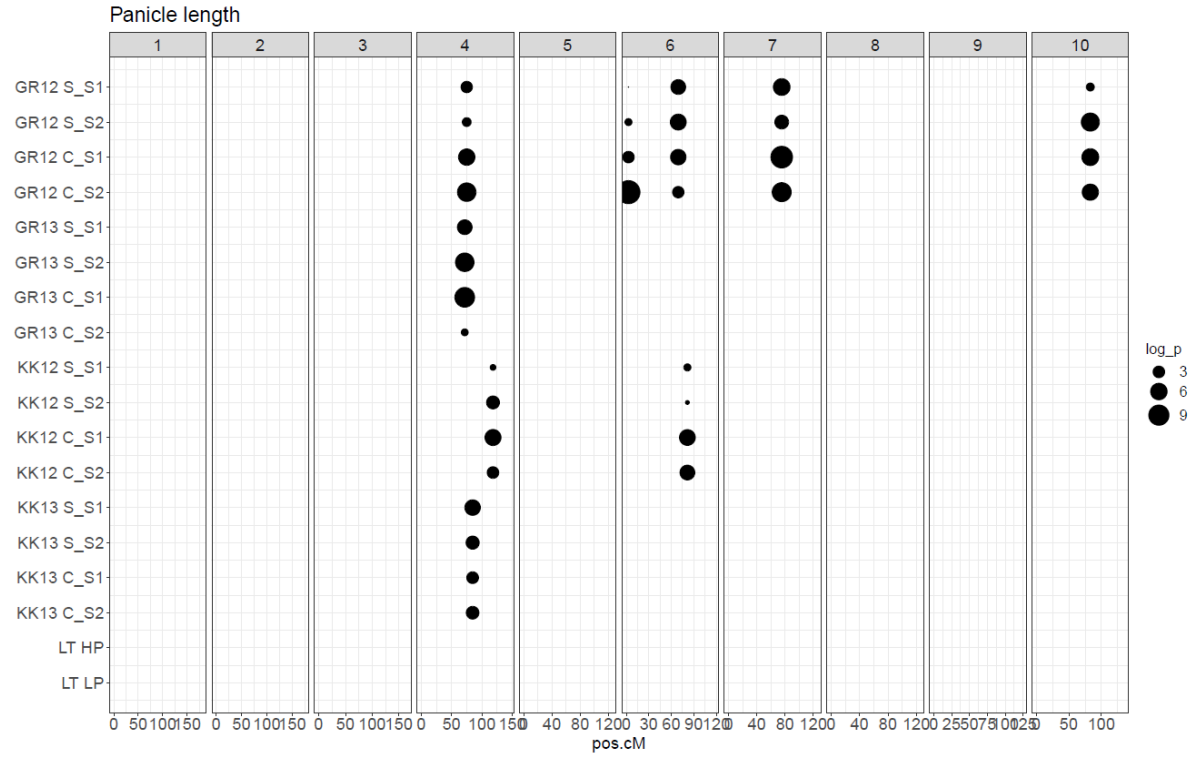

Significance of the QTL effect on the panicle length given the different populations: Grinkan 2012 (GR12), Grinkan 2013 (GR13), Kenin-Keni 2012 (KK12), Kenin-Keni 2013 (KK13), and Lata within the tested environments: Sotuba sowing 1 and 2 (S_S1-2), Cinzana sowing 1 and 2 (C_S1, 2), low/high phosphorus (LP, HP), and Kolombada. The size of the dot is proportional to the within environment significance

1000 grain weight (GWGH)

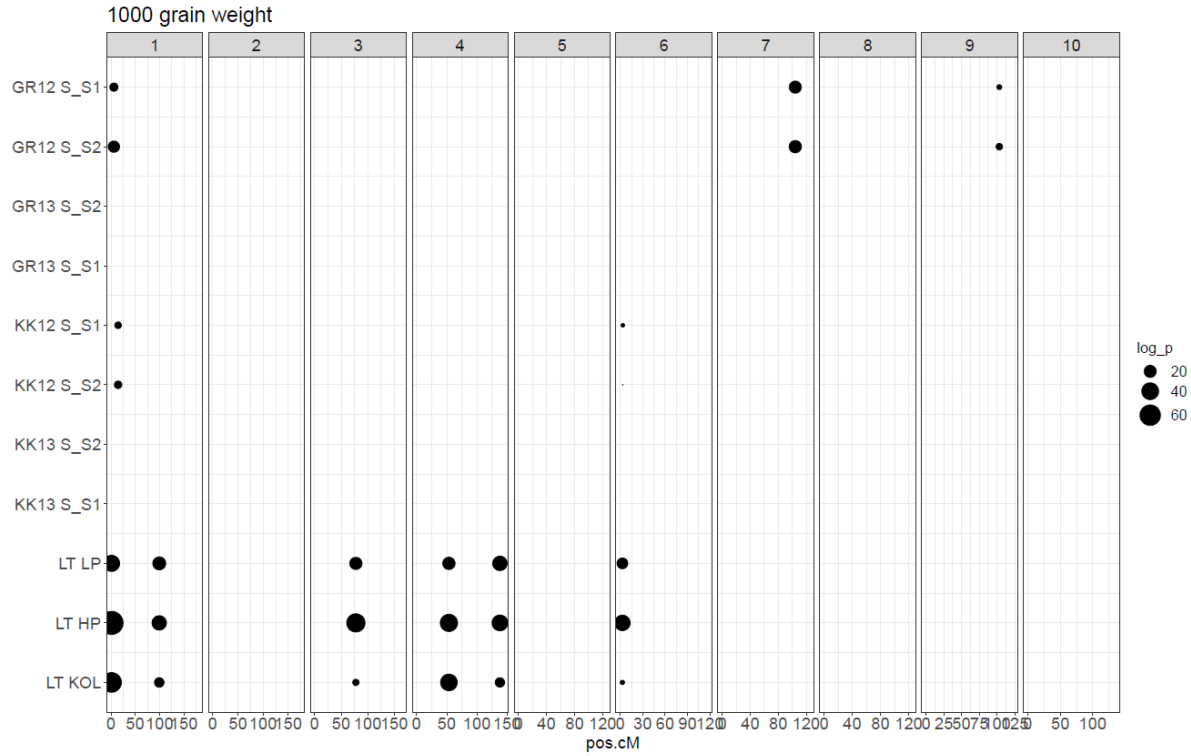

Significance of the QTL effect on 1000 grain weight given the different populations: Grinkan 2012 (GR12), Grinkan 2013 (GR13), Kenin-Keni 2012 (KK12), Kenin-Keni 2013 (KK13), and Lata within the tested environments: Sotuba sowing 1 and 2 (S_S1-2), Cinzana sowing 1 and 2 (C_S1, 2), low/high phosphorus (LP, HP), and Kolombada. The size of the dot is proportional to the within environment significance

Grain yield (YIELD)

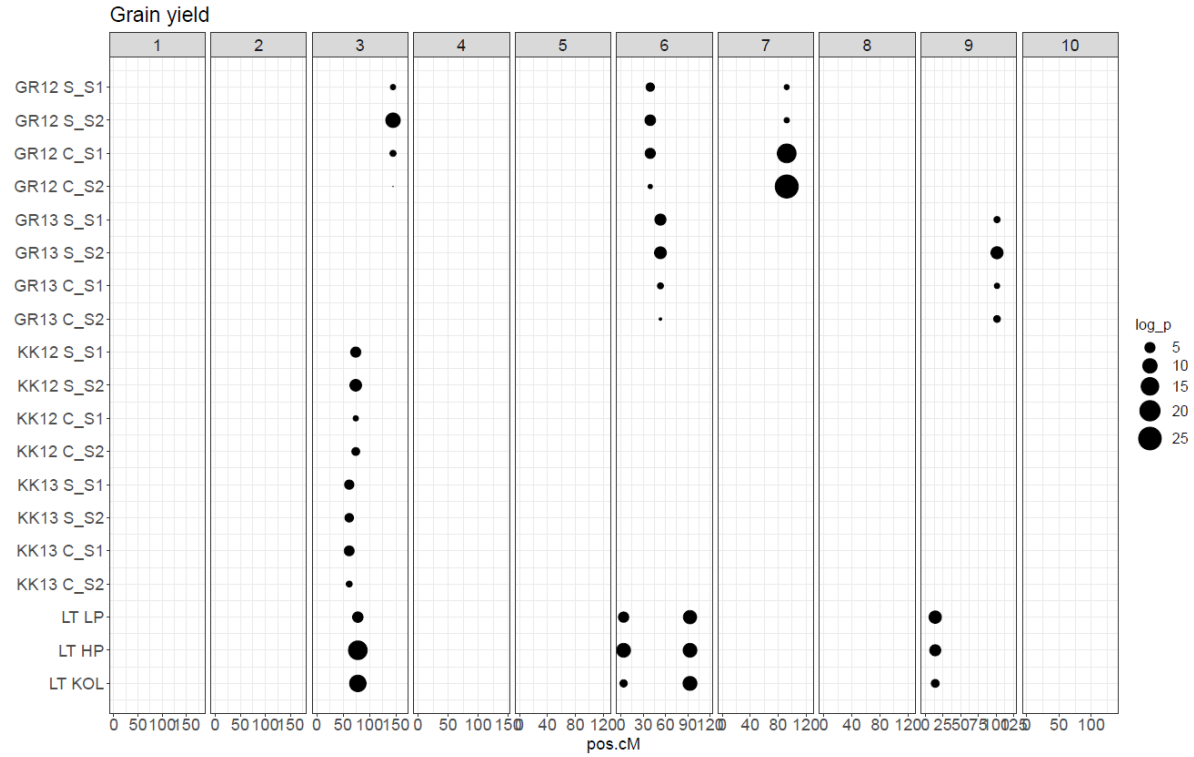

Significance of the QTL effect on grain yield given the different populations: Grinkan 2012 (GR12), Grinkan 2013 (GR13), Kenin-Keni 2012 (KK12), Kenin-Keni 2013 (KK13), and Lata within the tested environments: Sotuba sowing 1 and 2 (S_S1-2), Cinzana sowing 1 and 2 (C_S1, 2), low/high phosphorus (LP, HP), and Kolombada. The size of the dot is proportional to the within environment significance

Figure S7: Field trial locations, sowing dates and environmental description

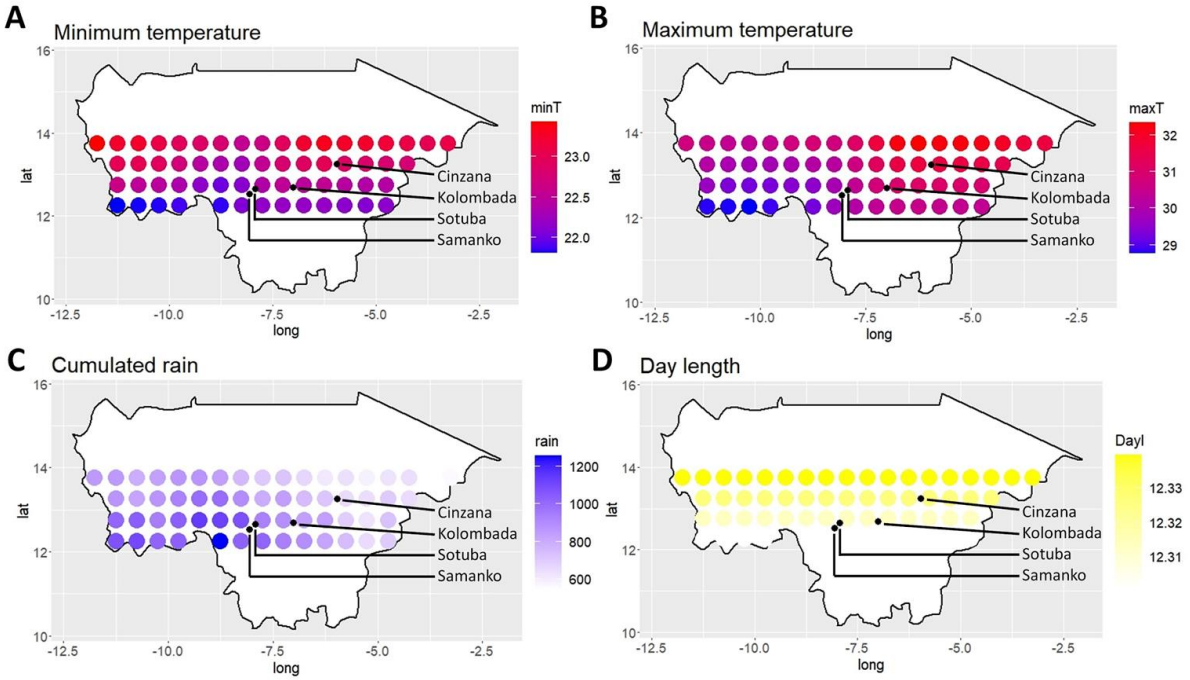

Environmental characterization of the field trial and neighbouring area during over the growing season (20 June to 20 Septembre 2012-2013) given A) minimum temperature, B) maximum temperature, C) cumulated rain and D) day length using synthetic climatic data from Nasapower (Spark 2018)

Figure S8: Cinzana and Sotuba environments principal component analysis based on ECs

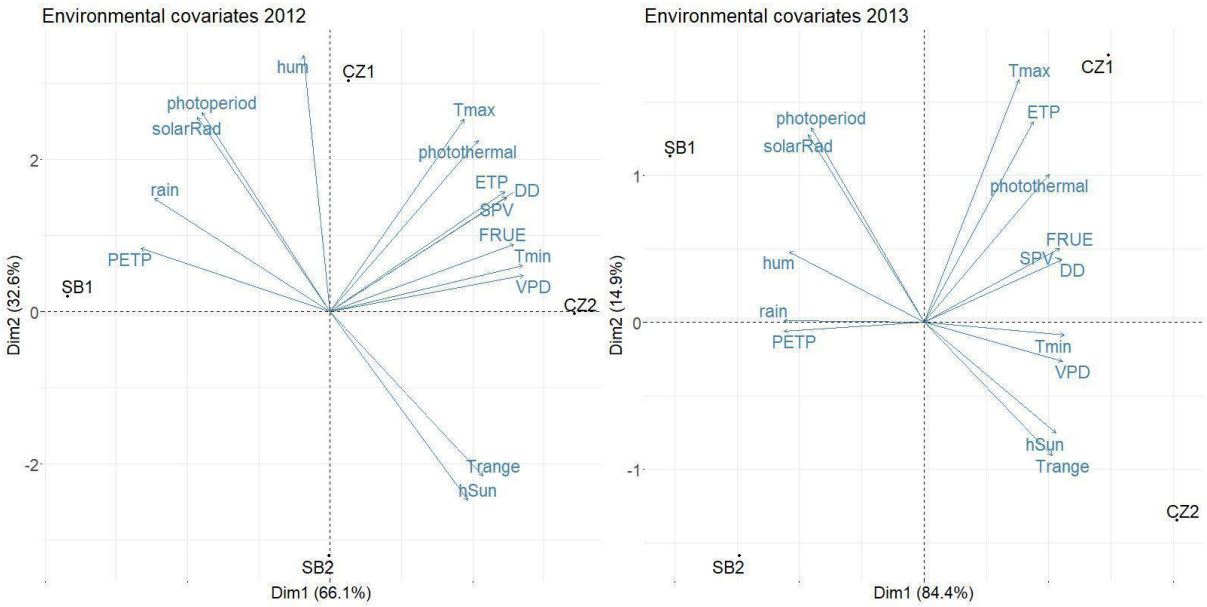

Four environments: Sotuba sowing 1 and 2 (SB1, SB2) and Cinzana (CZ1, CZ2). Environment covariables: cumulated rain over the season (rain), relative humidity (hum), vapour pressure deficit (VPD), slope of saturation VP curve (SVP), potential evapotranspiration (ETP), water deficit (PETP), minimum temperature (Tmin), maximum temperature (Tmax), temperature range (Trange), cumulated degree day (DD), temperature effect on radiation efficiency (FRUE), cumulated observed hour of sun (hsun), photoperiod, solar radiation (solarRad), photothermal (photoperiod * DD)

Supporting tables

Table S1: Consensus map statistics

Chr	N. markers[1]	Length [cM]	N. CO[2] Grinkan	N. CO Kenin-Keni	N. CO. Lata3
1	8154	179.8	6562	2591	2570
2	6717	173.8	5470	2425	2158
3	7258	164.8	5571	2450	2534
4	5593	144.9	4887	2035	2183
5	3940	124.6	4577	2327	1960
6	4380	117.2	4548	2076	1908
7	3674	124.9	3894	1474	1574
8	3533	124	3895	1648	1733
9	4463	123.1	3967	1693	1784
10	3833	134.9	4298	1624	1716
Total	51545	1411.9	47669	20343	20120

1. Number of polymorphic markers in the consensus map
2. N. CO: total number of crossing over estimated in the different single reference BCNAM (Grinkan, Kenin-Keni, Lata3)

Table S2: Number of QTL detected for the traits and reference genotype by year combinations. Total R^2 explained by the QTL are provided in parenthesis.

	FLAG	PH	NODE_N	NODE_L	PED	PAN	GWGH	YIELD
Grinkan 2012	6 (48.9)	3 (48)	4 (17.6)	2 (47.1)	6 (31.2)	5 (8.5)	3 (13.5)	3 (5.4)
Grinkan 2013	4 (32.1)	4 (44.5)	1 (9.6)	2 (42.6)	2 (21.1)	1 (4.6)	0	2 (7.3)
Kenin-Keni 2012	6 (53.4)	2 (9.6)	2 (16.8)	3 (18.8)	3 (14.3)	2 (5.2)	2 (7.9)	1 (3.9)
Kenin-Keni 2013	2 (35.5)	2 (12.7)	2 (22.3)	0	2 (16.9)	1 (5.8)	0	1 (5.9)
Lata3	4 (50.3)	2 (20.1)	2 (13.7)	1 (11)	2 (10.2)	0	6 (30.4)	4 (14.3)

Tables S3: Within cross variance components: genotypic variance (σ_g^2) genotype by environment variance (σ_{ge}^2), error variance (σ_e^2) and heritability (h2) of the different populations. Empty cells correspond to traits that have not been evaluated in a specific population.

Grinkan part characterized in 2012

		Flag leaf [d]				Plant height [cm]				Peduncle length [cm]				Panicle length [cm]				Grain weight [g]				Grain yield [ton/ha]			
Grinkan	N	Av	σ_g^2	σ_{ge}^2	h^2	Av	σ_g^2	σ_{ge}^2	h^2	Av	σ_g^2	σ_{ge}^2	h^2	Av	σ_g^2	σ_{ge}^2	h^2	Av	σ_g^2	σ_{ge}^2	h^2	Av	σ_g^2	σ_{ge}^2	h^2
Fara	117	83.6	15.9	13.8	0.82	175.7	1360.1	662.6	0.89	36.8	23.2	33.3	0.74	30.7	8.7	22.6	0.61	25.3	3.2	3.1	0.67	1.8	0.3	0.9	0.55
E36-1	125	76.3	35.0	14.7	0.91	166.6	738.3	645.0	0.82	34.6	20.7	35.1	0.7	28.0	4.3	11.3	0.6	25.4	2.9	2.8	0.68	2.5	0.2	1.1	0.41
IS15401	113	80.4	8.0	7.8	0.8	166.8	615.9	624.3	0.8	34.3	22.0	33.6	0.72	28.9	3.4	14.9	0.48	23.5	3.9	2.5	0.76	2.0	0.2	0.8	0.44
IS23540	61	77.8	15.9	9.4	0.87	176.3	1098.6	641.6	0.87	40.2	25.4	26.5	0.79	28.3	1.6	12.7	0.34	24.4	5.0	2.2	0.82	2.3	0.0	1.3	0.04
B35	118	79.1	25.4	19.9	0.84	156.7	888.6	489.9	0.88	38.1	36.4	36.0	0.8	27.6	5.7	13.0	0.64	23.7	4.6	1.4	0.86	1.5	0.2	0.5	0.6
Kono.	134	78.9	6.8	6.2	0.81	180.7	1837.9	823.9	0.9	35.0	36.8	25.5	0.85	29.1	8.0	12.7	0.72	26.8	6.1	3.7	0.77	2.1	0.2	0.9	0.44
SC566-14	142	74.5	53.5	23.9	0.9	173.2	1335.7	564.3	0.9	39.7	60.6	39.5	0.86	28.5	5.5	16.5	0.57	24.1	2.4	2.0	0.7	2.0	0.2	0.7	0.46
Framida	140	76.2	19.5	6.5	0.92	172.6	1077.2	445.4	0.91	36.5	24.3	19.4	0.83	28.6	6.8	9.5	0.74	24.5	2.0	3.6	0.52	2.2	0.1	0.7	0.35
CSM417	160	75.9	16.8	5.8	0.92	179.1	1974.4	946.5	0.89	40.4	45.2	35.9	0.83	30.8	5.1	22.3	0.48					2.1	0.2	0.9	0.41
CSM63	67	75.3	28.8	15.0	0.89	187.1	1697.7	1250.4	0.84	41.4	57.0	32.2	0.88	31.6	3.9	23.8	0.4	23.1	1.6	4.0	0.44	1.9	0.0	1.0	0
CSM388	149	76.6	24.1	4.8	0.95	201.7	1779.5	1283.5	0.85	40.5	30.6	41.5	0.75	32.0	5.2	21.0	0.5	23.2	1.7	3.1	0.52	2.2	0.1	1.0	0.28

Gadiaba	135	80.1	9.5	4.6	0.89	192.6	2466.6	1211.0	0.89	38.3	41.8	42.0	0.8	27.5	7.7	11.1	0.74	23.7	2.7	2.6	0.67	2.2	0.1	0.7	0.35
Wth Kaur	137	79.1	12.4	6.2	0.89	171.8	1780.4	663.7	0.91	39.5	87.6	31.2	0.92	28.7	4.6	12.8	0.59	24.3	4.7	3.7	0.72	2.2	0.2	0.7	0.54
Average	123	78.0	20.9	10.6	0.88	177.0	1434.7	788.6	0.87	38.1	39.3	33.2	0.81	29.3	5.4	15.7	0.57	24.3	3.4	2.9	0.68	2.1	0.1	0.9	0.37

Kenin-Keni part characterized in 2012

		Flag leaf [d]				Plant height [cm]				Peduncle length [cm]				Panicle length [cm]				Grain weight [g]				Grain yield [ton/ha]			
Keni-Keni	N	Av	σ_g^2	σ_{ge}^2	h^2	Av	σ_g^2	σ_{ge}^2	h^2	Av	σ_g^2	σ_{ge}^2	h^2	Av	σ_g^2	σ_{ge}^2	h^2	Av	σ_g^2	σ_{ge}^2	h^2	Av	σ_g^2	σ_{ge}^2	h^2
Fara	134	79.1	34.0	7.0	0.95	245.7	705.2	689.7	0.8	59.7	20.1	55.4	0.59	37.3	3.5	26.7	0.34	22.9	3.8	3.0	0.72	2.0	0.3	0.7	0.6
E36-1	144	70.0	37.8	11.1	0.93	207.9	1044.0	758.4	0.85	51.3	69.0	43.0	0.87	35.1	7.9	23.6	0.57	21.0	2.8	2.2	0.71	2.1	0.1	0.7	0.39
IS15401	138	75.0	23.3	9.0	0.91	223.1	642.9	577.3	0.82	55.7	25.2	45.3	0.69	35.6	4.3	29.6	0.37	22.7	2.3	2.5	0.65	2.2	0.1	0.8	0.27
B35	79	71.6	17.0	19.3	0.78	205.4	898.9	1324.1	0.73	55.1	51.4	61.6	0.77	36.6	3.4	39.4	0.26	20.3	4.0	4.2	0.65	1.7	0.2	0.4	0.65
CSM417	80	71.4	1.7	6.3	0.52	241.7	441.5	1040.8	0.63	64.4	10.1	44.8	0.47	40.0	5.7	41.4	0.36					2.4	0.0	1.1	0
Average	115	73.4	22.8	10.5	0.82	224.8	746.5	878.1	0.77	57.2	35.2	50.0	0.68	36.9	5.0	32.1	0.38	21.7	3.2	3.0	0.68	2.1	0.1	0.8	0.38

Grinkan part characterized in 2013

		Flag leaf [d]				Plant height [cm]				Peduncle length [cm]				Panicle length [cm]				Grain weight [g]				Grain yield [ton/ha]			
	N	Av	σ_g^2	σ_{ge}^2	h^2	Av	σ_g^2	σ_{ge}^2	h^2	Av	σ_g^2	σ_{ge}^2	h^2	Av	σ_g^2	σ_{ge}^2	h^2	Av	σ_g^2	σ_{ge}^2	h^2	Av	σ_g^2	σ_{ge}^2	h^2
E36-1	46	70.2	31.7	7.1	0.95	155.29	395.35	262	0.86	31.6	13.8	15.4	0.78	27.1	5.07	5.83	0.78					1.9	0.04	0.42	0.29
V33/08	67	73.1	6.5	6.1	0.81	157.43	655.28	555.2	0.83	36.1	35.06	44.9	0.76	29.9	7.63	9.1	0.77					1.5	0.05	0.46	0.29
Kalaban	115	70.4	19.2	7.1	0.92	153.5	461.43	318.5	0.85	35.2	11.75	28.9	0.62	26.7	2.02	9.09	0.47					1.68	0.05	0.44	0.31
Malisor	95	72.3	14.7	17.6	0.77	142.77	139.03	259.7	0.68	31.9	18.73	19.4	0.79	26.7	2.53	8.9	0.53	17.1	5.6	42.1	0.21	1.68	0.02	0.41	0.18
BimbG	100	79	15.2	10.9	0.85	177.86	1001.7	603.9	0.87	35.9	23.85	28.3	0.77	30.5	10.9	10.44	0.81	19.3	16.2	23.4	0.58	1.09	0.22	0.35	0.71
Hafijega	84	71.6	25.2	10.3	0.91	165.26	1310.7	614.2	0.9	35.7	34.89	26.8	0.84	31.2	9.57	11.31	0.77					1.27	0.1	0.38	0.53
CSM_388	47	69.5	24.5	6.5	0.94	185.67	1540.3	661	0.9	37.9	44.31	27.7	0.86	30.1	5.53	8.04	0.73					1.73	0.07	0.57	0.33
Sh Kaur	50	73.9	5.1	5.6	0.79	161.13	843.1	618.5	0.85	34.8	35.49	41.8	0.77	29	3.46	12.68	0.52					1.39	0.19	0.45	0.63
average	75.5	72.5			0.87	162.36			0.84	34.9			0.77	28.9			0.67	18.2			0.39	1.53			0.41

Kenin-Keni part characterized in 2013

		Flag leaf [d]				Plant height [cm]				Peduncle length [cm]				Panicle length [cm]				Grain weight [g]				Grain yield [ton/ha]			
	N	Av	σ_g^2	σ_{ge}^2	h^2	Av	σ_g^2	σ_{ge}^2	h^2	Av	σ_g^2	σ_{ge}^2	h^2	Av	σ_g^2	σ_{ge}^2	h^2	Av	σ_g^2	σ_{ge}^2	h^2	Av	σ_g^2	σ_{ge}^2	h^2
Sangatigui	35	68.2	28.3	8.7	0.93	213.36	477.75	358.7	0.84	57.2	17.01	50.2	0.58	39.99	4.97	15.58	0.56					1.49	0.14	0.46	0.55
IS23540	67	70.2	25.1	12.7	0.89	210.72	297.61	430.5	0.73	48.7	40.06	41.4	0.79	34.84	6.72	12.46	0.68					1.54	0.13	0.44	0.54
Kalaban	80	67.2	16.7	8.6	0.89	196	928.98	367.6	0.91	50.2	47.95	42.3	0.82	34.79	10.6	13.87	0.75					1.71	0.06	0.53	0.3
Malisor	66	69.8	20.9	22.8	0.79	182.62	769.19	421.5	0.88	48.7	54.06	28.5	0.88	34.85	8.45	16.75	0.67	15.3	2.2	19.8	0.18	1.4	0.12	0.53	0.47
BimbG	73	74.9	36.3	10.5	0.93	218.56	546.97	414	0.84	52.3	13.23	57.8	0.48	39.82	5.1	19.71	0.51	16.4	0	38.1	0	1.43	0.33	0.57	0.7
CSM417	23	66.5	0.55	6.5	0.25	223.3	407	376.8	0.81	59.6	31.63	65.2	0.66	40.91	13.2	12.68	0.81					2.06	0.25	0.37	0.73
average	57.3	69.5			0.78	207.43			0.84	52.8			0.7	37.53			0.66	15.8			0.09	1.61			0.55

Lata3 population characterized in 2013

		Flag leaf [d]				Plant height [cm]				Peduncle length [cm]				Panicle length [cm]				Grain weight [g]				Grain yield [ton/ha]			
Lata	N	Av	σ_g^2	σ_{ge}^2	h^2	Av	σ_g^2	σ_{ge}^2	h^2	Av	σ_g^2	σ_{ge}^2	h^2	Av	σ_g^2	σ_{ge}^2	h^2	Av	σ_g^2	σ_{ge}^2	h^2	Av	σ_g^2	σ_{ge}^2	h^2
Grinkan	95	81.2	24.7	0.3	0.97	238.2	1596.8	105.8	0.93	42.8	27.2	1.4	0.88	29.2	6.1	1.3	0.77	2.1	0.04	0.01	0.86	2.47	0.31	0.05	0.8
IS23645	54	83.2	40.3	0.9	0.97	250.6	3387.6	1.9	0.97	41.0	49.1	2.1	0.89	30.8	9.8	0.0	0.84	1.86	0.08	0.01	0.92	1.46	0.22	0.09	0.78
SK5912	76	86.0	34.4	1.4	0.97	248.9	1170.1	74.6	0.92	43.4	27.6	0.3	0.9	28.1	6.1	1.7	0.73	2.33	0.09	0.01	0.91	2.07	0.21	0.08	0.77
DouaG	72	83.7	24.9	0.9	0.97	276.9	558.5	0.0	0.87	48.6	23.2	0.3	0.87	30.5	4.4	0.0	0.75	2.13	0.05	0	0.95	2.32	0.09	0.07	0.56
Framida	60	81.6	56.6	1.3	0.98	245.2	369.7	0.0	0.78	42.2	33.1	0.8	0.92	28.0	6.4	1.0	0.76	2.28	0.07	0.01	0.91	2.01	0.14	0.16	0.56
Gnossiconi	67	79.9	18.1	0.6	0.96	269.5	269.8	64.0	0.74	46.5	14.1	0.0	0.77	29.2	3.6	0.0	0.68	2.24	0.04	0	0.89	2.37	0.05	0.05	0.4
IS15401	89	85.2	49.1	1.6	0.97	274.7	799.7	7.5	0.91	43.8	24.3	4.3	0.83	28.5	5.9	0.0	0.87	2.36	0.06	0.01	0.9	2.45	0.19	0.13	0.67
IS23540	68	82.0	52.9	3.6	0.96	237.7	1011.8	20.2	0.93	39.8	30.0	2.9	0.88	26.0	4.6	1.6	0.69	2.24	0.08	0.01	0.91	2.18	0.11	0.06	0.6
Fara	82	90.0	42.9	0.9	0.97	295.2	924.6	70.8	0.86	47.2	22.9	0.0	0.86	32.2	7.6	0.5	0.78	2.25	0.07	0.01	0.91	2.07	0.18	0.05	0.74
Ngolofing	76	82.0	2.1	0.0	0.8	275.8	331.2	0.0	0.82	44.9	12.9	0.0	0.81	30.8	3.1	0.0	0.66	2.2	0.02	0.01	0.76	2.28	0.03	0.09	0.31
Sambalma	88	86.3	31.2	0.0	0.97	265.9	628.5	32.5	0.88	43.0	18.0	1.7	0.84	32.7	7.3	0.9	0.78	2.27	0.04	0.01	0.84	2.46	0.14	0.07	0.65
SC566-14	69	82.5	74.7	5.8	0.96	253.5	1465.7	124.1	0.92	43.0	28.3	0.3	0.89	28.1	10.9	0.1	0.88	2.22	0.04	0.01	0.88	2.21	0.28	0.07	0.78
average	74	83.6	37.7	1.43	0.95	261	1042.8	41.8	0.88	43.9	25.9	1.2	0.9	29.5	6.3	0.6	0.77	2.21	0.06	0.01	0.89	2.2	0.16	0.08	0.64

Tables S4: Lists of the five most influential environmental covariables on each trait

Table of most influential EC on traits with recurrent parent, year of phenotyping, trait, most influential EC in order of influence, average R2 trait-EC of the different tested window, R2 trait-EC of the best window, starting and end day of the best sowing window, value of the EC in the environment during the best window

RP	year	trait	EC	R2_av	R2_win	start	end	SB1	SB2	CZ1	CZ2
Grinkan	2012	FLAG	photoperiod	0.997	1	28	67	12.4	12.1	12.4	12.2
Grinkan	2012	FLAG	solarRad	0.844	0.999	9	88	3003.5	2928	3002.5	2937.1
Grinkan	2012	FLAG	Trange	0.82	1	3	82	8.8	9.4	8.9	9.4
Grinkan	2012	FLAG	hSun	0.629	0.997	1	80	512.1	542.9	511.3	538
Grinkan	2012	FLAG	rain	0.378	0.959	17	76	573.6	417.4	540.4	408.7
Grinkan	2012	PH	photoperiod	0.775	0.895	1	20	12.7	12.5	12.7	12.6
Grinkan	2012	PH	solarRad	0.746	0.995	23	42	756.5	752.6	758.9	754.5
Grinkan	2012	PH	Trange	0.628	0.985	6	65	8.8	8.9	8.7	8.8
Grinkan	2012	PH	hSun	0.621	0.999	16	75	389.4	407.2	376.7	398.8
Grinkan	2012	PH	hum	0.523	0.999	14	113	77.2	74	79.8	75.4
Grinkan	2012	N_N	photoperiod	0.819	0.915	1	20	12.7	12.5	12.7	12.6
Grinkan	2012	N_N	solarRad	0.758	0.901	1	60	2266.3	2248.7	2272.4	2255
Grinkan	2012	N_N	Trange	0.633	0.974	46	65	8.8	9.8	9	9.3
Grinkan	2012	N_N	hSun	0.62	0.994	7	66	376.3	396.7	373.6	383.1
Grinkan	2012	N_N	hum	0.388	0.841	19	118	76.9	73.1	78.8	74.2
Grinkan	2012	N_L	FRUE	0.32	0.956	34	113	1	1	1	1
Grinkan	2012	N_L	rain	0.291	0.967	9	48	359.8	419.7	436.6	396.7
Grinkan	2012	N_L	PETP	0.275	0.963	5	24	4.7	-0.5	-1.8	1.4
Grinkan	2012	N_L	ETP	0.168	0.644	74	93	9.1	9.9	10.3	10.1
Grinkan	2012	N_L	hSun	0.145	0.919	22	41	137.2	120.2	114.8	124.6

Grinkan	2012	PAN	PETP	0.356	0.999	8	67	-0.4	0.2	0.5	-1.9
Grinkan	2012	PAN	rain	0.345	0.995	7	66	516.6	539.1	554.9	449.7
Grinkan	2012	PAN	VPD	0.322	0.634	52	71	0.8	1	0.9	1.3
Grinkan	2012	PAN	Tmin	0.295	0.549	68	87	31.3	33.2	32.4	35.8
Grinkan	2012	PAN	hum	0.277	0.924	7	26	78.6	78.6	77.9	81.9
Grinkan	2012	PED	DD	0.857	0.979	88	107	377	396.8	433.4	452.4
Grinkan	2012	PED	SVP	0.85	0.974	88	107	0.2	0.2	0.2	0.3
Grinkan	2012	PED	Tmin	0.809	0.993	19	78	30.6	31.3	31.9	32.4
Grinkan	2012	PED	ETP	0.788	1	53	112	9.1	9.5	9.9	10.1
Grinkan	2012	PED	FRUE	0.772	0.997	4	63	1	1	1	1
Grinkan	2012	YIELD	Trange	0.382	0.995	20	39	8.6	8.6	8.3	8.9
Grinkan	2012	YIELD	hSun	0.352	0.976	2	61	376.3	377	371.1	381.7
Grinkan	2012	YIELD	hum	0.346	0.869	69	88	76.4	74.5	83.2	72.4
Grinkan	2012	YIELD	rain	0.33	0.998	5	64	509.8	524.2	584.4	460.2
Grinkan	2012	YIELD	photoperiod	0.32	0.321	2	101	12.4	12.1	12.3	12.1

RP	year	trait	EC	R2_av	R2_win	start	end	SB1	SB2	CZ1	CZ2
Grinkan	2013	FLAG	photoperiod	0.92	0.926	15	34	12.6	12.4	12.5	12.3
Grinkan	2013	FLAG	solarRad	0.693	0.866	64	83	741.5	710.8	708.1	674.2
Grinkan	2013	FLAG	hSun	0.623	0.991	61	80	145	175.7	163.2	181.5
Grinkan	2013	FLAG	hum	0.584	0.993	9	28	75.9	80.7	78.3	81.8
Grinkan	2013	FLAG	Trange	0.514	0.954	58	77	8.2	10.4	9.7	12
Grinkan	2013	PH	solarRad	0.887	0.961	41	60	755.5	742.5	741.7	718.6
Grinkan	2013	PH	photoperiod	0.874	0.884	5	24	12.7	12.5	12.6	12.4
Grinkan	2013	PH	Trange	0.848	1	16	75	8.3	8.7	9.1	10.2
Grinkan	2013	PH	VPD	0.822	0.998	66	85	1	1.3	1.7	2.6
Grinkan	2013	PH	hum	0.814	0.998	45	64	80.7	79.1	77.9	74.6
Grinkan	2013	N_N	photoperiod	0.774	0.812	1	20	12.7	12.6	12.6	12.4
Grinkan	2013	N_N	solarRad	0.65	0.726	85	104	712.6	670	665.8	630.8
Grinkan	2013	N_N	hSun	0.565	0.995	2	21	155.6	130.1	147.8	128
Grinkan	2013	N_N	Trange	0.523	0.873	58	77	8.2	10.4	9.7	12
Grinkan	2013	N_N	hum	0.452	0.998	3	42	77.1	80	78.3	80.6
Grinkan	2013	N_L	VPD	0.781	0.976	4	63	1	1	1.3	1.3
Grinkan	2013	N_L	SVP	0.772	0.998	12	51	0.2	0.2	0.2	0.2
Grinkan	2013	N_L	DD	0.772	0.998	13	52	764.4	742.9	786.3	807.1
Grinkan	2013	N_L	Tmin	0.754	0.998	13	52	31.2	30.6	32.2	32.8
Grinkan	2013	N_L	photothermal	0.728	0.997	25	64	9380.2	9144.8	9741.9	9961.7
Grinkan	2013	PAN	SVP	0.814	0.994	11	50	0.2	0.2	0.2	0.2
Grinkan	2013	PAN	DD	0.813	0.991	11	50	762.5	740.9	791	804

Grinkan	2013	PAN	VPD	0.795	0.995	5	64	1	0.9	1.3	1.3
Grinkan	2013	PAN	Tmin	0.79	0.998	13	52	31.2	30.6	32.2	32.8
Grinkan	2013	PAN	photothermal	0.765	0.998	25	64	9380.2	9144.8	9741.9	9961.7
Grinkan	2013	PED	SVP	0.804	0.993	12	51	0.2	0.2	0.2	0.2
Grinkan	2013	PED	DD	0.803	0.991	20	59	755.8	739.9	784.7	812.5
Grinkan	2013	PED	VPD	0.801	0.989	5	64	1	0.9	1.3	1.3
Grinkan	2013	PED	Tmin	0.788	1	13	52	31.2	30.6	32.2	32.8
Grinkan	2013	PED	photothermal	0.75	0.998	25	64	9380.2	9144.8	9741.9	9961.7
Grinkan	2013	YIELD	hum	0.746	1	10	69	79.2	79.6	78.9	76.9
Grinkan	2013	YIELD	VPD	0.736	0.991	33	52	0.9	0.9	1.1	1.5
Grinkan	2013	YIELD	solarRad	0.693	0.893	21	40	756.5	755	755.8	744.7
Grinkan	2013	YIELD	Trange	0.651	0.986	24	43	8.3	7.8	8.5	9.7
Grinkan	2013	YIELD	Tmin	0.642	0.934	26	45	31.1	30.4	31.8	33.1

RP	year	trait	EC	R2_av	R2_win	start	end	SB1	SB2	CZ1	CZ2
Kenin-K	2012	FLAG	photoperiod	0.995	0.999	43	62	12.4	12.1	12.4	12.1
Kenin-K	2012	FLAG	solarRad	0.817	0.997	49	68	753.5	728.2	752.4	730.7
Kenin-K	2012	FLAG	Trange	0.8	1	3	82	8.8	9.4	8.9	9.4
Kenin-K	2012	FLAG	hSun	0.58	0.994	1	80	512.1	542.9	511.3	538
Kenin-K	2012	FLAG	photothermal	0.553	0.997	12	31	2600.1	2224.2	2598.4	2282.5
Kenin-K	2012	PH	hum	0.551	0.998	48	87	77.2	75.8	83.9	77.8
Kenin-K	2012	PH	Tmax	0.504	0.996	19	38	22.2	21.9	23.9	22.5
Kenin-K	2012	PH	solarRad	0.414	0.959	18	37	756	754.6	758.7	756.5
Kenin-K	2012	PH	photoperiod	0.371	0.523	1	20	12.7	12.5	12.7	12.6
Kenin-K	2012	PH	hSun	0.365	0.985	12	71	393.5	396.2	375.2	392.6
Kenin-K	2012	N_N	photoperiod	0.684	0.836	1	20	12.7	12.5	12.7	12.6
Kenin-K	2012	N_N	solarRad	0.668	0.994	9	48	1511.7	1505.7	1516.7	1509.6
Kenin-K	2012	N_N	hSun	0.54	0.994	15	74	389.3	405.2	380.1	395.2
Kenin-K	2012	N_N	hum	0.52	0.991	7	106	77.7	74.8	80.4	76.8
Kenin-K	2012	N_N	Trange	0.517	0.97	6	65	8.8	8.9	8.7	8.8
Kenin-K	2012	N_L	FRUE	0.593	0.972	3	22	1	1	1	1
Kenin-K	2012	N_L	rain	0.439	0.999	15	54	277	404.2	409.4	377.2
Kenin-K	2012	N_L	PETP	0.438	0.976	18	57	-2.1	1	0.7	0.3
Kenin-K	2012	N_L	ETP	0.397	0.895	75	94	9.2	9.9	10.2	10
Kenin-K	2012	N_L	Tmin	0.344	0.55	47	66	30.5	31.8	31.6	32.5
Kenin-K	2012	PAN	photoperiod	0.937	0.941	33	52	12.5	12.2	12.5	12.2
Kenin-K	2012	PAN	solarRad	0.843	0.932	56	75	749.7	717.6	747.4	720.2

Kenin-K	2012	PAN	Trange	0.802	0.999	56	75	8.8	10.2	9.2	9.8
Kenin-K	2012	PAN	hSun	0.714	0.995	53	72	131.9	147.5	133.9	142.4
Kenin-K	2012	PAN	photothermal	0.544	0.986	17	36	2676.2	2350.1	2577.4	2425.7
Kenin-K	2012	PED	rain	0.268	1	34	53	162.9	255.4	262.2	131
Kenin-K	2012	PED	PETP	0.261	0.999	37	56	-2	3.1	3.9	-3.5
Kenin-K	2012	PED	hum	0.131	0.601	7	26	78.6	78.6	77.9	81.9
Kenin-K	2012	PED	photothermal	0.127	0.982	27	46	2525.5	2194.5	2236.6	2627.2
Kenin-K	2012	PED	hSun	0.113	0.989	23	62	258.3	251.5	249.5	261.6
Kenin-K	2012	YIELD	FRUE	0.385	0.964	14	113	1	1	1	1
Kenin-K	2012	YIELD	Tmax	0.305	0.736	12	31	21.8	22	23.9	22.9
Kenin-K	2012	YIELD	ETP	0.288	0.886	7	26	8.6	8.9	10	8.8
Kenin-K	2012	YIELD	hum	0.267	0.774	59	78	78	78	84.6	79
Kenin-K	2012	YIELD	DD	0.254	0.724	7	26	358.5	364	403.8	384.4

RP	year	trait	EC	R2_av	R2_win	start	end	SB1	SB2	CZ1	CZ2
Kenin-K	2013	FLAG	photoperiod	0.975	0.978	4	43	12.6	12.4	12.5	12.3
Kenin-K	2013	FLAG	solarRad	0.842	0.999	55	74	749.1	725.3	723.4	692.8
Kenin-K	2013	FLAG	hSun	0.69	0.996	14	73	416.7	442.1	446.7	487.8
Kenin-K	2013	FLAG	Trange	0.686	0.998	36	75	8.1	9.2	9.4	10.7
Kenin-K	2013	FLAG	hum	0.645	0.999	49	68	80.7	77.7	77	72.8
Kenin-K	2013	PH	photoperiod	0.966	0.972	23	42	12.6	12.3	12.4	12.2
Kenin-K	2013	PH	solarRad	0.83	0.945	88	107	707.3	663.8	659.4	625.2
Kenin-K	2013	PH	Trange	0.714	0.976	58	77	8.2	10.4	9.7	12
Kenin-K	2013	PH	hSun	0.707	0.999	54	73	141.3	162.2	157.5	172.8
Kenin-K	2013	PH	hum	0.627	0.961	9	28	75.9	80.7	78.3	81.8
Kenin-K	2013	N_N	photoperiod	0.769	0.773	32	51	12.5	12.2	12.3	12
Kenin-K	2013	N_N	solarRad	0.584	0.737	90	109	703.7	659.7	655.2	621.6
Kenin-K	2013	N_N	hSun	0.581	1	67	86	159.1	176.1	167.9	175.9
Kenin-K	2013	N_N	Trange	0.487	0.808	58	77	8.2	10.4	9.7	12
Kenin-K	2013	N_N	hum	0.401	0.999	5	44	77.4	80.2	78.8	80.2
Kenin-K	2013	N_L	photoperiod	0.956	0.96	1	80	12.5	12.2	12.3	12.1
Kenin-K	2013	N_L	solarRad	0.911	0.991	55	74	749.1	725.3	723.4	692.8
Kenin-K	2013	N_L	Trange	0.852	1	25	104	8.8	10.1	10.6	12.4
Kenin-K	2013	N_L	hum	0.777	0.998	49	68	80.7	77.7	77	72.8
Kenin-K	2013	N_L	Tmin	0.776	0.99	62	81	31	33	34.3	36.7
Kenin-K	2013	PAN	VPD	0.85	1	18	77	1	1	1.3	1.6
Kenin-K	2013	PAN	Tmin	0.832	1	33	52	30.6	30.7	32	33.7

Kenin-K	2013	PAN	Trange	0.8	0.994	26	45	7.9	8	8.5	9.6
Kenin-K	2013	PAN	solarRad	0.782	0.865	34	53	756.7	748.4	748.2	729.3
Kenin-K	2013	PAN	hum	0.774	0.998	6	105	78.2	77.4	72.8	67.1
Kenin-K	2013	PED	SVP	0.714	0.99	12	51	0.2	0.2	0.2	0.2
Kenin-K	2013	PED	photothermal	0.713	1	21	60	9447.8	9132.6	9683.7	9869.8
Kenin-K	2013	PED	DD	0.713	0.992	12	51	763.3	741.5	788.6	804.8
Kenin-K	2013	PED	VPD	0.708	0.994	11	50	1.1	0.9	1.1	1.2
Kenin-K	2013	PED	Tmin	0.674	0.988	9	48	31.2	30.4	32.1	32.5
Kenin-K	2013	YIELD	photoperiod	0.714	0.807	1	20	12.7	12.6	12.6	12.4
Kenin-K	2013	YIELD	solarRad	0.664	0.727	1	60	2266.2	2254.1	2256.4	2220.1
Kenin-K	2013	YIELD	hum	0.502	0.996	5	24	75.4	80.3	75.7	82.1
Kenin-K	2013	YIELD	hSun	0.493	0.98	1	20	154.4	131.4	147.7	126.4
Kenin-K	2013	YIELD	Trange	0.491	0.867	57	76	8.4	10.2	9.6	12

Tables S5: QTL parental allele effects detailed statistics (significant effect, QTLxE effect, QTLxEC effect)

Total significant parental alleles

	FLAG	PH	NODE_N	NODE_L	PED	PAN	GWGH	YIELD	Total
GR2012	39	29	25	22	43	40	24	21	243
GR2013	17	17	5	12	9	5	0	8	73
KK2012	19	10	8	9	7	6	0	3	62
KK2013	9	5	9	0	7	3	0	1	34
Lata	28	8	17	5	12	0	44	26	140
Total	112	69	64	48	78	54	68	59	552

Proportion of significant parental alleles

	FLAG	PH	NODE_N	NODE_L	PED	PAN	GWGH	YIELD	Total
GR2012	0.5	0.74	0.48	0.85	0.55	0.62	0.67	0.54	0.62
GR2013	0.53	0.53	0.62	0.75	0.56	0.62	0	0.5	0.59
KK2012	0.63	1	0.8	0.6	0.47	0.6	0	0.6	0.67
KK2013	0.75	0.42	0.75	0	0.58	0.5	0	0.17	0.53
Lata	0.58	0.33	0.71	0.42	0.5	0	0.61	0.54	0.53
Total	0.6	0.6	0.67	0.65	0.53	0.59	0.64	0.47	0.59

Total significant parental alleles with GxE

	FLAG	PH	NODE_N	NODE_L	PED	PAN	GWGH	YIELD	Total
GR2012	21	14	9	9	21	13	12	14	113
GR2013	5	11	2	6	5	2	0	4	35
KK2012	7	4	3	4	3	2	0	1	24
KK2013	1	4	2	0	3	2	0	0	12
Lata	15	3	2	0	5	0	16	13	54
Total	49	36	18	19	37	19	28	32	238

Proportion of significant parental alleles with GxE

	FLAG	PH	NODE_N	NODE_L	PED	PAN	GWGH	YIELD	Total
GR2012	0.27	0.36	0.17	0.35	0.27	0.2	0.33	0.36	0.29
GR2013	0.16	0.34	0.25	0.38	0.31	0.25	0	0.25	0.28
KK2012	0.23	0.4	0.3	0.27	0.2	0.2	0	0.2	0.26
KK2013	0.08	0.33	0.17	0	0.25	0.33	0	0	0.19
Lata	0.31	0.12	0.08	0	0.21	0	0.22	0.27	0.17
Total	0.21	0.31	0.19	0.25	0.25	0.25	0.28	0.22	0.24

Number of parental alleles with at least one significant EC interaction

	FLAG	PH	NODE_N	NODE_L	PED	PAN	YIELD	Total
GR2012	15	13	3	6	17	5	8	67
GR2013	3	9	2	6	4	1	3	28
KK2012	5	2	3	3	3	1	0	17
KK2013	1	3	1	0	1	0	0	6
Total	24	27	9	15	25	7	11	118

Proportion of parental alleles with at least one significant EC interaction

	FLAG	PH	NODE_N	NODE_L	PED	PAN	YIELD	Total
GR2012	0.18	0.31	0.05	0.21	0.2	0.07	0.19	0.17
GR2013	0.08	0.25	0.22	0.33	0.22	0.11	0.17	0.2
KK2012	0.14	0.17	0.25	0.17	0.17	0.08	0	0.14
KK2013	0.07	0.21	0.07	0	0.07	0	0	0.07
Total	0.12	0.24	0.15	0.24	0.17	0.07	0.09	0.15

Table S6: Number of significant QTL parental allele by environmental covariable interaction

Category		FLAG	PH	NODE_N	NODE_L	PED	PAN	YIELD	Total
Atmospheric	rain	20	0	0	5	12	1	4	42
	hum	4	26	9	0	14	0	9	62
	VPD	0	9	0	6	20	1	3	39
	SVP	0	0	0	6	4	6	0	16
	ETP	0	0	0	6	0	5	0	11
	PETP	0	0	0	5	12	0	0	17
Temperature	Tmin	0	0	0	8	20	6	3	37
	Tmax	0	1	0	0	0	0	0	1
	Trange	23	24	8	0	3	1	7	66

	DD	0	0	0	6	4	6	0	16
	FRUE	0	0	0	5	0	4	0	9
Radiation	hSun	23	16	9	3	2	1	4	58
	photoperiod	22	26	8	0	0	1	7	64
	solarRad	22	27	8	0	1	1	2	61
Photothermal	photothermal	0	1	0	6	4	1	0	12
	Total	114	130	42	56	96	34	39	511

Table S7: Significance of the QTL effect on yield after correction for a component trait (flag leaf appearance or plant height)

We estimated the effect of QTL position on yield an the residual of yield (yield corrected) after correcting for the component trait by using a linear regression.

KK2012 QTL chr 3 74 cM Grain yield flag leaf corrected

		-log10(pval)	
Par	env	yiel d	yield corrected
IS15401	SB1	0.37	0.01
IS15401	SB2	2.46	0.12
IS15401	CZ1	0.96	0.72
IS15401	CZ2	0.37	1.25

GR2012 QTL chr 6 39 cM Grain yield flag leaf corrected

		log10(pval)	
Par	env	yield	yield (corrected)
B35	SB1	0.08	0.9
B35	SB2	0.01	0.82
B35	CZ1	0.88	1.91
B35	CZ2	2.65	0.81
SC566-14	SB1	2.38	10.14
SC566-14	SB2	0.15	1.57
SC566-14	CZ1	5.48	9.21
SC566-14	CZ2	0.01	2.65

Table S8: Sowing dates of the field trials

	2012		2013	
	Sw1	Sw2	Sw1	Sw2
Sotuba	26-Jun	24-Jul	29-Jun	21-Jul
Cinzana	29-Jun	21-Jul	21-Jul	07-Aug
Samanko			28-Jun	
Kolombada			28-Jun	

Table S9: Environmental description of the multi-location trials

Location	lat	lon	year	sowing	cum rain [mm]	av. Humidity [%]	av. temp. [d]	av. maxT [d]	av. minT [d]	av. photop. [h]
Sotuba	12.65	-7.93	2012	Sw1	851.5	77.1	26.6	31.3	21.9	12.3
				Sw2	570.3	74.3	27	32.3	21.7	12.0
			2013	Sw1	799.8	77.7	27.2	31.8	22.6	12.3
				Sw2	698.2	75.7	27.1	32.4	21.9	12.0
Cinzana	13.25	-5.96	2012	Sw1	707.9	79.3	28.1	32.9	23.3	12.3
				Sw2	529.3	75.5	28.7	34.1	23.3	12.0
			2013	Sw1	377.1	70.3	28.7	34.2	23.3	12.0
				Sw2	338.5	65.9	28.7	34.6	22.7	11.9
Samanko	12.53	-8.07	2013	LP	967	79.8*	27.5	33.3	21.7	12.3
				HP	967	79.8*	27.5	33.3	21.7	12.3
Kolombada	12.69	-7.01	2013	std	439.7	77.6*	26.7*	31.2*	22.3*	12.3

*: Synthetic data from Nasapower (Spark 2018)

Table S10: Detail of the phenotyping per population, year environment, and trait

Population	Year	Env	FLAG	PH	NODE_N	NODE_L	PED	PAN	GWGH	YIELD
Grinkan	2012	Sotuba Sw1	X	X	X	X	X	X	X	X
		Sotuba Sw2	X	X	X	X	X	X	X	X
		Cinzana Sw1	X	X	X	X	X	X		X
		Cinzana Sw2	X	X	X	X	X	X		X
	2013	Sotuba Sw1	X	X	X	X	X	X	X	X
		Sotuba Sw2	X	X	X	X	X	X	X	X
		Cinzana Sw1	X	X	X	X	X	X		X
		Cinzana Sw2	X	X	X	X	X	X		X
Kenin-Keni	2012	Sotuba Sw1	X	X	X	X	X	X	X	X
		Sotuba Sw2	X	X	X	X	X	X	X	X
		Cinzana Sw1	X	X	X	X	X	X		X
		Cinzana Sw2	X	X	X	X	X	X		X
	2013	Sotuba Sw1	X	X	X	X	X	X	X	X
		Sotuba Sw2	X	X	X	X	X	X	X	X
		Cinzana Sw1	X	X	X	X	X	X		X
		Cinzana Sw2	X	X	X	X	X	X		X
Lata3	2013	Samanko LP	X	X	X	X	X	X	X	X
		Samanko LP	X	X	X	X	X	X	X	X
		Kolombada	X	X	X	X			X	X

Table S11: List of environmental covariables at the environment trials (Sotuba, Cinzana)

Category	EC	Abbreviation	Unit	Observed/ inferred	Sum/mean
Atmospheric	cumulated rain	cum rain	mm	obs	sum
	humidity	hum	%	obs	mean
	vapour pressure deficit	VPD	kPa	inf	mean
	slope of saturation VP curve	SVP	kPa/d	inf	mean
	potential evapotranspiration	ETP	mm/day	inf	mean
	water deficit	PETP	mm/day	inf	mean
Temperature	minimum temperature	Tmin	d	obs	mean
	maximum temperature	Tmax	d	obs	mean
	temperature range	Trange	d	obs	mean
	cumulated degree day	DD	dd	obs	sum
	T effect on radiation use efficiency	FRUE	0-1	inf	mean
Radiation	cumulated hour of sun	hsun	h	obs	sum
	photoperiod	photo	h	inf	mean
	solar radiation	SolRad	MJ/m^2/day	inf	sum
Photothermal	Photothermal (photoperiod * DD)	photothermal	h*dd	obs	sum

Supporting experimental procedure

Methods S1: Diversity tree construction methodology

This analysis was based on 137'003 SNPs common to the SAP (Boatwright et al. 2022) and SGT (https://www.globalsorghuminitiative.org/) panels. From a merge of these 2 studies, we excluded all wild accessions and kept SNP with less than 20% of missing data and with a Minor Allele Frequency (MAF) higher than 5%. To lighten the matrix without losing too much precision, we pruned with bcftools (Danecek et al, 2021) with these parameters : windows (-w) 1000 and r^2 (-m) bigger than 0.8. The software Darwin (https://darwin.cirad.fr/) were used to calculate the dissimilarity matrix and draw the tree (NJ method).

Methods S2: Phenotype by environmental covariable analysis

To determine the ECs influence on the different traits, we applied the same method as Li et al. (2018), which consists of calculating the correlation between the trait mean across the environments and the EC values (Figure A) inside time windows of different size (20, 40, 60, 80, or 100) starting at different days of the plant cycle (Figure B). For each configuration of population (GR12, GR13, KK12, KK13) x traits we selected the five ECs with the highest average correlation and determined the most influential window and corresponding EC values as the one with the highest EC-trait correlation. Those values were later used in the QTLxEC models.

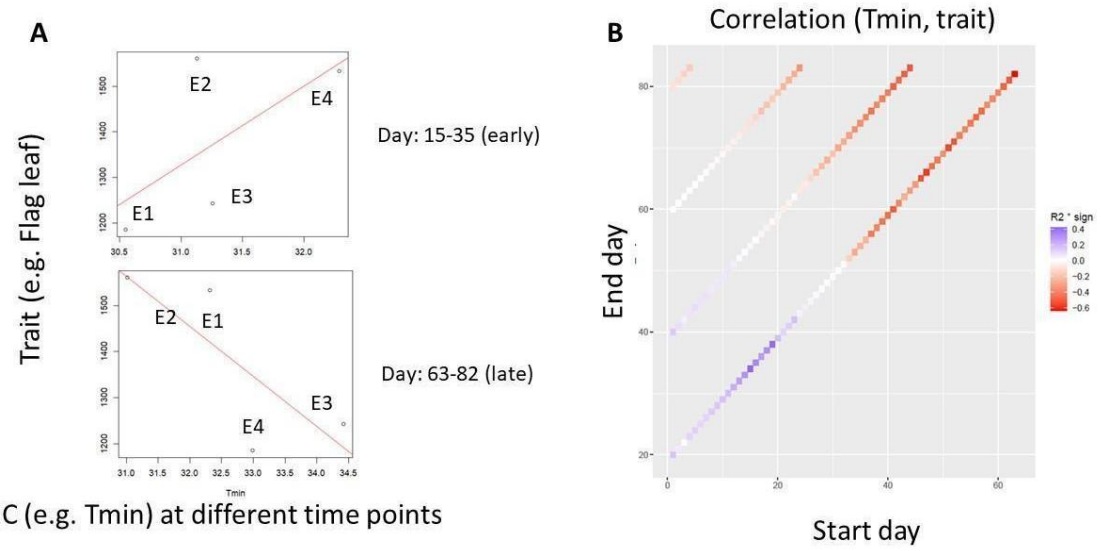

Method S3: QTL detection procedure and QTL detection threshold

For each combination of population and trait, we performed the following QTL detection procedure:

a) Simple interval mapping (SIM) scan.

b) Selection of cofactors based on the SIM scan profile. Positions with -log10(p-val) larger than the threshold were selected. We selected a maximum of one cofactor per chromosome.

c) Cofactor and QTL detection threshold. The false positive rate for individual cofactors/QTL detection (Type I error) was set to alpha = 0.05. To account for multiple tests, we applied a correction accounting for the number of independent tests, so alpha = 0.05/Meff, where Meff is calculated according to the procedure defined by Li and Ji (2005).

d) Composite interval mapping scan using the selected cofactors

e) The final QTLs were recursively selected per chromosome using the -log10(pval) results of the CIM profile. We first selected the most significant position and then applied an exclusion window of 20 cM around the QTL position. We continued to search for the next most significant position until no more significant positions could be selected.

f) Estimation of the QTL effects. We estimated the QTL effect simultaneously by including all detected QTLs in the estimated model. We also estimated the global R squared of the whole QTL set as well as partial R squared for each final selected QTL position using a linear model. The R squared values were adjusted for the number of degrees of freedom.

QTL detection threshold

Population	**-log10(p-val)**
GR2012	4.647689
GR2013	4.483628
KK2012	4.181491
KK2013	4.187031
Lata	4.428637

Methods S4: Approximate mixed model computation and QTL test statistic

To reduce the computational power needed to perform the QTL scan we implemented an approximate mixed model computation similar to the generalized least square strategy implemented in Kruijer et al. (2015). The procedure consists of estimating a general VCOV ($\hat{V}$) using model 2 without the tested QTL position, which means estimating the VCOV of model 2 without the QTL term for the SIM scan and the same model with selected cofactors for the CIM scan. The statistical significance of the tested QTL positions and the different allelic effect was obtained by using $\hat{V}$ to get the following Wald statistic $W_Q = \beta^T V(\beta)^{-1}\beta$, where $\beta = (X^T V^{-1} X)^{-1} X^T V^{-1} y$, $V(\beta) = (X^T V^{-1} X)^{-1}$, X represents the fixed effect matrix including the QTL position, and y the vector of phenotypic values. W_Q follows a chi-square distribution with degree of freedom equal to the number of tested QTL allelic effects ($(N_{par} - 1) * N_{env}$ for the main QTL term).

Method S5: Synonyms of the parental lines' names

This Study	germplasm_ Name	VARNM	ALNM	BCNAM_PROJECT _ICRISAT_CODE	BCNAM_PROJECT_ IER_CODE	ICRISAT_ACCN O	USDA_ACCNO
Grinkan	Grinkan		02-SB-F4DT-275	1085	V12		
Kenin-Keni	Keninkeni		V248/08		V13		
Lata3	Lata3	Lata 3	GPN01 S01 267-9-3-3-vr	1097	V14		
Fara-Fara	IS24887	Fara Fara		1096	V20	IS24887	
E36-1	E36-1				V15	IS30469	
IS15401	IS15401	Soumalemba		1086	V17	IS15401	
IS23540	IS23540	Ganga		1087	V18	IS23540	
B35	B35				V33		
Konotene	Konotene				V5	IS25705	
SC566-14	SC566-14			1089	V19		PI533871
Framida	Framida			1084	V16		
CSM417	CSM417	Tiemantieteli			V11		
CSM63	CSM63E	Jakumbe			V2		
CSM388	CSM388	Jigi Seme			V3		
Gadiaba Dié	Gadiaba Dié				V4	IS25916	PI525840,PI585749
W. Kaura	White Kaura		SSV 20043		V25		
V33/08	V33/08		G03-1-118		V7		
Kalaban	Kalaban		00KOF5DT19		V10		
Malisor 84-7	Malisor84-7	Dabitinnen			V9		

BimbG	BimbG	Bimbiri Soumalen	BB_G_5_34		V35		
Hafijeka	IS23645	Hafijega		1088	V21	IS23645	
S. Kaura	Short Kaura		SK-5912	1090	V22	IS10699	
Sangatigui	Sanga Tigi		98-BE-F5P-84		V8		
DouaG	Doua-G			1092	V31		
Gnossiconi	Gnossiconi			1093	V23		
Ngolofing	CSM660	Ngolofing		1091	V29		
Sambalma	Sambalma (4)	Sambalma		1095	V26		

References

Boatwright, J.L., Sapkota, S., Jin, H., Schnable, J.C., Brenton, Z., Boyles, R. and Kresovich, S. (2022), Sorghum Association Panel whole-genome sequencing establishes cornerstone resource for dissecting genomic diversity. Plant J, 111: 888-904. https://doi.org/10.1111/tpj.15853

Danecek P, Bonfield JK, *et al*. Twelve years of SAMtools and BCFtools. *Gigascience* (2021) 10(2):giab00

Li, J., & Ji, L. (2005). Adjusting multiple testing in multilocus analyses using the eigenvalues of a correlation matrix. *Heredity*, *95*(3), 221-227.

Sparks, A. H. (2018). nasapower: a NASA POWER global meteorology, surface solar energy and climatology data client for R. *Journal of Open Source Software*, *3*(30), 1035.